Universitat Politècnica de Catalunya
Institut de Tècniques Energètiques

DESIGN OF a 4 π NEUTRON DETECTOR FOR β-delay NEUTRON DETECTION EXPERIMENTS

PhD Thesis presented in
Universitat Politècnica de Catalunya
to obtain PhD degree

Author: Vitaly Gorlychev

UPC supervisor: Dr. Guillem Cortès Rossell

Barcelona, January 2014

Contents

List of Figures

List of Tables

Chapter 1

Introduction

Decay studies lie at the very frontier of the field of exotic nuclei, since once the existence of an isotope has been demonstrated, the next elementary information is sought is how it decays, even an imprecise number on the half live of a new isotope can tell a lot about the allowed or forbidden character of the decay. At the same time decay spectroscopy provides often primary information on excited states of nuclei far from stability. The advantage of the decay experiments is that they can be based on a relatively small number of events.

The study of the decay properties of neutron rich nuclei away from the valley of beta stability provides the opportunity to extend the information on the structure of atomic nuclei and its dependence with the N/Z ratio, to obtain information relevant to the understanding of the rapid neutron capture nucleosynthesis process and to obtain data useful for reactor technology applications [6]

As these nuclei are involved in supernova explosions the study of delayed neutron emission in beta decay is of fundamental importance in astrophysics for understanding the r-process. Beta delayed neutron emission is also important in terms of nuclear technology, since it is one of the key features for the safe operation of actual nuclear power plants.

Mechanisms for detecting neutrons are based on indirect methods. Neutrons are neutral and they do not interact directly with the electrons in matter, as gamma ray. The process of neutron detection begins when neutrons, interacting with various nuclei, initiate the release of one or more charged particles. The electrical signals produced by the charged particles can then be processed by the detection system.

The neutron can be scattered by a nucleus, transferring some of its kinetic energy to the nucleus. If enough energy is transferred the recoiling nucleus ionizes the material surrounding the point of interaction. This mechanism is only efficient for neutrons interacting with light nuclei. In fact, only hydrogen and helium nuclei are light enough for practical detectors. Seems the neutron can cause a nuclear reaction. The products from these reactions, such as protons, alpha particles, gamma rays, and fission fragments, can initiate the detection process. Some reactions require minimum neutron energy (threshold), but most take place at thermal energies.

Gas-filled thermal-neutron detectors use either BF_3 or ^{3}He detecting gas. In case of BF_3, the gas is enriched in ^{l0}B. Helium-3 is only about 1 ppm of natural helium, so it is usually obtained by separation from tritium produced in reactors. The nuclear reactions that take place in these gases are

$$^3\mathrm{He} + \mathrm{n} \rightarrow {}^3\mathrm{H} + {}^1\mathrm{H} + 765\ \mathrm{keV}$$
$$^{10}\mathrm{B} + \mathrm{n} \rightarrow {}^7\mathrm{Li}^* + {}^4\mathrm{He} + 2310\ \mathrm{keV}$$
$$^7\mathrm{Li}^* \rightarrow {}^7\mathrm{Li} + 480\ \mathrm{keV}$$

These reactions are exothermic and release energetic charged particles into the gas. The counters are operated in the proportional mode, and the ionization produced by these particles

initiates the multiplication process that leads to detection. The amount of energy deposited in the detector is the energy available from the nuclear reaction. In case of ^{3}He, the neutron causes the breaks up of the nucleus into a tritium nucleus (^{3}H) and a proton (^{1}H). The tritium and the proton share the 765-keV reaction energy. In case of ^{10}B, the boron nuclei breaks up into a helium nucleus (alpha particle) and lithium nuclei, with 2310 keV shared between them. Ninety-four percent of the time the lithium nucleus is left in an excited state from which it subsequently decays by emitting a 480-keV gamma ray. This gamma ray is usually lost from the detector, in which case only 2310 keV is deposited. About 6% of the lithium nuclei is left in the ground state, so that 2790 keV is deposited in the detector. This double reaction mode yields an additional small full-energy peak in the pulse height spectrum of BF_3 tubes.

The objective of the thesis is to design and construct a 4π neutron detector in order to detect neutrons at the experiment DESPEC [7] and in JYFL [6]. This neutron detector should be used to study beta delayed neutron emission. The first important part of the work is the design of the detector. According to simulation done with MCNPX (see Chapter 3) the detector is made of a matrix of polyethylene to moderate the neutrons. In the center of the matrix there is a 10 cm diameter hole to allow the ion beam impact the target located inside the matrix. Two rings of ^{3}He proportional counters are around the beam hole. The first ring consists of 8 proportional counters and the second one consists of 12 proportional counters (see Figure 5.11). Because inside the beam hole of the neutron detector might be placed many devices as the implantation target, a germanium detector, etc, the matrix of polyethylene should be dismountable in order to have access to the center of the detector. This means that it needed to design a procedure to mount and dismount the setup easily. It is important to have stable efficiency for the working neutron energy range to decrease the uncertainty in the measurement of the ratio of delayed neutron, emitted per β-decay. The next important thing to be defined is the proportional counters specifications. There are various types of detecting gas, length, diameters and cathode material.

The Technical University of Catalonia (UPC) bought one position sensitive proportional counter and a standard one manufactured by LND Inc (see Table 3.4) to make some tests of the counters and preamplifiers. These preliminary tests were done during the year 2008 at the laboratory of Nuclear Engineering Section (SEN). According to the tests results the standard 60 cm length counters by LND Inc were bought for the detector construction.

Another activity part of this work was the choice of electronics for the detector. Different electronics components will be used for the detector: high voltage power supply, amplifiers, pre-amplifiers, components of acquisition system (TDC, ADC etc).
In case of high voltage (HV) the most important problems are the noise and ripple of HV supply. In order to have clear signal from the counters the noise must be as low as possible. After a process of selection of different High Voltage power supply we chose one which specifications respond to the problem. The model of power supply is ISEG NHQ203M (see Figure 4.16). This 2 channel supply has maximum ripple and noise 2 mV and provides output current 4mA which is enough for all proportional counters of the detector.

According to the simulation and cost study there will be 20 proportional counters with ^{3}He detection gas. In order to supply all the counters a special distribution box was designed at

the laboratory of Institute of Energy Technologies (INTE). This box distributes the current from two input channels to 20 output channels. For acquisition system, Time to Digital Converter (TDC) CAEN V767 was selected. This TDC has 64 channels which is enough for the detector. The same TDC was used at NERO [4] experiment in MSU, an experiment with similar objectives.

There were two options with the preamplifiers. The first one was to buy two standard MESYTEC pre-amplifiers of 16 channels. The second option was to make the preamplifiers by ourselves and adapt them to the detector setup. The problem of using standard ones was the cable length between the counters and preamplifiers. The long cable gives large noise, but our adapted preamplifiers might be directly connected without any cable to the counters. These preamplifiers are based on CREMAT CR-110 chip. Some preamplifiers based on this chip were made and tested at SEN laboratory.
As the weight of the detector will be more than 300 kg, another work to be done is the design of a special support to make possible to move the detector in the experimental area and also to adjust the ion beam into the center of the detector.
This work was carried out in collaboration with other research centers and universities. The Gamma Ray Spectroscopy Group of IFIC (Valencia) led the development of the beta-detection and acquisition system software. Researchers from CIEMAT (Madrid) helped with the tests of the counters and electronics. As they have experience in neutron study they help in the detector construction. The first test of the detector will be made in JYFL (Finland). It will be a prototype for DESPEC experiment.

The project FAIR (Facility for Antiproton and Ion Research) [8] is an international accelerator facility of the next generation. It builds on the experience and technological developments already made at the existing GSI (Germany) facility, and incorporates new technological concepts. Different experiments with different objectives will be made at this accelerator. One of these experiments is Decay Spectroscopy (DESPEC) experiment. One of the important objectives of DESPEC is the study of r-process and the influence of delayed neutron emission. An unique feature of FAIR will be the access to regions where the waiting points for the r-process occur. For our understanding of the r-process nucleo-synthesis of heavy elements in supernova explosions we need to know the beta decay half life, the neutron branching ratios and the neutron (or two-neutron) separation energy of these nuclei.

At DESPEC it will be possible to measure the first two quantities. If the number of decays is high enough, detailed spectroscopy will be possible and then questions such as isospin symmetry can be tested in mirror nuclei or the long standing Gamow Teller quenching problem in beta decay can be addressed in combination with charge exchange reactions.

For the most exotic nuclei it is possible to expect some unusual decay modes such as beta-delayed multi-neutron emission, beta delayed fission, or even direct neutron radioactivity.

Another very important aspect of DESPEC is the possibility to study the decay properties of isomeric levels in nuclei which survive the flight time from the moment of production until the time of arrival to our set-up. All of the experiments at DESPEC involve deep implantation of the ions in an active stopper prior to the decay, as the AIDA device [7]. The detector will be highly pixellated, which allows us to correlate in time and space the signal of the initial pulse from implantation of the heavy ion with the signal produced in the same detector in

the subsequent beta decay. Neutron and high resolution gamma-ray detectors in a compact arrangement around the active stopper in a highly flexible and modular geometry will be at the heart of this set-up. Complementary measurements using the Total Absorption Gamma technique and measurements of nuclear g-factors and quadruple moments as well as level half lives are also foreseen.

In particular the determination of the beta decay probability distribution over the entire accessible energy window (Q_β), the determination of the total neutron emission probability (P_n), and the determination of the energy distribution of the emitted neutrons serves to all three purposes. In order to obtain this information complementary setups are required: the use of a Total Absorption Spectrometer (TAS) [6] to measure accurately the beta-decay intensity distribution (I_β) below the neutron separation energy (S_n) in the daughter nucleus, the use of a 4π neutron (4πn) detector to obtain accurate values of P_n and the use of a Time of Flight neutron detector array (ToF)[6] to measure the beta delayed neutron energies. The complementary analysis of the ToF and 4π data will be used to control the systematic uncertainties specific to each technique. Hence, both neutron detectors should allow reconstructing the beta-decay intensity distribution above the neutron separation energy. The use of the Penning trap as a mass separator of very high resolution will ensure the purity of the sources required for obtaining high quality data. This collaboration is working on the design of three detectors for DESPEC-FAIR similar to the ones that will be used in the experiment in this proposal.

The measurements at JYFL will be complementary to the ones that will be carried out in FAIR and will allow the beta decay delayed neutron experimental program to start before the FAIR facility becomes available.

Chapter 2

State of art

2.1 Introduction to neutron detection

As neutrons are neutral particles, they do not interact electromagnetically directly with the electrons in matter. The mechanisms of the detection are based on indirect methods. In order to detect a neutron it should interact with a nuclei and then initiate a release of one or more charged particles. The detection system can process the electrical signals produced by the charged particles. There are two basic types of neutron interactions with matter [9]:

- The neutron can be scattered by a nucleus and transfers some of its kinetic energy to the nucleus. The recoiling nucleus ionizes the material surrounding the point of interaction, if enough energy is transferred. This mechanism is efficient for interacting with light nuclei. Actually, only hydrogen and helium nuclei are light enough for practical detectors.

- The neutron can cause a nuclear reaction. The products from these reactions can initiate the detection process. It can be protons, alpha particles, gamma rays and fission fragments. Some reactions require a minimum neutron energy (threshold), but most of them take place at thermal energies. Around the detectors which use thermal reactions moderating material is used.

Detectors that use either the recoil or reaction mechanism can use solid, liquid or gas-filled detection media. The detecting media can be quite varied, leading to many options, but the choice of the reactions is limited. This chapter describes some types of neutron detectors. They are gas-filled proportional counters, scintillator, fission chambers.

2.1.1 General properties of gas-filled detectors

Gas-filled detectors were among the first detectors. This type of detectors are able to detect thermal neutrons via nuclear reactions and fast neutrons via recoil interactions. The gas detector consists of a metal cylinder with an electrical connector at one end or at both ends in case of position-sensitive detector. Detector walls are made of stainless steel or aluminium. Sometimes the interior of walls are coated with activated charcoal in order to absorb electronegative gases which build up during neutron irradiation. The neutron transfer some or all of its energy to charged particles. The charged particles will then ionize and excite the atoms along its path until its kinetic energy is exhausted.

^{3}He and BF_3 Thermal Neutron Detectors

Gas-filled thermal-neutron detectors use either BF_3 or ^{3}He detecting gas. In case of BF_3, the gas is enriched in ^{10}B. The nuclear reactions that take place in these gases are

$$^{3}He + n \rightarrow ^{3} H + ^{1} H + 765keV; \tag{2.1}$$

$$^{10}B + n \rightarrow ^{7} Li^{*} + ^{4} He + 2310keV \tag{2.2}$$

$$^{7}Li^{*} \rightarrow ^{7} Li + 480keV \tag{2.3}$$

These reactions are exothermic and issue energetic charged particles into the gas. The cross-section for the ^{3}He reaction is 5330 b for thermal neutrons and the cross section for the ^{10}B reaction is 3840 b. Figure 2.1 illustrates these cross-sections.

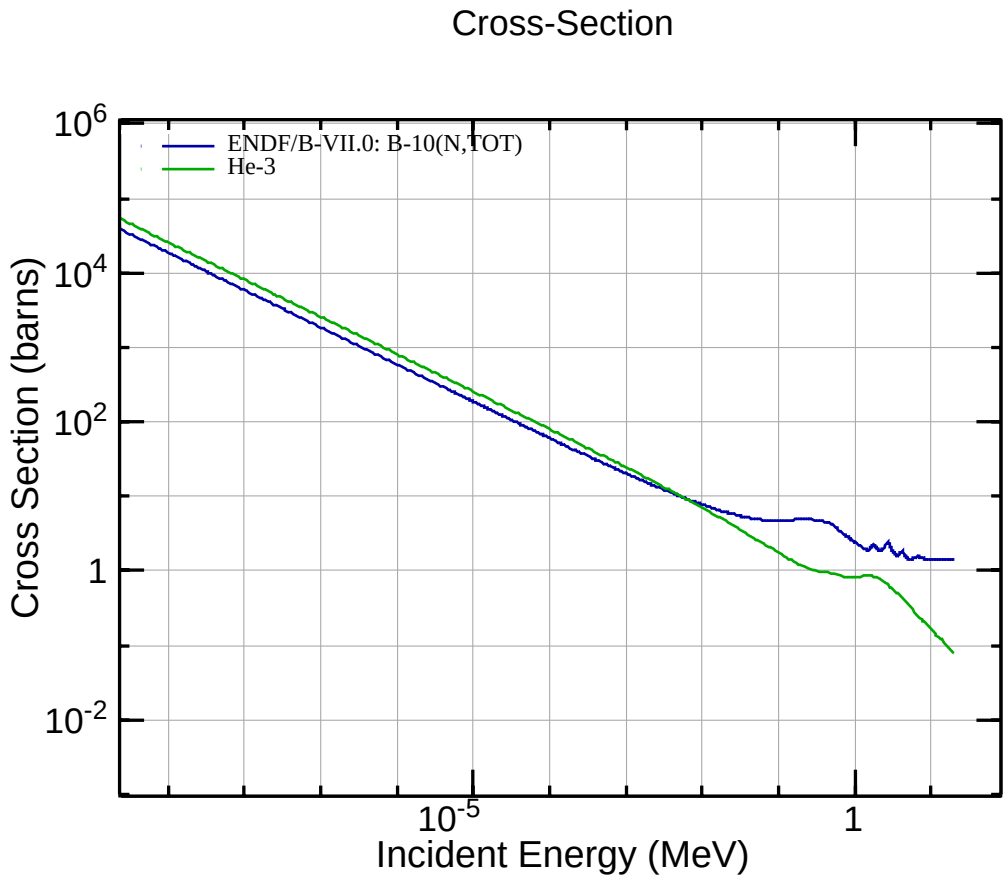

Figure 2.1: Neutron cross-section capture for ^{3}He and BF_3. This data was taken from ENDF-06

In order to increase the probability of the reaction the first thing which should be done is moderate the neutrons. Moderation is the process of the reduction of the initial high kinetic energy of the free neutron. Since energy is conserved, this reduction of the neutron kinetic

energy takes place by transfer of energy to a material known as a moderator. As a moderator can be used a material consisting of light-nuclei. For one strike neutron lose

$$\frac{2A}{(A+1)^2} \tag{2.4}$$

of its energy. Some properties of neutron moderators are presented on Table 2.1 where N is number of strikes, t is moderation time from 1 MeV to 0.1 eV, and L is mean of square distance of moderation from 1 MeV to 0.1 eV.

Material	N	t, μs	L, cm
Lead	1600	1300	200
Coal	110	70	43
Water	23	30	13

Table 2.1: Characteristics of some neutron moderators

As the counters are operated in the proportional mode the ionization produced by these particles initiates the multiplication process which leads to detection. The energy available from the nuclear reaction is deposited in the detector. In case of ^{3}He, the neutron causes the breaks up of the nucleus into a tritium nucleus (^{3}H) and a proton (^{1}H). This two particles share the 765 keV of reaction energy. In case of ^{10}B, the boron nuclei breaks up into a helium nucleus (alpha particle) and lithium nuclei. This two particles share 2310 keV of reaction energy. Ninety-four percent of the time the lithium nucleus is left in an excited state from which it subsequently decays by emitting a 480 keV gamma ray. This gamma ray is usually lost from the detector, in which case only 2310 keV is deposited. About 6% of the lithium nuclei is left in the ground state, so that 2790 keV is deposited in the detector. This double reaction mode yields an additional small full-energy peak in the pulse height spectrum of BF_3 tubes.
The cross-section for the ^{3}He reaction is 5330 b for thermal neutrons and the cross section for the ^{10}B reaction is 3840 b. Figure 2.1 illustrates these cross-sections. Figure 2.2 is a typical pulse-height spectrum from ^{3}He proportional counter. In this figure the electronic noise can be observed in channels from 0 to 20. The first wall effect corresponds to channel 25 and the second wall effect could be observed in channels near to the 80, but it is overlapped with the main peak of energy deposition. The main peak corresponds to the energy 765 keV and it is around channel 98. The wall effect arises because the proton and triton daughter products of the reaction have discrete energies (573 keV and 191 keV respectively) and their ranges in the detector are usually larger than the dimensions of the detector. When one of the daughter products collides with the wall of the detector, its energy is dissipated and does not contribute to the full energy peak, thus creating the discrete steps in the spectrum.

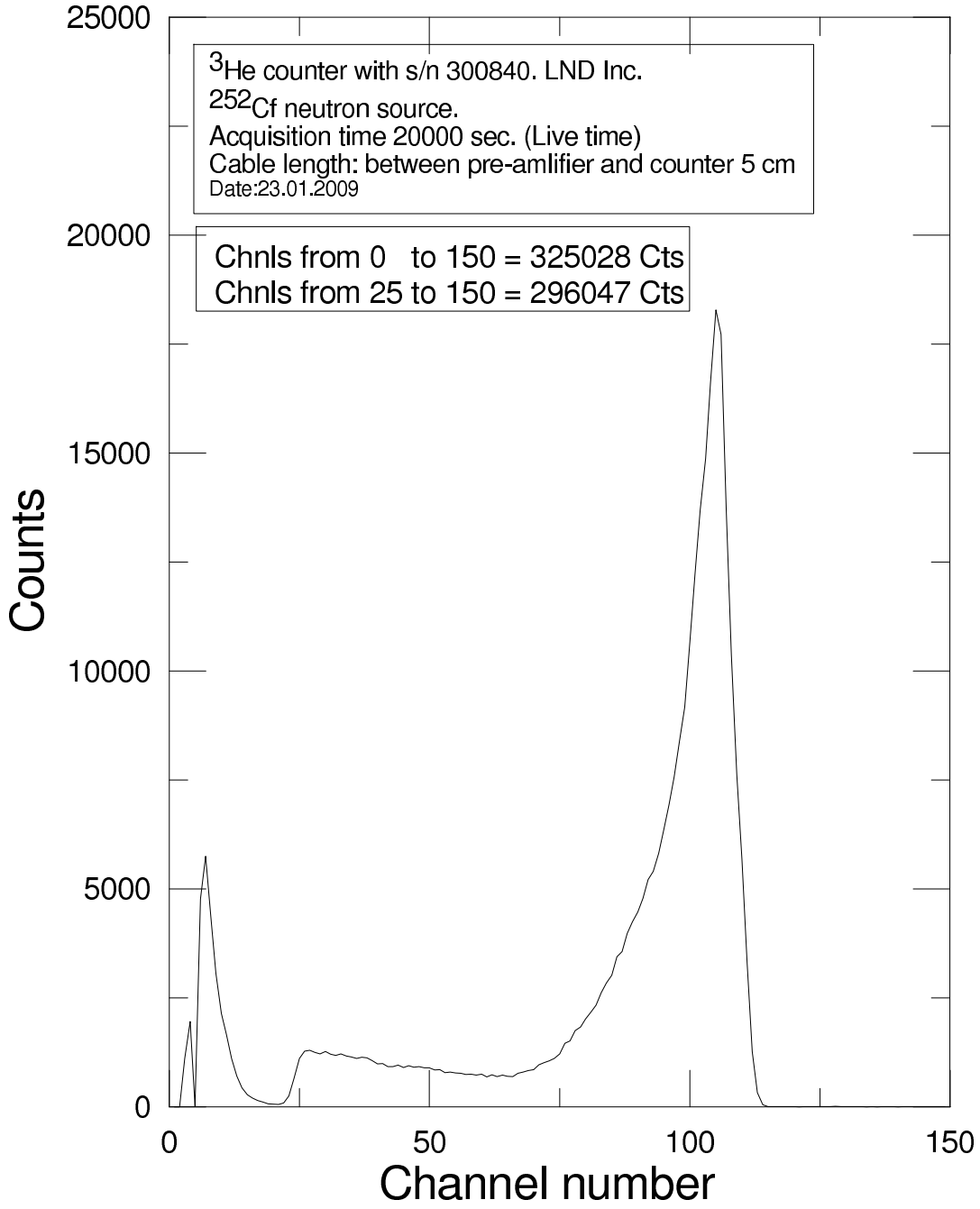

Figure 2.2: Differential pulse-heigh spectrum for thermal neutrons detected by a ^{3}He-filled counter. This spectra was obtained at UPC-SEN laboratory.

^{4}He and CH_4 Fast Neutron Detectors

Helium-4 and CH_4 fast-neutron detectors are based on the recoil of light nuclei in order to ionize the gas in the tube. The interaction is the elastic scattering of the neutron by a light nucleus. If the recoiling nucleus is only a hydrogen nucleus (proton), the maximum possible energy transfer is the total neutron kinetic energy. For heavier elements the maximum energy transfer is always less. For a nucleus of atomic weight A, the maximum energy transfer is the same like equation 2.5:

$$E_{(max)} = \frac{2AE}{(A+1)^2} \tag{2.5}$$

Where $E_{(max)}$ is maximum energy transfer and E is neutron energy.

For a single scattering event, the energy transferred to the recoiling nucleus lies between 0 and $E_{(max)}$. It depend on the scattering angle and has equal probability for any value in this range.
Equation 2.5 shows that the target nucleus must have low atomic weight in order to receive a significant amount of energy from the neutron. In this case hydrogen is the best choice. It can be used in a gaseous, liquid form or plastic scintillator. Popular gas detector employs methane CH_4 or ^{4}He.

Fission chambers

Fission chambers are a variation of the gas-filled counters. They detect neutrons which induce fissions in fissionable material coated on the inner walls of the chamber. As the fissionable material is usually used uranium highly enriched in ^{235}U. A very thin layer is electroplated on the inner walls. After a fission event, the two fission fragments travel in nearly opposite directions. The ionization caused by the fission fragment which entered the gas is sensed by the detector, the fragment travelling in the opposite direction is absorbed in the detector walls.
Two fragments share about 160 MeV of energy. Since the coating must be kept thin to allow the fission fragments to enter the gas, the fission chamber uses only small quantity of fissionable material and has a low detection efficiency. For thermal neutrons, the intrinsic efficiency is typically 0.5 to 1. Fast neutrons can also be detected, but with lower efficiency.

2.1.2 Plastic and liquid scintillators

Plastic and liquid scintillators are often used for fast-neutron detection because of their fast response and low cost. Fast response is particulary beneficial for coincidence counting applications where the ratio of real to accidental coincidence events can have a significant impact on the statistical precision of the measurement. Also liquid scintillators have response time of a few nanoseconds, the coincidence resolving time is usually dictated by the dynamic range of neutron flight time from the sample to the detector.
The main disadvantages of scintillator is their high gamma-ray sensitivity. Detection probabilities for neutrons and gamma rays are comparable, and the pulse-high spectra resulting

from monoenergy radiation of both types are broad and overlapping.

2.1.3 Example of some actual neutron detectors

This section will describe some 4π neutron detectors which were used for other experiments with neutron detection.

Neutron detector based NE-213 scintillation counters.

A group from Physikalisch-Technische Bundesanstalt, Braunschweig, Germany and Physikalisches Institut der Universität, Göttingen, Germany designed a neutron detector based on scintillation counters [1]. This detector was designed for β-delayed neutron detection. The energy range was from 260 keV till 6 MeV.

The neutron detection system consists of sixteen individual NE 213 detectors with two differently shaped scintillator tanks (See Figure 2.3). A ring of eight detectors with the axis in the beam direction encircles the implantation spot and the second ring of eight detectors surrounds the beam line. The number of sixteen segments was chosen as a compromise between simplicity of construction and the chance to measure neutron multiplicities.

The calculation of efficiencies for NE 213 neutron counters requires accurate knowledge of the detection threshold and of the light output function for the secondary charged particles. In the energy region of β-delayed neutrons ($E_n < 3$ MeV), only recoil protons from n-p scattering have to be considered. A precise way to determine the energy of neutrons is to measure their time-of-flight. The efficiency as a function of neutron energy can be measured.

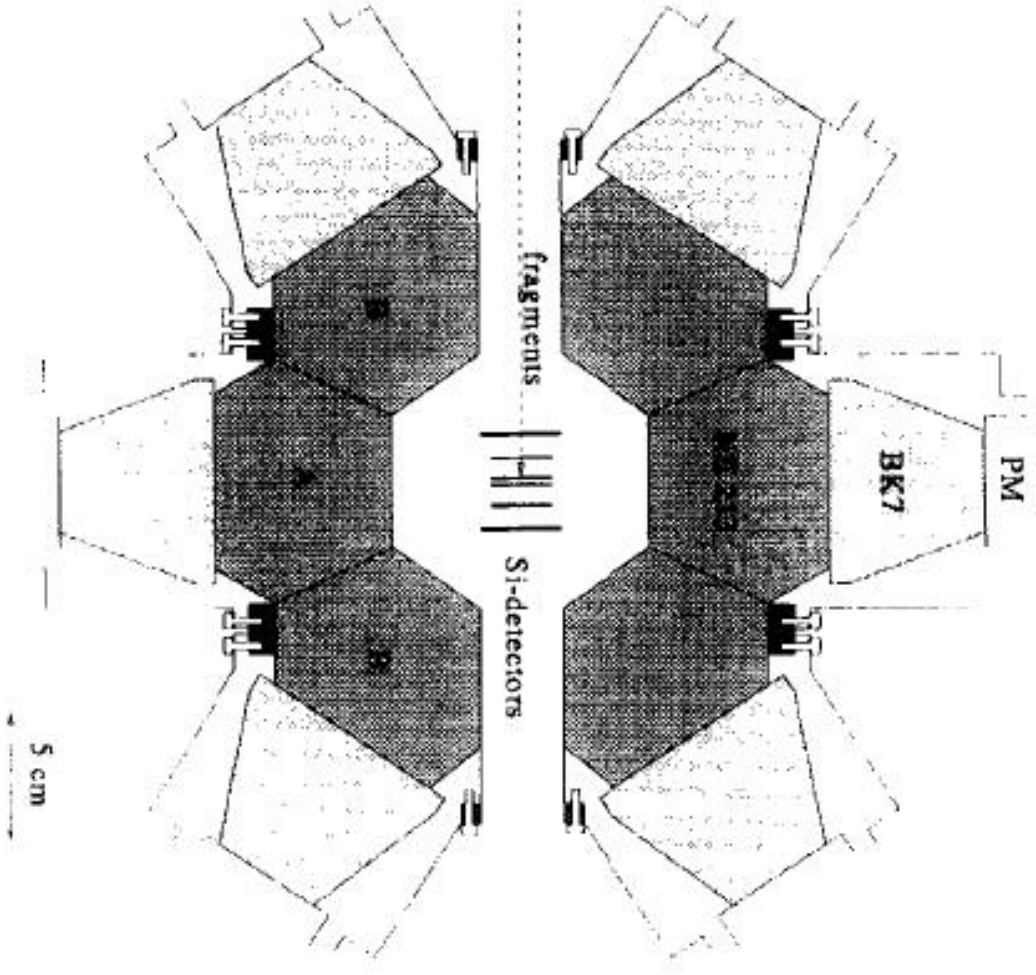

Figure 2.3: Arrangement of NE 213 scintillator for neutron detection in measuring geometry. Six of sixteen segments mounted in 4Π geometry are visible. This image was taken from reference [1]

.

Examples of neutron time-of-flight spectra are shown in Figure 2.4. The numbers l-3 correspond to energy thresholds in the pulseheight branch of about 50, 155, and 260 kV. The γ -line at TOF = 10 ns is due to the imperfect pulse-shape discrimination at low energies and is only present for the lowest detection threshold. Several corrections need to be applied in the off-line data evaluation. The corrected TOF spectra were transformed into a linear energy scale. The resulting neutron energy spectra for the different thresholds are shown in Figure 2.5 a (curves l- 3). together with the ^{252}Cf reference spectrum. Since significant deviations of the ^{252}Cf neutron distribution from a Maxwellian shape were observed, a careful evaluation of the experimental data available were used. The efficiency $\varepsilon(E)$ as a function of neutron energy was then obtained by dividing the measured spectra (curves 1-3 on Fig-

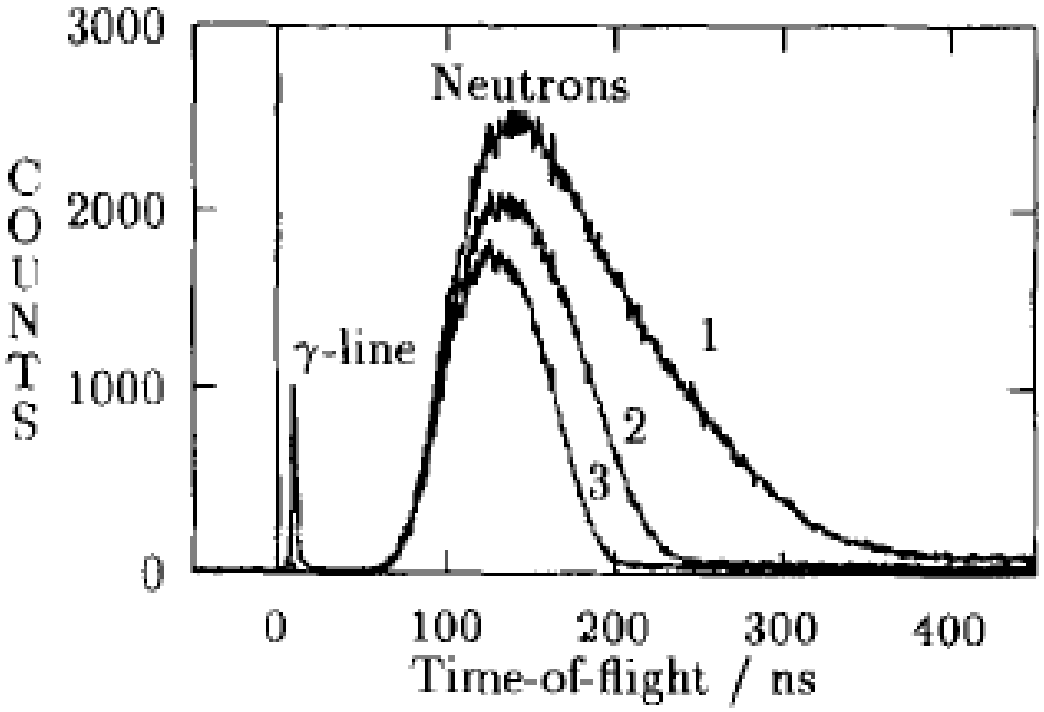

Figure 2.4: Neutron time-of-flight spectra of ^{252}Cf measured with detector B and 3 m flight path (recording time 14.9 h, time calibration 0.72 ns/channel). The numbers correspond to different energy thresholds. This image was taken from reference [1]

ure 2.5) by the calculated reference spectrum. The results are shown in Figure 2.5 b together with Monte Carlo calculations.

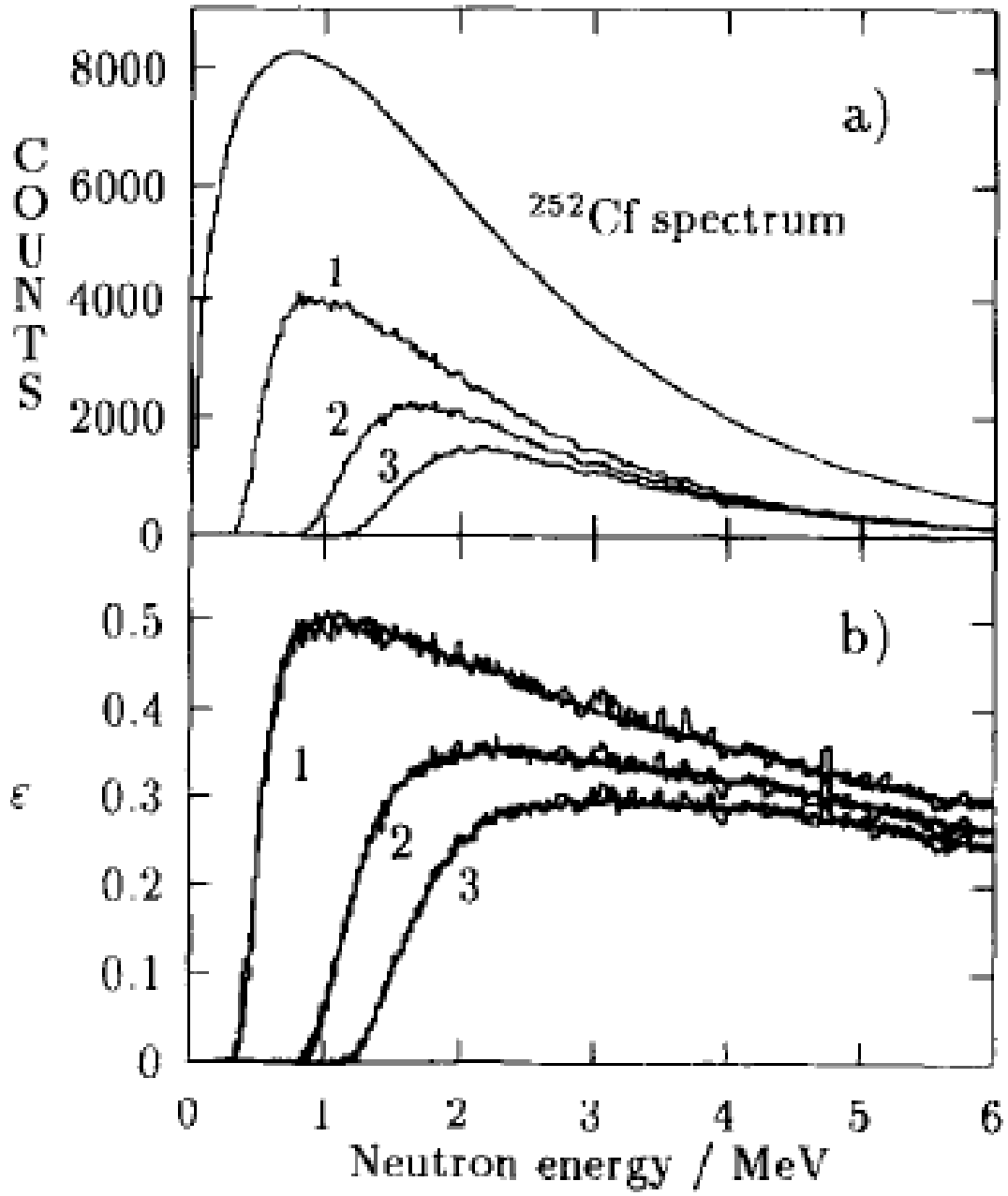

Figure 2.5: (a) Neutron energy spectra from ^{252}Cf spontaneous fission measured with detector B and n flight path of 3 m for three different thresholds together with the ^{252}Cf reference spectrum (see text). (b) Experimental efficiency curves (thin lines) obtained after dividing the upper curves I to 3 by the reference spectrum. Monte Carlo calculations (thick lines) are given for comparison. This image was taken from reference [1]

4Π moderation based neutron detector with ^{3}He-filled proportional counters.

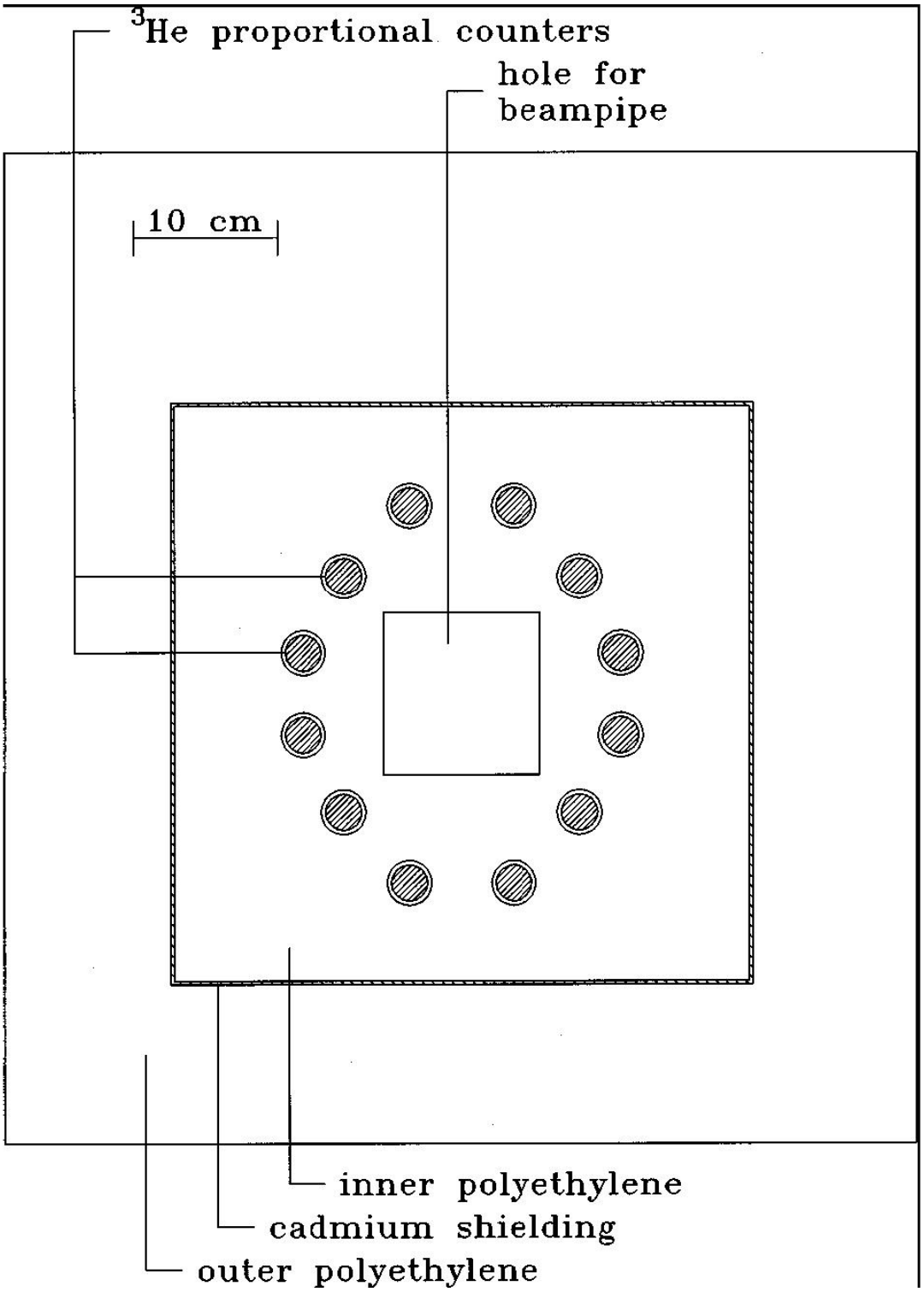

Figure 2.6: Front view of the polycube. This image was taken from reference [2]

In Radiation Laboratory in California Institute of Technology total cross sections for the ^{19}F(α,n)^{22}Na and ^{22}Ne(p,n)^{22}Na reactions were measured. The neutron detector for this experiment, called as the "polycube", is a 4π detector consisting of 12 ^{3}He-filled proportional counters embedded in a polyethylene moderator (See Figure 2.6). The moderator is in the form of a cube, 40 cm on a side, with a 11.5 cm x 11.0 cm channel through the center for insertion of the beam pipe. The channel downstream from the beam pipe end is plugged with graphite. The 12 proportional counters are placed about the beam pipe channel in an ellipse whose vertical semimajor axis is 13.2 cm, and horizontal semiminor axis is 11.1 cm. Each proportional counter is 2.5 cm in diameter and 54 cm long, with an active length of 46 cm. The polycube is mounted on rails that allow it to be positioned such that the target is at the center of the cube. Surrounding the 40 cm cube of polyethylene is a 4π layer of cadmium shielding, 0.6 mm thick, which is in turn surrounded by a 4π layer of polyethylene and borated paraffin, approximately 10 cm thick, and a 3π paraffin wax "house" $25 - 50$ cm thick. Since the efficiency of the neutron detector depends on the neutron energy, Monte Carlo calculations were required to model the low-energy behavior of the polycube, and determine the detection efficiency as a function of neutron energy. The simulation results are presented on Figure 2.7

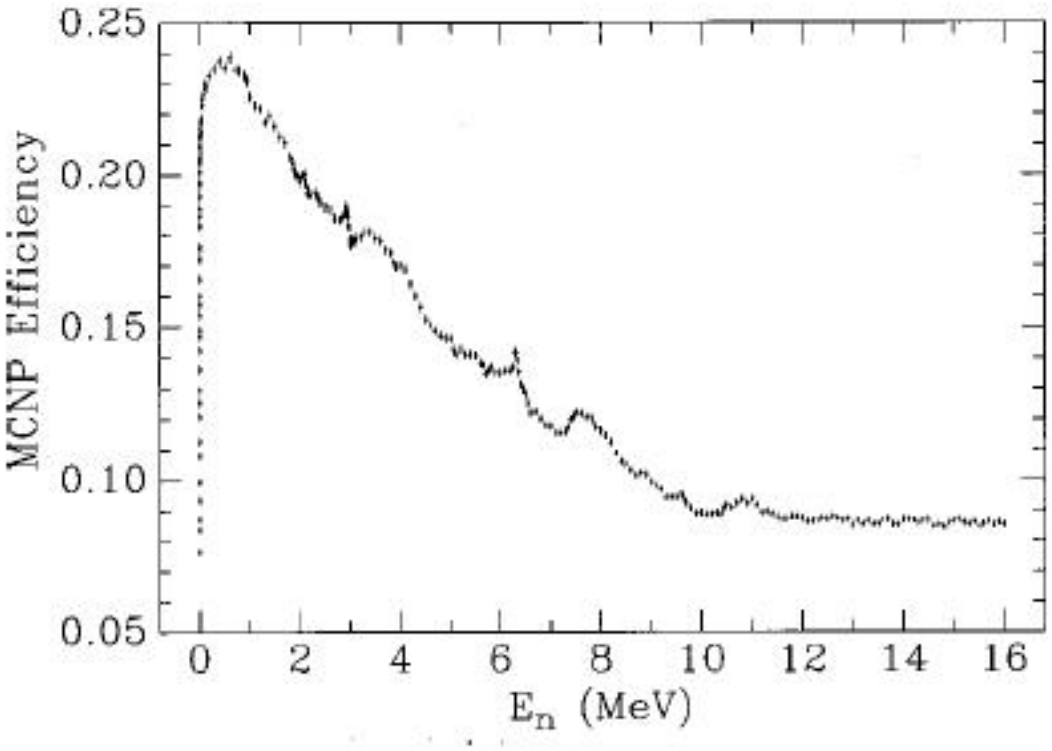

Figure 2.7: The MCNP[3] efficiency vs neutron energy for monoenergetic, isotropic neutrons. This image was taken from reference [2]

Two radioactive sources, ^{252}Cf and ^{241}Am-Be, and two nuclear reactions, t(d,n)^{4}He and ^{7}Li(p,n) ^{7}Be, were used to test the results from MCNP. The results of the test with these isotopes are presented on Table 2.2

	$\overline{E_n}$	Experimental	MCNP
^{252}Cf	2.35	0.196(6)	0.1927(15)
AmBe	4.46	0.155(6)	0.1500(14)
t(d,n)^{4}He	14.1	0.0468(14)	0.0481(2)

Table 2.2: Efficiency of 4Π neutron detector consisted of 12 ^{3}He-filled proportional counters embedded in a polyethylene moderator.This table was taken from reference [2]

The production of ^{22}Na involves the interaction of exothermic (p,γ), (n,p), and (n,α) reactions and β-decay. In this experiment partial reaction rates is determined for the destruction mechanisms ^{22}Na(n,p$_0$)^{22}Ne and ^{22}Na(n,α_0)^{19}F, where the subscript means that the products of nuclei ^{22}Ne and ^{19}F are in their ground states.

The NERO detector

The Neutron Emission Ratio Observer (NERO), has been constructed for use at the National Superconducting Cyclotron Laboratory (NSCL) to work in conjunction with the Beta Counting System (BCS) in order to detect β-delayed neutrons. It consists of an axially symmetric set of proportional gas counters embedded in a moderating matrix. The main feature of the detector system is a large diameter hole which allow to insert the implantation detector which stops the nuclei of interest and allows for β - delayed neutron decay to occur in the center of NERO, thus providing a solid angle of almost 4π.

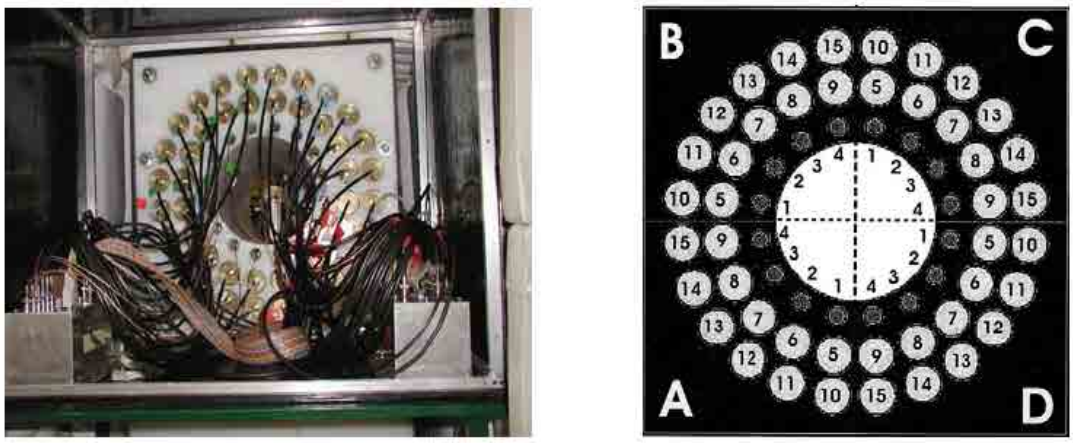

Figure 2.8: Views of NERO. (a) The tubes are inserted and high voltage cables come out of the proportional tubes to the preamp boxes. In the beamline hole, a special holder allows a source to be placed in the middle of NERO. (b) Cross section of NERO. For the purpose of electronics, NERO was divided into four quadrants, and the proportional counters were numbered by quadrant. This image was taken from reference [4]

The final design of NERO (Figure 2.8) included a polyethylene moderating matrix 60x60x80 cm^3, being longer along the beam axis. The detector contains 60 proportional counters, 16 ^{3}He and 44 BF_3 tubes, arranged in three concentric rings. The inner ring has a radius of 13.6 cm and contains 16 ^{3}He tubes. The middle ring has a radius of 19.2 cm and contains 20 BF_3 tubes, and the outer ring has a radius of 24.8 cm with 24 BF_3 tubes. The rings are all concentric around the cylindrical beamline hole of radius 11.2 cm, running the length of the detector along the beamline direction. Two models of ^{3}He proportional counters were used in NERO. All of the BF_3 counters are 100% BF_3 gas enriched in ^{10}B to greater than 96%.

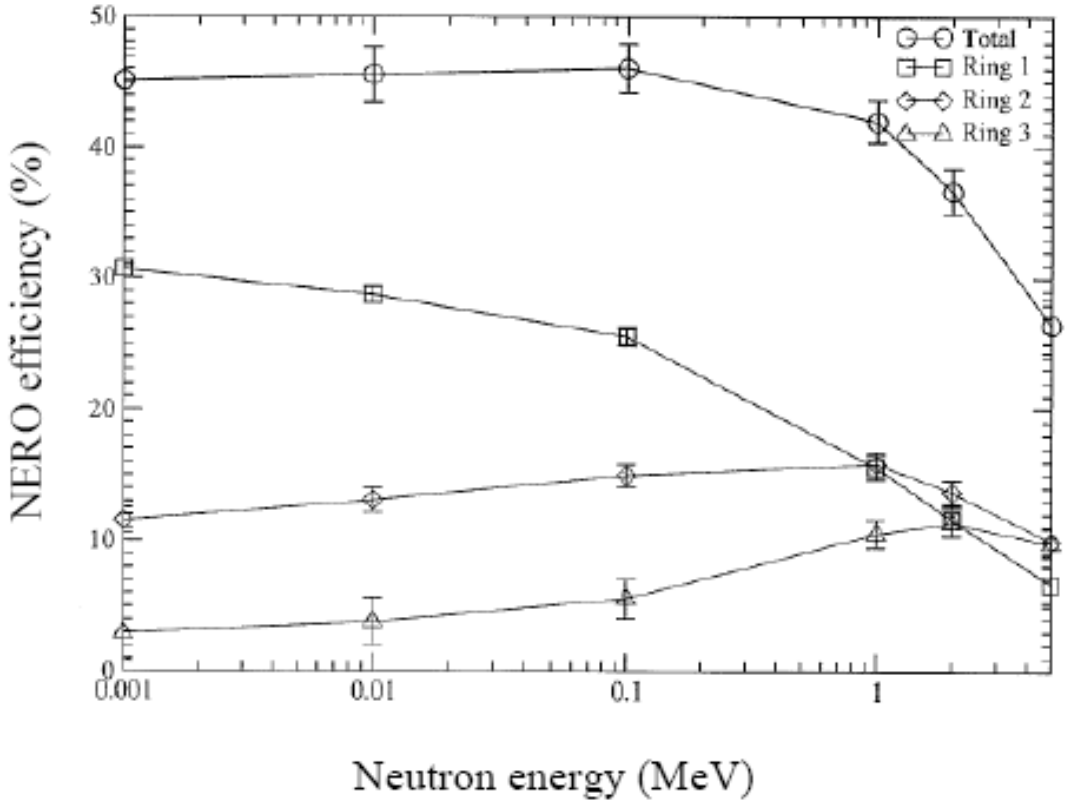

Figure 2.9: The calculated efficiency curve for NERO. This image was taken from reference [4]

The detection of neutrons with proportional gas counters takes advantage of the fairly large neutron capture cross section of ^{3}He and ^{10}B at low neutron energy (less then 0.5 eV). The flat efficiency (see Figure 2.9) is achieved by the placement of rings of proportional counters at various radii from the center of the detector. Three rings also allow for the possibility of extracting some average energy of the emitted neutrons which may be desiderable since the energy information of an individual neutron is lost in moderation. The beamline-hole requirement was a particular challenge in order to put the target inside. The larger the hole, the further away the tubes are from the center of the detector and therefore the lower solid angle that is covered with the same number of tubes.
A boron carbide shield was added around NERO. This shield was used in order to protect the detector from background neutrons. The boron carbide shield was fabricated by mixing boron carbide powder in epoxy and pouring the mix into a frame. Inside the sheet, fiberglass ribbons provide added support.
The NERO final design has a relatively constant calculated detection efficiency of about 45% from 1keV to 500keV, dropping off to around 26% at 5MeV. Figure 2.9 shows the NERO efficiency versus the neutron energy as calculated in the code MCNP. The plot includes the total NERO efficiency, as well as the efficiency of each one of the three rings of proportional counters.

Test with ^{252}Cf source was performed for calibration of neutron detector. It has a neutron production rate of 0.116 neutrons/s/Bq. The emitted neutrons cover a broad range of energy from 0 MeV to 7 MeV. This was compared to the neutron rate measured by NERO with

the source located at the target position. Their ratio, the average efficiency weighted by the source neutron energy spectra, was calculated to be 27 ± 4%. The response of the MCNP code for this quantity is 34.48 ± 0.06% and the nature of this discrepancy is still under discussion.
This work extended the nuclear physics data to ^{78}Ni and examined the influence of new measurements on understanding of nuclear structure and the r-process in this mass region.

Neutron detector of cylindrical polyethylene moderator

This detector consists of a cylindrical polyethylene moderator and a matrix of 16 ^{3}He-filled proportional counters. These counters are placed in two concentric rings around the target chamber, with each ring consisting of 8 counters (See Figure 2.10). The distances from the axis of the target chamber to the counter rings were 8 cm and 12 cm, respectively. This configuration of the detector leads to a large efficiency of up to 38%.

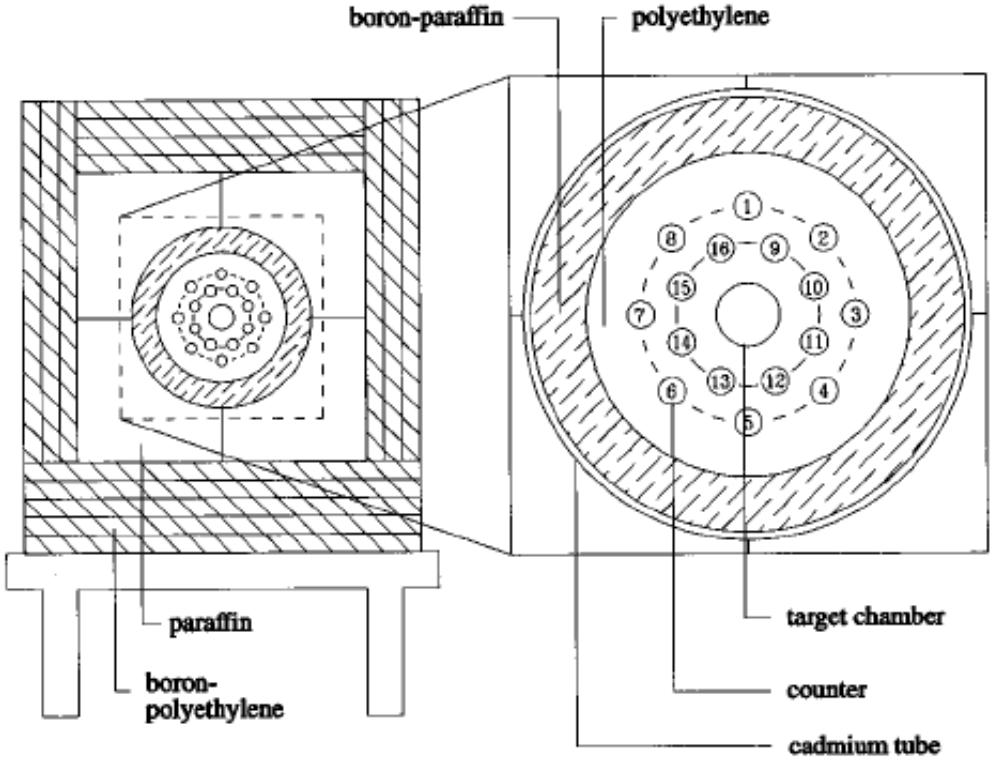

Figure 2.10: Cross section of the 4Π neutron detector. This image was taken from reference [5]

The efficiency of the detector in dependence of the neutron energy has been determined by Monte Carlo simulations using the code MCNP. The resulting curve is shown in Figure 2.11. These calculations have been tested by efficiency measurements with a calibrated ^{252}Cf-neutron source and some other nuclear reactions. These tests resulted in a good agreement of better than 3% relative deviation between measurement and simulation. The uncertainty

assigned to the efficiency was less than 5%, depending on the neutron energy.

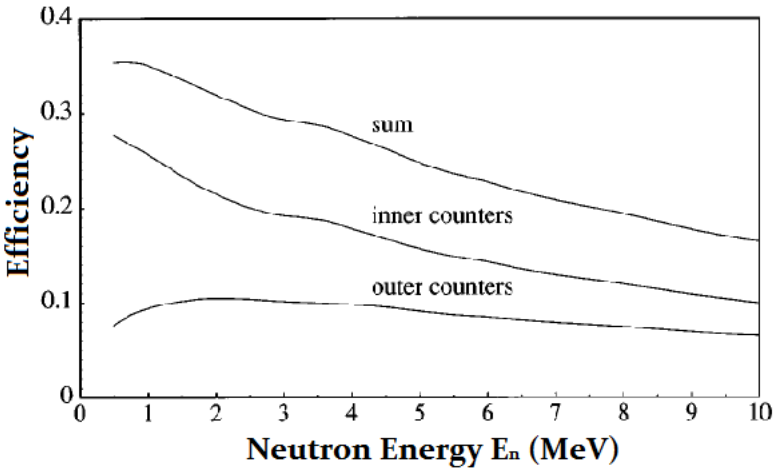

Figure 2.11: Energy dependence of the efficiency ε of the two counter rings separate and as sum for neutron energies from 0.5 to 10 MeV. This image was taken from reference [5]

The measurements have been performed at the 4MV DYNAMITRON accelerator of the Institut für Strahlenphysik at Stuttgart. The reaction ^{9}Be(α,n) ^{12}C has been examined in the energy range from 366 up to 3552 keV

Chapter 3

Design of neutron detector

3.1 Introduction

The aim of this work is to design a neutron detector for measuring neutron emission ratio per β-decay. The design of the detector will be based on the design of NERO [4]. This detector should be re-disigned and optimized for the actual work. The main objective of the design is flat efficiency curve for wide energy range of neutrons. In this work wide range is considered as a range between 100 keV and 6 MeV. Other important things for this detector is efficiency as high as possible.
In order to design the detector with these properties it is important to make some calculation such as dimensions, detection properties, detection reaction, etc.
It is difficult to make all this calculation without Monte Carlo simulation. Monte Carlo simulation helps to obtain main characteristics of the detector, such as geometry properties or the material choice for the construction. Simulation results will provide future properties of the final setup such as efficiency, trigger time and some other properties. Simulation permits to obtain response function from the simulated detector as it would be a real one. Next section will describe some Monte Carlo simulation codes.

3.2 Simulation codes overview

There are a lot of different Monte Carlo simulation codes for the radiation transport. They are GEANT [10], MCNPX [3], FLUKA [11], PENELOPE [12] and others. Each of them is used for different particles and energies.
Geant4 (for GEometry ANd Tracking) is a toolkit for simulating the passage of particles through matter. It includes a complete range of functionality including tracking, geometry, physics models and hits. The physics processes offered cover a comprehensive range, including electromagnetic, hadronic and optical processes, a large set of long-lived particles, materials and elements, over a wide energy range starting, in some cases, from 250 eV and extending in others to the TeV energy range. It has been designed and constructed to expose the physics models used, to handle complex geometries, and to enable its easy adaptation for optimal use in different sets of applications. The toolkit is the result of a worldwide collaboration of physicists and software engineers. It has been created exploiting software engineering and object-oriented technology and implemented in the C++ programming language. It has been used in applications in particle physics, nuclear physics, accelerator design, space engineering and medical physics.

FLUKA (FLUktuierende KAskade) is a Monte Carlo simulation package developed for the interaction and transport of particles and nuclei in matter. This simulation code has many applications in particle physics, high energy experimental physics and engineering, shielding, detector and telescope design, cosmic ray studies, dosimetry, medical physics and radiobiology. FLUKA is developed using the FORTRAN language. Under Linux the g77 compiler is at present necessary to build and run user programs. The software is sponsored and copyrighted by INFN and CERN.

The computer code system PENELOPE performs Monte Carlo simulation. This code lets

simulation of electrons, positrons and photons in energy range from 50 eV till 1 GeV in arbitrary materials. Initially, this simulation code was developed to simulate the PENetration and Energy LOss of Positrons and Electrons in matter; photons in this code were introduced later. The simulation code is based on Fortran77 programming language.

MCNPX (Monte Carlo N-Particle Transport Code) is a software package for simulating particle interactions involving neutrons, photons, and electrons, and particle interactions of 34 different types of particles at all energies. This code can be used to judge whether or not nuclear systems are critical and to determine doses from sources, amongst other things. MCNPX was chosen to make this simulation due to we have a wide experience in this simulation code.

The geometry of the problem to be simulated is defined in the input file. This geometry requires the description of surface, materials and cells. Surfaces can be spheres, cylinders, planes and their combinations. Materials can be defined as a simple element or as compounds. Cells are built as the intersection of many surfaces. An MCNPX input file contains descriptions of surfaces, materials and cells.
The input file contains description of tallies of the problem. The user can choose different types of tallies for the input file.
The input file contains a description of the source of the problem. The particle source can be defined as a constant source or as a distribution to be sampled from in space, energy and direction coordinates. Predefined distributions are available through the SP (Source Probability) card. Information on the geometrical extent of the source can be provided with the SI (Source Information) card.

An output file of MCNPX contains the the source of input file and different table and results which was asked in the output file.

3.3 Simulation equipment

The simulations were done on cluster ARGOS [13] at UPC-SEN with MCNPX 2.5.0 simulation code [3].
The cluster consists of three parts. The first one is a Server (server Argos): This is the front end where users can launch the simulations to the nodes (also called clons). Every user has his personal folder and useful tools such compilers, editors, etc. The second part called Nodes (Clons). Every node is always waiting for submitted jobs from the server. Every user has also his own personal folder (different from the server), but shared with the other nodes. If a file is modified on any node, all the nodes will have this modified file in real time. Every node has his own local hard disk where simulation outputs must to be recorded. And the third part is a monitoring and information server. It shows the live statistics of the cluster services. It is also used to host the web information service where users can share and publish his documents. On the Figure 3.1 a schematic view of three parts of cluster is shown.

There are two types of processes running into the cluster:
Parallel processes (PVM and MPI): small processes are sent to aggregated nodes and when all of them finishes, the server sends new jobs. Nodes that calculate faster, has to wait until

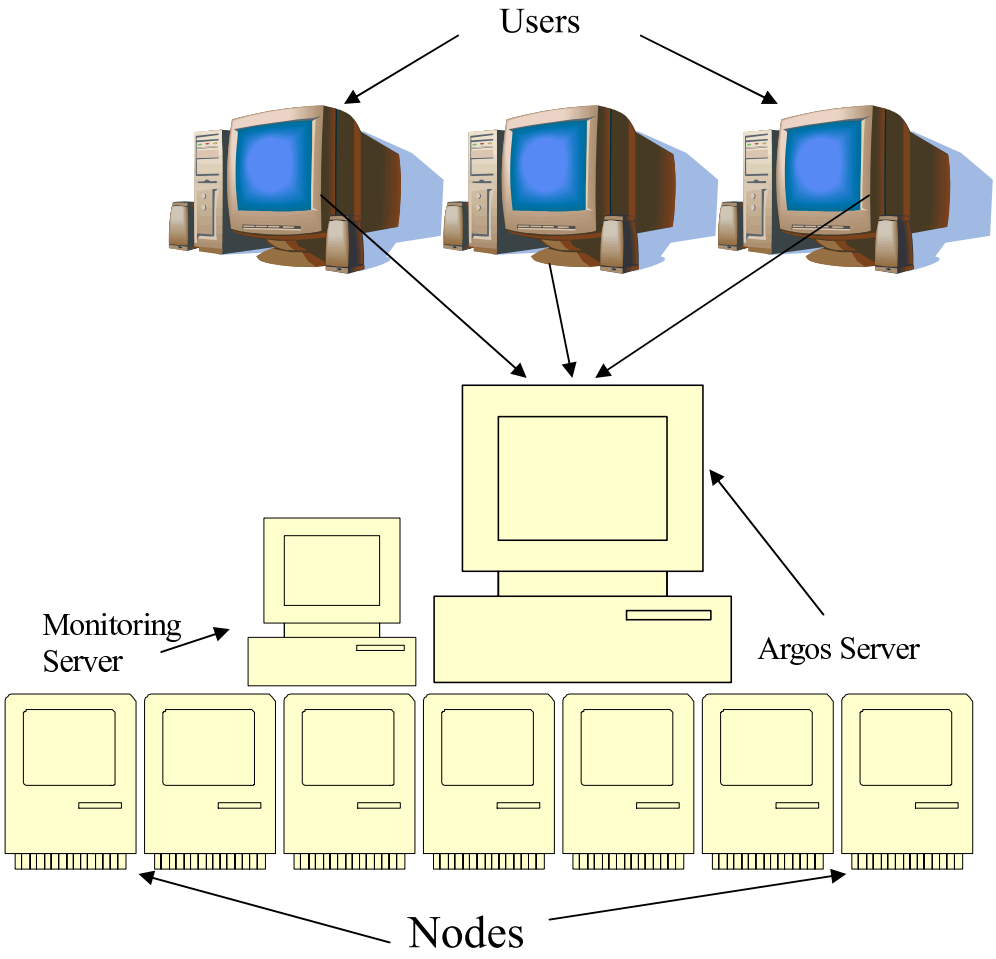

Figure 3.1: Schematic view of Cluster Argos

nodes slower finish its processes, so efficiency depends with the slower node.
Processes non-parallelized: every sent process to each node is independent. The finalization of the simulation will depend with the slower node, but in this case, faster nodes will not have to wait the others.

3.4 Design and optimization of the neutron detector with MCNPX

This section will describe simulation steps in order to find optimal characteristics of neutron detector.
The detector consists on a matrix of polyethylene with a beam hole in the center of the parallelepiped matrix. In order to deliver the radioactive nuclei inside. The beam hole will be surrounded by proportional counters. (See Figure 3.2)

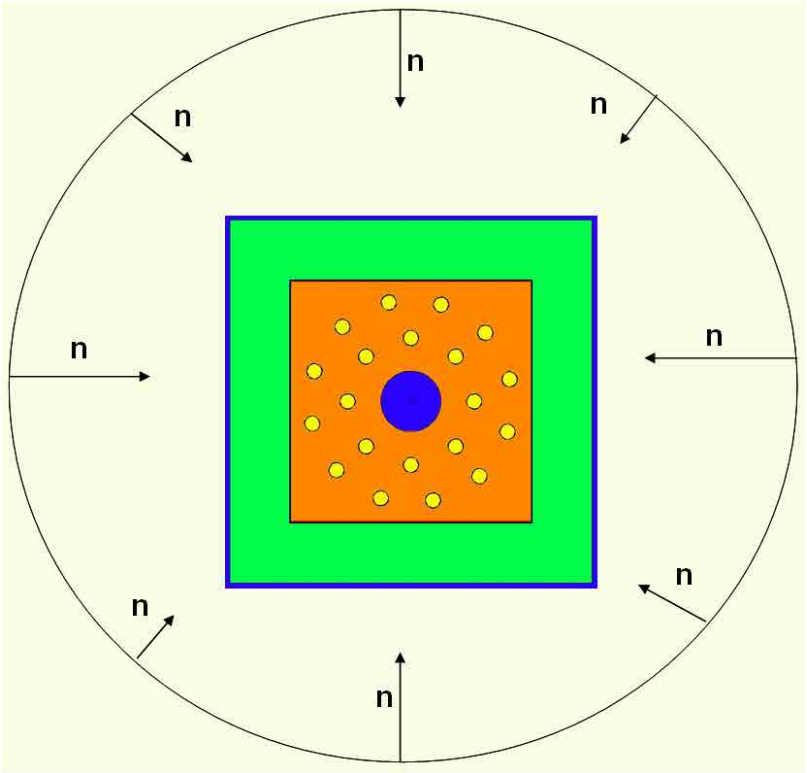

Figure 3.2: View of future neutron detector simulated in MCNPX

The first study consisted in calculation of the neutron propagation time and neutron moderation in the matrix of polyethylene. It is important to find moderation distance of neutrons with different energies at the different periods of moderation time, to define the dimensions of the detector. It is also important to know which part of neutrons will be moderated at different period of moderation time. It will help to have some idea about time correlation

between the β-decay and detection of the neutron from this decay.
After this, next study is the influence of beam hole diameter on neutron propagation distance. This study is important to know moderation distance in the polyethylene and have some idea about the dimensions of the detector. The study about the propagation of neutrons with different moderation time also have influence of the dimensions of the detector.

After defining the dimensions of the matrix of polyethylene is need to do a study of number of counters, its length, gas pressure in order to obtain maximum detection efficiency. Also a study of optimal number of rings of proportional counters was performed. After performing all these previous studies all different combinations of ring radii should be checked in order to obtain a flat efficiency curve for wide energy range of the source. At this work the neutron energy range is from 10 keV to 6 MeV. It was important to find a compromise between cost of the detector and its efficiency.

Other study that was done is the influence of beam hole radii on the neutron propagation inside the polyethylene matrix. The beam hole is used to deliver radioactive nuclei into the center of the detector and it can be also used in order to put additional equipment inside of the detector.
The results obtained let us define the optimal geometry dimensions and structure of the polyethylene matrix. Next step was the choice of the optimal number of counter rings surrounding the beam hole and number of counters in each ring. In order to simulate all possible combinations of the counters a program on fortran was written. We have simulated by Monte Carlo simulation a large number of different combinations of number of counters and their position in the matrix in order to find the optimal structure of the detector. The main objective in this study was to have efficiency plot as flat as possible for working range of energies (from 0.01 MeV to 6 MeV).
Once obtained the geometry a shielding study was done. It was studied the need of a shielding and its composition and dimensions. This shielding is used to protect the detector from background neutrons. These neutrons can be cosmic neutrons or neutrons from the experiment facility.
Once defined the optimal dimensions, optimal number of counters and counter rings, composition and dimension of the shielding, neutron propagation time inside of the detector was studied in order to have an idea about measure time and time correlation between the β-decay and neutron detection at the experiment.
In the following section have shown the simulations done, in order to find optimal properties described above. Firstly, some preliminary tests were done. An "infinite" matrix of polyethylene was taken for this study. The real dimensions of this matrix was 400x400x400 cm^3. The neutron point source was placed in the center of the matrix.

3.5 Neutron moderation and propagation analysis

The aim of this analysis is to find the distance length where the neutron moderates from the energy of neutron source to thermal energy (0.025 eV) in the matrix of polyethylene. Neutrons must be moderated to thermal energies because the cross-section of the reaction for the neutron detection is higher with lower energy (See Figure 3.3).

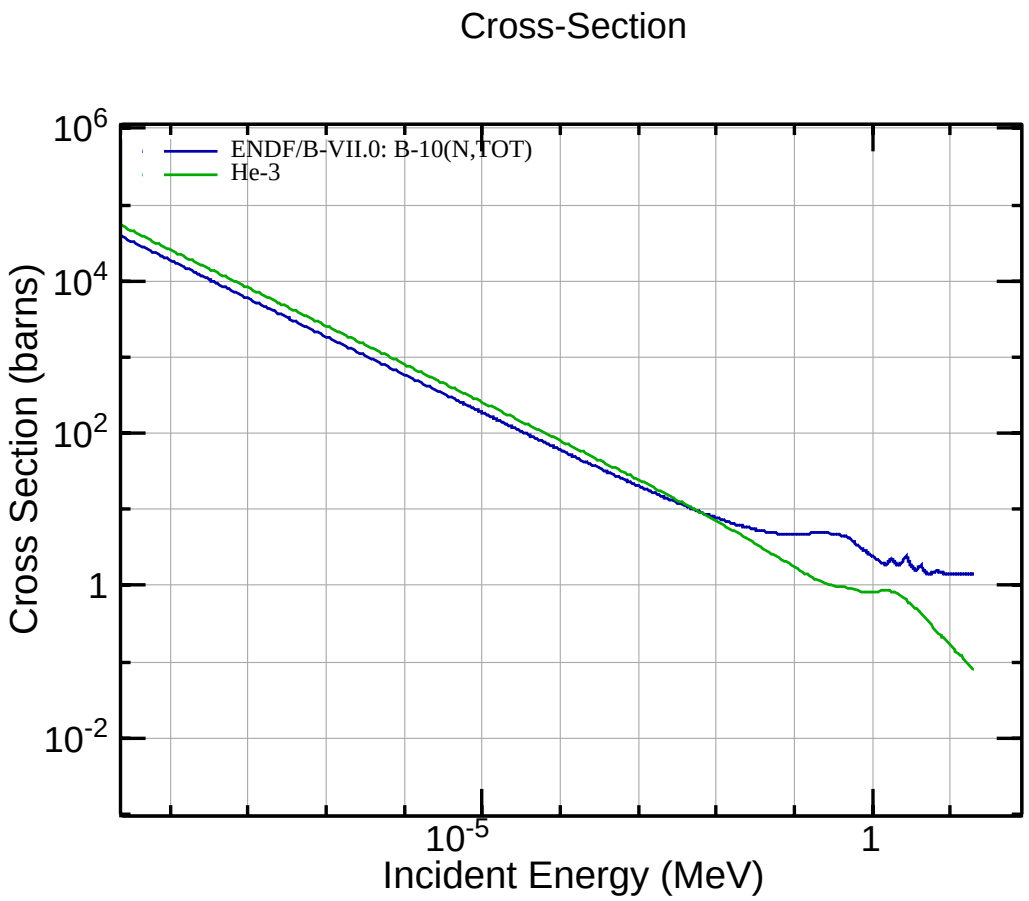

Figure 3.3: Cross-section of the reaction of neutron with ^{3}He and BF_3

In this simulation a matrix of polyethylene was studied to find the optimal dimensions of future neutron detector prototype and moderation distance of neutrons at the different period of moderation time. The dimensions of the matrix were 400x400x400 cm^3 which was considered as an "infinite" matrix for this simulation. The neutron point source was placed in the center of the polyethylene matrix.

The neutron energies, of the point source were set to 1 eV, 1 keV, 5 MeV, and 10 MeV to study the moderation time and perform the propagation analysis. The simulation was made for 10 μs, 50 μs, 100 μs, 150 μs, 200 μs moderation time and for an infinite time. Infinite time in this simulation is considered the time elapsed between the emission of a neutron from the source to its capture or lose. This times were taken from reference [4]. The number of neutrons emitted from the source in each simulation were 10^5. This value is enough to see the neutron propagation and could not be increased because the simulation time in this case increases too much. For the simulations the mesh tally with tally cell of 2 cm was used. Decreasing the tally cell till 1 cm produced error in executing the simulation because the resources of simulation equipment did not permit to simulate with small tally. Since cross section for neutron detection is higher for thermal energies (see Figure 3.3), a condition is applied in the simulation to observe only neutrons with energy range from 0 till 10^{-7} MeV.

The distribution of fluence for neutrons of energy range from 0 to 10^{-7} MeV for the different moderation time is shown on Figure 3.4. For a source with neutron energies of 1 eV with 10 μs and 50 μs moderation time we do not observe thermal neutrons in the polyethylene matrix. All neutrons are moderated and captured at the distance of propagation of neutrons of less than 40 cm from the source. The cube of polyethylene is cut through the center like shown on the figure 3.4 with dotted line. In order to compare the data, the number of neutrons is normalized. These data are repeated on Figure 3.5. This figure shows the moderation distance from the neutron source in the matrix of polyethylene. In this figure the moderation distance is defined as the distance where 90 % of issued neutrons are moderated. On the Table 3.3 is shown percent of neutrons which have the energy from 0 till 10^{-7} MeV during the moderation time. This value has been calculated for all volume of the polyethylene matrix. To obtain these values next condition in MCNPX is used:

cut:N 1000 1e-7 0 0 0

- 1000 is time cutoff in shakes. 1 shake is 10^{-8} seconds;
- 1e-7 is minimum energy cutoff in MeV. 10^{-7} MeV in this case

The output file generates a summary with information about the simulation results. This data is shown on Table 3.1 for the conditions presented above. In this table in the first column

neutron loss	weight
escape	0
energy cutoff	9.69E-01
time cutoff	1.56E-02
capture	1.46E-02
total	1.00E+00

Table 3.1: Problem summary in output file. Source energy 1 eV, time cut off 10 μs.

possible ways of neutron loosing are described. And the second one indicates a probability of the event. Bellow is presented description of each possible event:

- **Escape.** When a neutron goes out of the universe volume.
- **Energy cutoff.** When the energy of a neutron is below a set limit. This line is the most important to find moderated neutrons at energies lower than 0.025 eV.
- **Time cutoff.** This is franction of neutrons which have not escaped, have not captured and have not reached the energy limit during 10^{-5} seconds.
- **Capture.** Shows a number of captured neutrons in all the volume of universe.

Table 3.2 shows the distance oat which 90 % of the neutrons emitted from the source are moderated. These values was calculated analyzing the output files generated by the MCNPX simulation for the conditions were the source energy and propagation time. We obtained in total of 25 output files. In order to analyze them a program on fortran was written. The

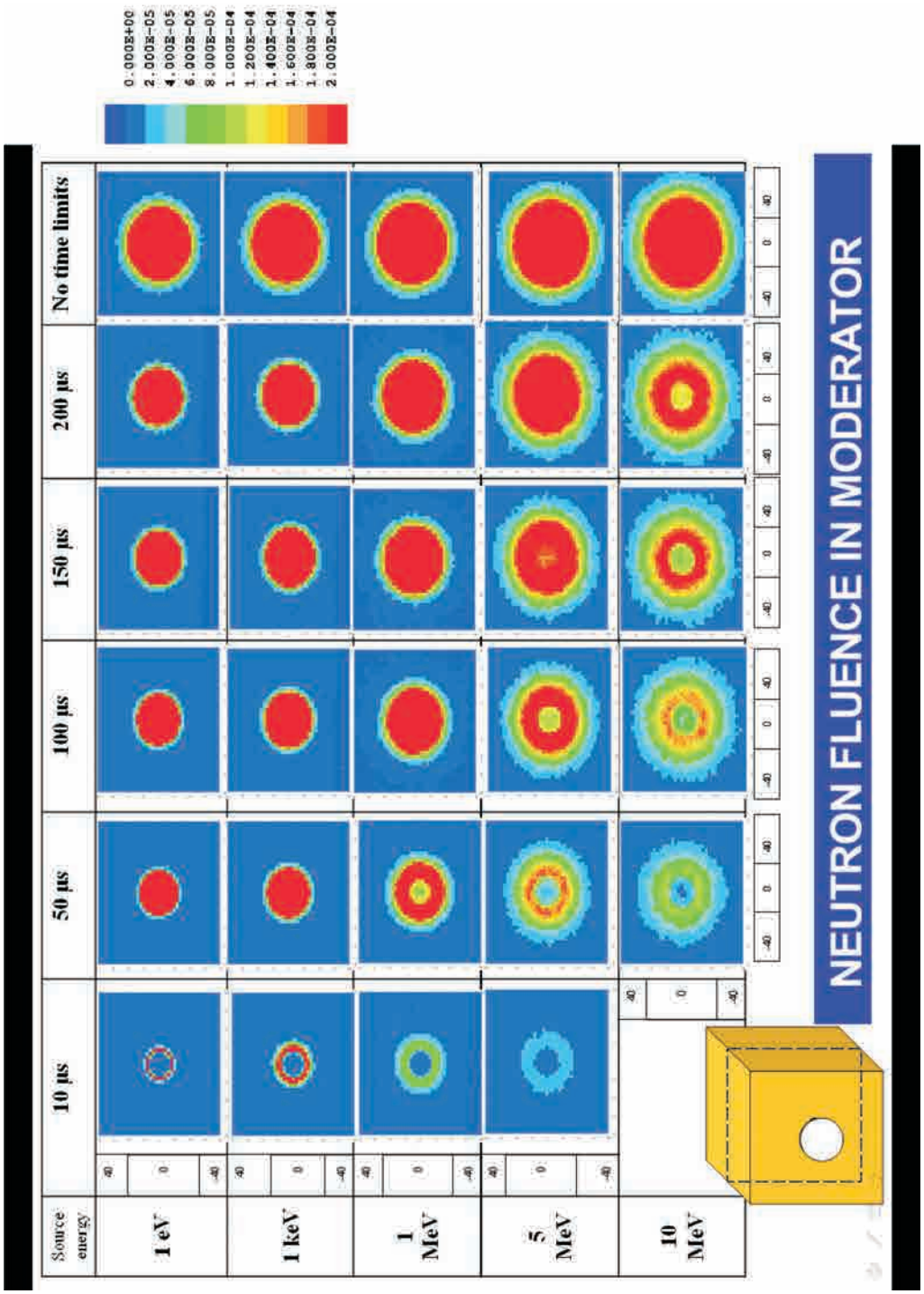

Figure 3.4: Neutron fluence in the moderator

Neutron source energy	**10 μs**	**50 μs**	**100 μs**	**150 μs**	**200 μs**
1 eV	3 cm	6 cm	7 cm	8 cm	9 cm
1 keV	7 cm	8 cm	9 cm	10 cm	11 cm
1 MeV	13 cm	14 cm	15 cm	15 cm	16 cm
5 MeV	28 cm	28 cm	29 cm	29 cm	29 cm
10 MeV	38 cm	39 cm	39 cm	39 cm	39 cm

Table 3.2: Distance from the center where 90% of all the neutrons are moderated

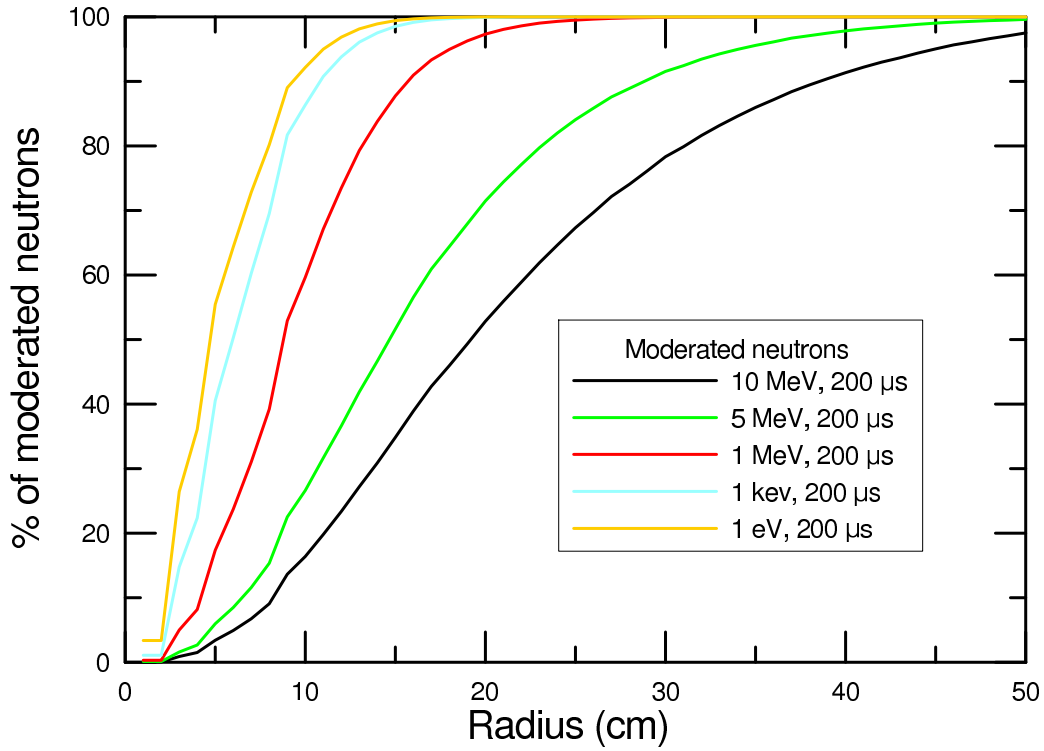

Figure 3.5: Propagation distance for different neutron energies and 200 μs moderation time

Neutron Source Energy	**Max. Moderation time**	
	10 μs	**100 μs**
1 eV	96.9 %	98.0 %
1 keV	96.2 %	98.2 %
1 MeV	96.2 %	98.3 %
5 MeV	94.9 %	97.0 %
10 MeV	87.1 %	89.0 %

Table 3.3: Value in % of neutrons with energy from 0 till 10^{-7} MeV.

program calculated the number of neutrons in total volume of the moderator and number of neutrons in the sphere around the source. The radius of the sphere increased from 0 cm to "infinite". A condition applied to the sphere was to contain 90 % of all the moderated neutrons in the volume. This condition is shown on equation 3.1 where N_i is the number of neutrons inside the sphere and N_{total} is the number of neutrons emitted by the source.

$$\sum N_i / \sum N_{total} \geq 0.9 \tag{3.1}$$

The radii of these spheres are presented on the table 3.2. As it can be observed the most of the neutrons in moderator are moderated in a radius less than 40 cm from the source. The value of 40 cm was taken here as a reference. The 90% of neutrons emitted with an energy of 10 MeV and propagation time 200μs moderates at this distance. For a source of neutron energies less than 1 MeV the best place to detect neutrons in moderator is less than 10 cm from the source. And for a source of energies more than 1 MeV the best place to detect neutrons in moderator is less than 15 cm from the source. The main part of all neutrons is moderated during the 10 μs, but the distance from the source is too small and it is not possible to place proportional counters in order to detect the neutrons. In order to increase the distance from the source it would be better to detect the neutrons with moderation time more than 100 μs for energies up to 1 MeV and more than 50 μs for energies large than 1 MeV

3.6 Analysis of beam hole radii

The beam hole radii have an influence on the maximum distance (from the center of detector) at which neutrons are moderated. Also an increase of the beam hole radii implies an increase of dimensions and weight of polyethylene matrix. This is the reason to reduce the beam hole as small as possible, taking in account that inside it, additional equipment will be placed. In order to evaluate the effect of beam hole radii the simulation was done with two kinds of neutron source located inside the beam hole at the center of the polyethylene matrix.

The neutron sources were point sources and non-point ones. The non-point neutron source had dimensions 8x8x4 cm^3. The study of the influence of non-point source is important for future detector because of possible geometry of the target will be a matrix of silicon detectors.

As in the previous section a matrix of polyethylene with dimensions 400x400x400 cm^3 was used and we consider this matrix as an "infinite" one with a beam hole in the center (see Figure 3.6). Neutron source was put in the center of the matrix.

A moderation time of 200x10^{-6} seconds was used for the simulations and the number of neutrons emitted by the neutrons source were 10^6. The neutron energy was set set to 1 MeV For this simulation mesh tally with range from -100 cm to 100 cm for each axis with tally cell 2 cm was used. Mesh tally divided all the cube into many small cubes with dimensions 2x2x2 cm^3 to see the neutron propagation. In order to see influence of non-point neutron source the simulation was repeated for neutron source with dimensions 4x8x4 cm^3. The results of thermal neutron propagation in the polyethylene matrix for point and non-point

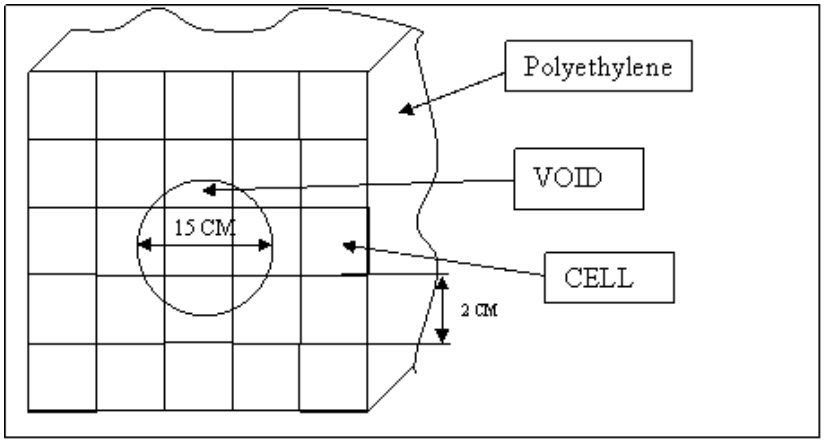

Figure 3.6: Schematic view of polyethylene matrix and its division in cells in order to study neutron propagation.

neutron source are presented on Figure 3.7 These values was calculated by analyzing the output file from simulation with different conditions (beam hole radius and geometry form of the source). In order to analyze the output files an analyzing program on fortran was written. The analyzing procedure was

- **The program calculated the number of neutrons in total volume of the moderator**
- **This number was considered as a 100% of the neutrons.**
- **The program set a cylinder around the beam hole.**
- **The program calculated the number of neutrons inside the cylinder.**
- **The next step was a calculation of percentage of neutrons inside the cylinder related to the neutrons in total volume.**
- **If the number of neutrons inside the cylinder was less than 90% the program increased the cylinder radius and repeated the calculation.**
- **In case of reaching 90% of the neutrons the program stopped and recorded the cylinder radius**

A conclusion of this study is that the moderation distance increases with the increase of the beam hole radius. See Figure 3.8. The results are the same for two geometries of neutron source. The maximum moderation distance for the beam hole diameter of 10 cm is less than 20 cm. Increasing the beam hole diameter till 40 cm the moderation distance increases till 45 cm. The results show that for both neutron sources (point source and extended one) the neutron moderation is similar for beam hole diameters less than 30 cm. For beam hole diameters greater than 30 cm the moderation distance for point source is less than extended source, but the difference is not sufficient. The beam hole diameter will be less than 20 cm. This diameter will be enough to install additional equipment inside the detector. As the

Cylinder Diameter (cm)	Point source	Non point source
10	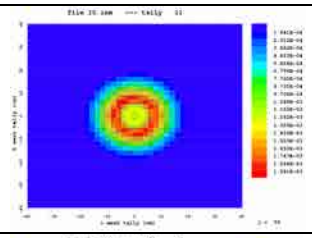	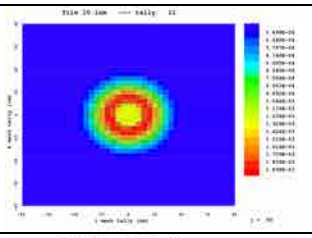
15	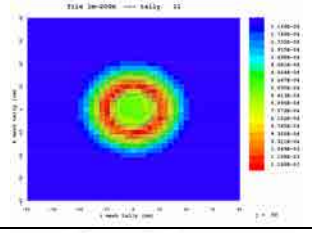	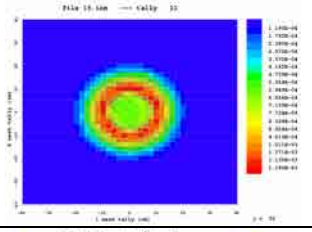
20	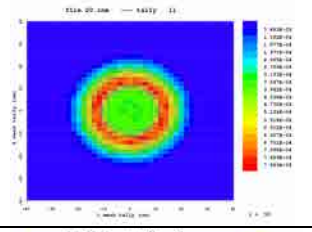	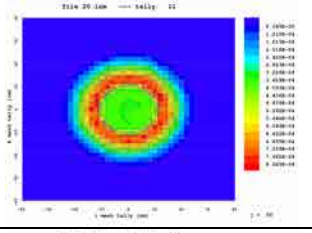
25	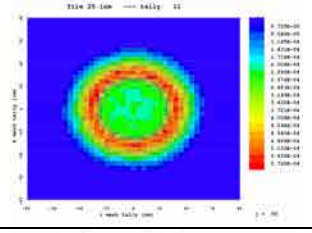	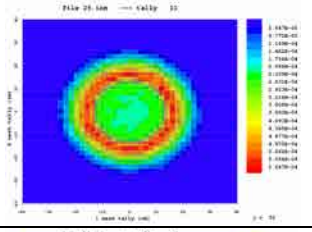
30	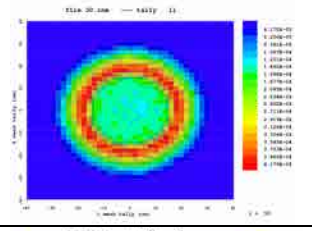	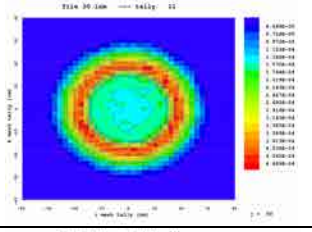
35	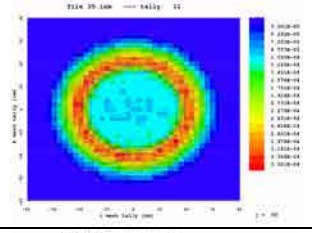	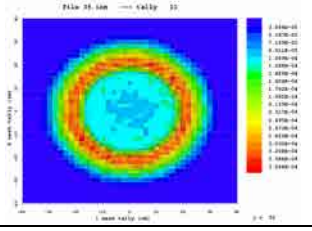
40	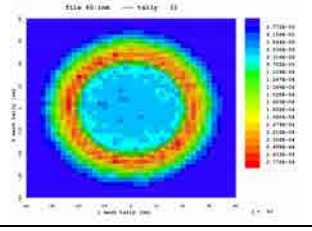	**N.D.**

Table 1 Summary of thermal neutron flux

Figure 3.7: Maximum of neutron propagation distance to see 90% of neutrons moderated related to the beam hole diameter

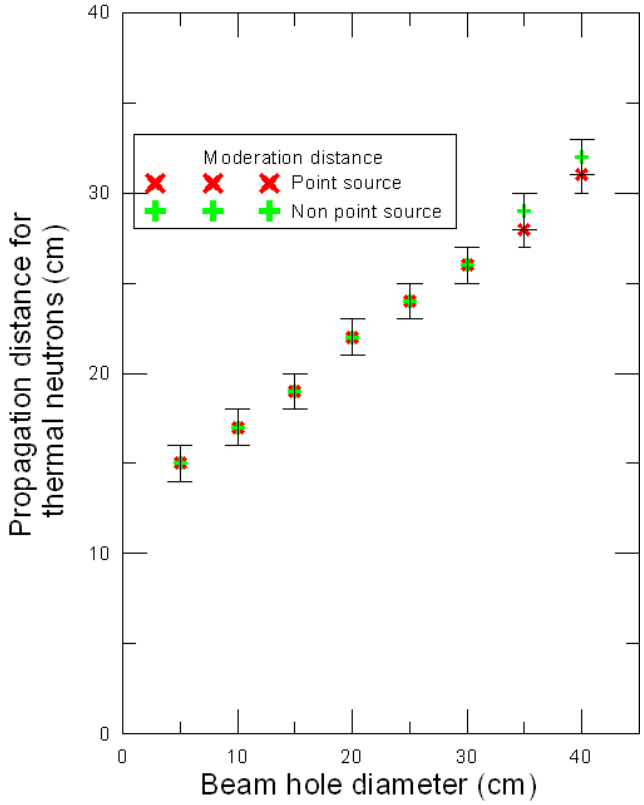

Figure 3.8: Sphere radii, centered at polyethylene matrix center, which contains 90% of moderated neutrons

diameter of beam hole is less than 30 cm we can avoid the influence of non-point (extended) neutron source. According to this simulation it is possible to use a point neutron source for future simulation of this detector.

3.7 Optimization of design parameters

This section will describe the simulation in order to obtain optimal number of counters, number of rings, the length of counters and gas pressure for future detector. These data will help to obtain the high efficiency and efficiency curve as flat as possible.

3.7.1 Number of counters

Next study was made to define number of counters in order to make the detector with high detection efficiency and to use each counter of the detector as efficient as possible. For polyethylene matrix with beam hole diameter 16 cm, neutron point source with energy 1 MeV and infinite propagation time, we did many simulations with different number of counters placed around the beam hole. These counters were placed in a position inside the matrix in order to obtain maximum efficiency. All the counters were placed in one ring around the beam hole. After this test in order to check other geometries these counters were placed in two rings around the beam hole (See Figure 3.9). We can see the efficiency of the setup with two rings of proportional counters increases. The results of this simulation can be observed on Figure 3.10. These data explain a combination of the counters. Horizontal axis shows a total number of counters surrounding the beam hole. Example of combinations of the counters in the rings is shown on table 3.4. The efficiency in this simulation is considered as number of reactions inside the proportional counters divided by the number of neutrons emitted from the source and is calculated as:

$$\eta = \frac{N_{det}}{N_{source}} \tag{3.2}$$

Where N_{det} is a number of detected neutrons and N_{source} is a number of neutrons emitted by the source. Crosses (see Figure 3.10) are referred to all counters are located in an unique ring. The efficiency plot begins to be flat with number of counters more than 18. Other cases were studied in order to distribute the counters to the other rings. There were studied cases for 8, 12 and 16 proportional counters in the first ring and all the rest counters were placed in the second ring. The efficiency curve grows if the number of rings are two. If there are 8 or 12 counters in the first ring and total number of counters are 20 the efficiency is the same and it is higher if put 16 counters in the first ring. This figure confirms that it should be used two counter rings. The number of counters in the first ring should be 8 and in the second one 12 counters. The first conclusions of the simulation are:

- **Number of counters: 20;**
- **This counters should form two rings;**

- **The first ring (ring A) should contain 8 counters and the second ring (ring B) should contain 12 counters.**

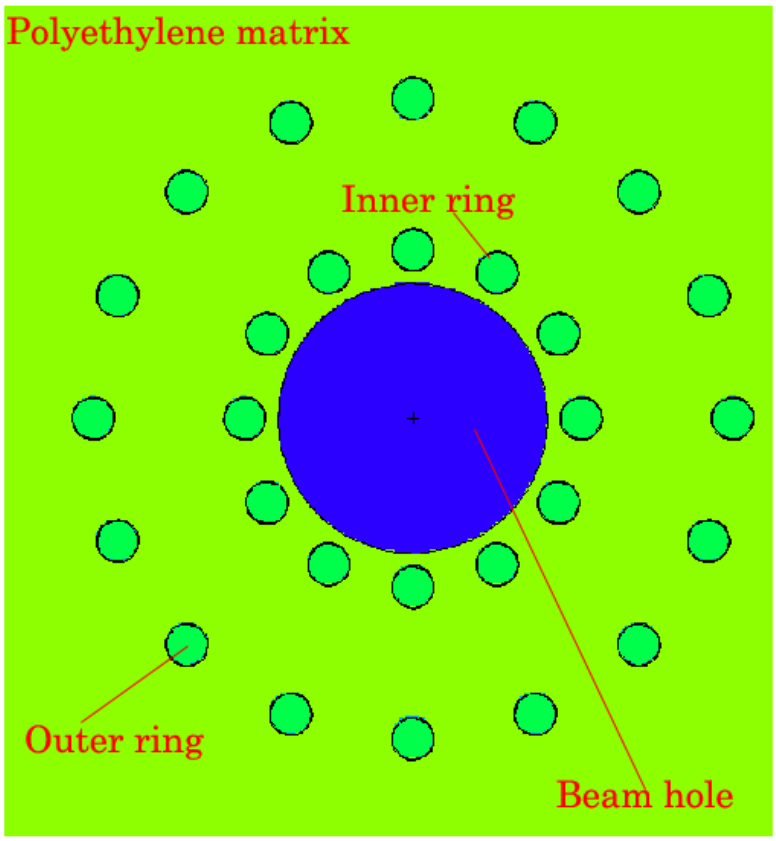

Figure 3.9: Example of the proportional counters distribution around the beam hole inside the polyethylene matrix. Inner ring is labeled as "A" and the outer ring is labeled as "B"

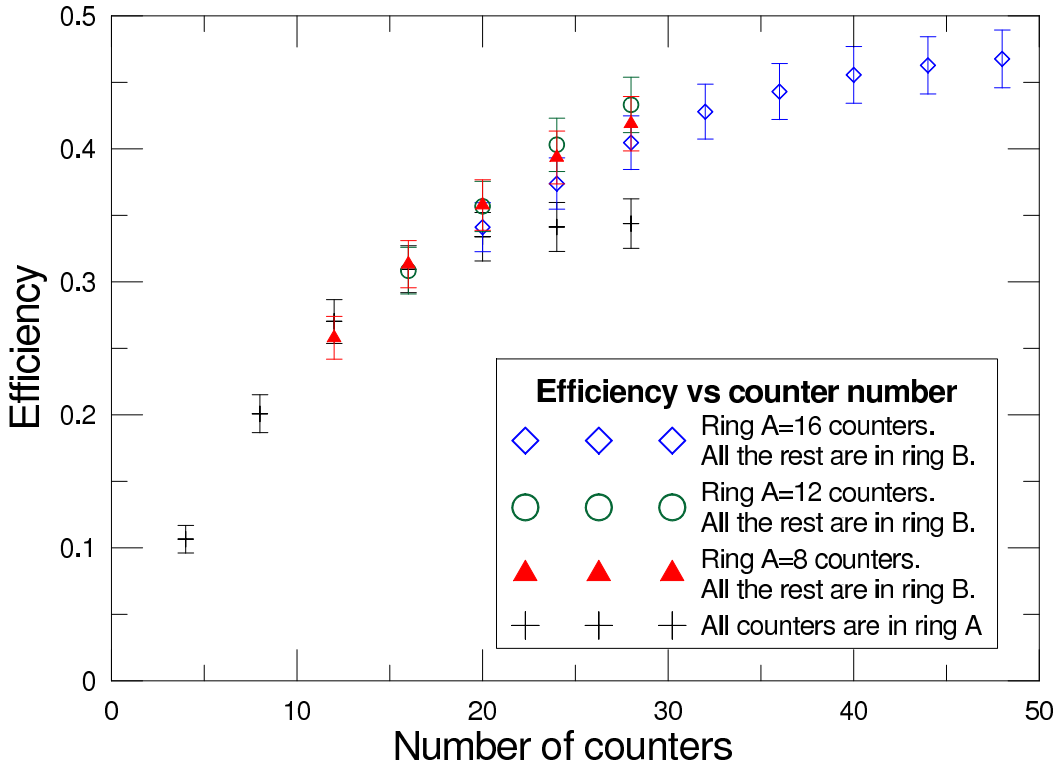

Figure 3.10: Dependency of detection efficiency as a function of total number of counters placed in one ring configuration and two rings configurations. This figure was obtained for source energy = 1 MeV and infinite propagation time.

Ring A	**Ring B**	**Total**
20	0	20
8	12	20
12	8	20
16	4	20

Table 3.4: Example of counters distribution in the rings. This example is showed for 20 counters

3.7.2 Length of counters

In order to find optimal length of counters next study was done. Inside the matrix of polyethylene all counters were placed to obtain maximum efficiency. The source energy was set to 1 MeV and infinite neutron propagation time. We simulated 30 cm, 40 cm, 50 cm, 60 cm and 70 cm of effective length of the proportional counters. The side view of the simulation setup can be observed on figure 3.11

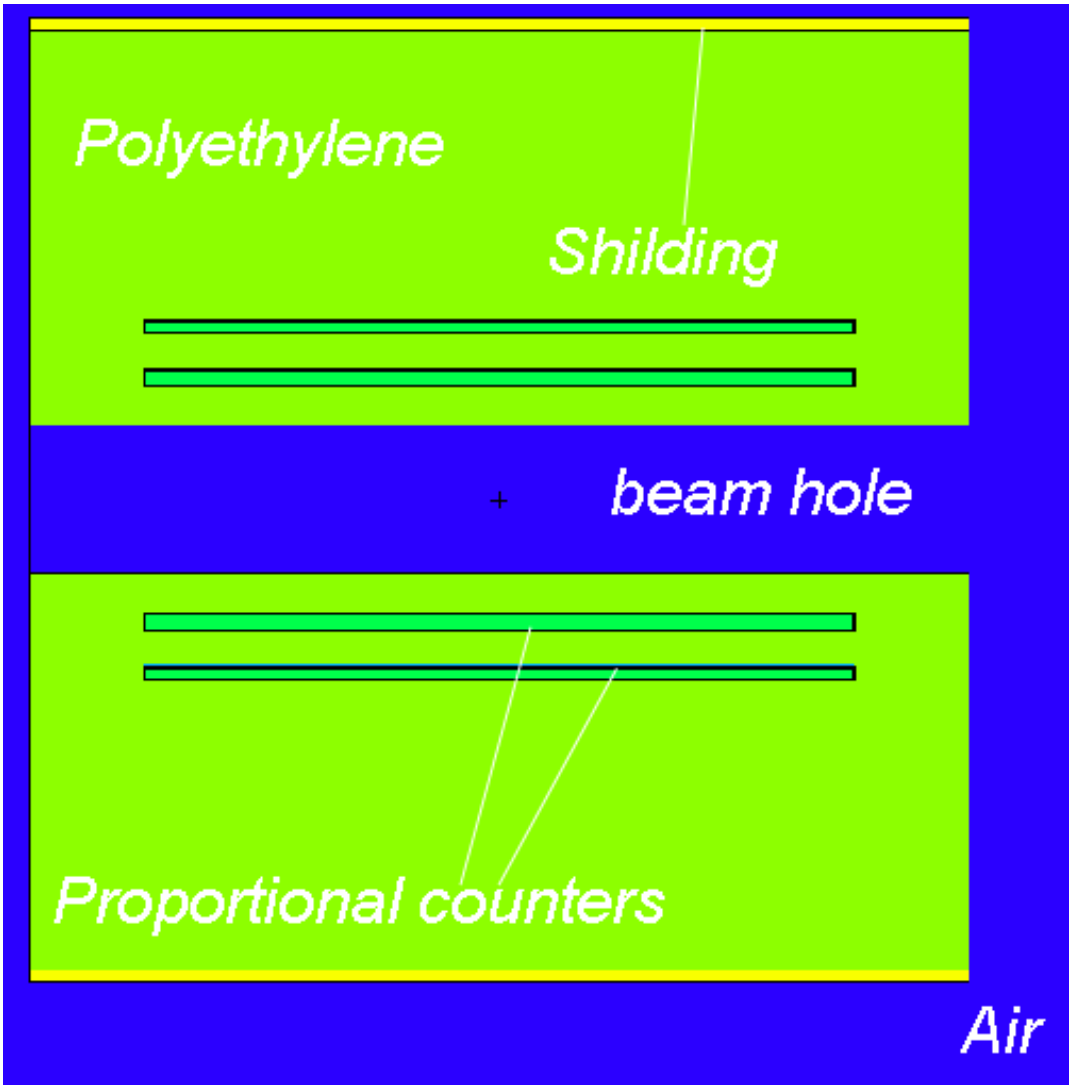

Figure 3.11: Side view of simulation setup with proportional counters

The efficiency curve as a function length of counters is presented on Figure 3.12

The gain of efficiency between lengths of 50 cm and 60 cm is about 2%, but the gain between lengths of 60 cm and 70 cm is about 1%. The efficiency curve begins to be flat with length of 60 cm and each additional 10 cm of length increase the total efficiency on less than 1%. The compromise between length of counters and contribution in the total efficiency should

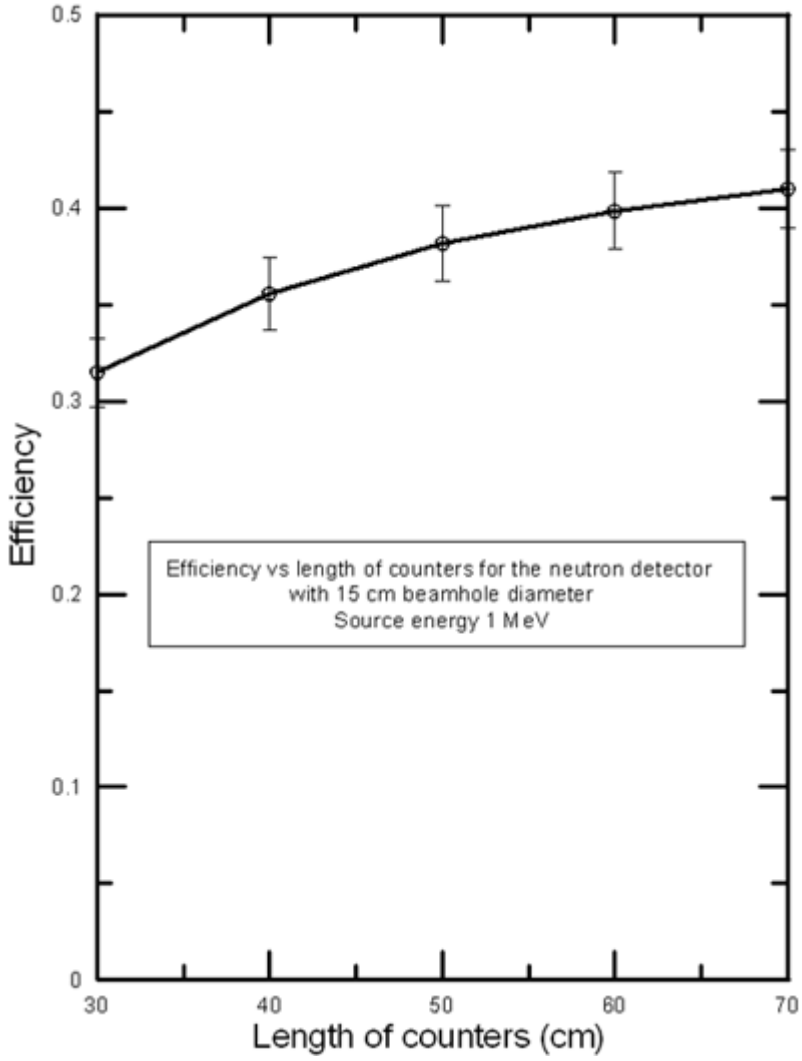

Figure 3.12: Dependency of detection efficiency as a function of length of counters

be found on 60 cm of effective length of counters. The conclusion of the simulation is:

- **Effective length of counters is 60 cm.**

3.7.3 Gas pressure

During this simulation a study of gas pressure was done. The counters were placed in the same position like in previous section and the gas pressure of 15200, 11400, 7600, 3800 torr (aprox. 20, 15, 10 and 5 bar) was simulated. This values of pressure was taken from technical characteristics of proportional counters manufactured by LND Inc. The energy of the source was set to 1 MeV and propagation time was set to infinite. The results can be observed on table 3.5.

Gas pressure (torr)	Efficiency %
3800 torr (5 bar)	23.6 %
7600 torr (10 bar)	27.3 %
11400 torr (15 bar)	28.7 %
15200 torr (20 bar)	29.4 %

Table 3.5: Detection efficiency for different pressure of the detection gas ^{3}He in the proportional counters.

The higher detection efficiency provide the highest pressure of the detecion gas. The proportional counters with highest detection gas pressure were chosen for the following simulation and detector constraction.

- **Detecting gas pressure of 15200 torr (aprox. 20 bar) was chosen.**

3.8 Optimal geometry choice

3.8.1 Ring radii

This section describes a way to find an optimal detector geometry. According to the data obtained in previous simulations the neutron detector is made with 20 proportional counters shared in two rings around the beam hole. The inner ring contains 8 proportional counters and the outer ring contains 12 proportional counters. The effective length of this counters is 60 cm and the detection gas pressure 15200 torr (aprox. 20 bar). The matrix of polyethylene have a centered beam hole of 10 cm in diameter. The dimensions of the beam hole allows to deliver radioactive nuclei inside the detector and the installation of additional equipment for the detection of β particles emitted by impacted nuclei. The aim of the simulation was to find the radii of the counters ring in order to have efficiency curve as flat as possible for wide neutron energy range.

The flat efficiency related with neutron energy is important to reduce the uncertainty of neutron emission ratio for the studied nuclei. The information about neutron energy is lost during the neutron moderation in the polyethylene matrix, a flat neutron detection efficiency avoids to know this neutron energy due the probability of neutron detection will be the same for all neutron energies. Taking in account the nuclei we will measure, the neutron detection efficiency has to be flat for a neutron energy range from 0.01 MeV to 6 MeV.

In order to parameterize the neutron detection efficiency planarity it has been defined the

"Efficiency factor", (F). This factor is a relation of maximum and minimum efficiencies for the neutron source energies in the region of interest (ROI). It is described with equation 3.3 where η_{max} is the maximum efficiency and η_{min} is the minimum efficiency on the ROI of neutron energy. The objective is an efficiency factor to be close to the unit ($F = 1$).

$$F = \frac{\eta_{max}}{\eta_{min}} \tag{3.3}$$

The mean efficiency $\overline{\eta}$ was calculated according to equation 3.4

$$\overline{\eta} = \frac{1}{E_1 - E_0} \int_{E_0}^{E_1} \eta(E) dE \tag{3.4}$$

Where E_0 is minimum energy in the ROI, E_1 is a maximum energy in the ROI.

The proportional counters simulated were manufactured by LND Inc with ^{3}He as a detection gas; their main specifications are presented on Table 3.6. The counters are placed in two rings around the beam hole in the matrix of polyethylene.

Counter	Gas	Maximum length (mm)	Effective length (mm)	Maximum diameter (mm)	Effective diameter (mm)	Gas pressure (torr)	Cathode material
2527 LND inc	^{3}He	686.84	604.8	25.4	24.38	15200	Stainless Steel

Table 3.6: General specifications of the ^{3}He proportional counter.

In order to generate input files for MCNPX with all possible combinations of counter ring radii a program on fortran was written. This program generated input files for MCNPX with different combinations for ring radii and different neutron source energies. The minimum and maximum radii of the inner ring were set from 8 cm to 15 cm respectively and for the outer ring the minimum and maximum radii were set from 15 cm to 22 cm respectively. The increment step of each radius was 1 cm. For these radii combinations and a neutron point source with energies 0.01 MeV, 0.1 MeV, 1 MeV, 2 MeV, 4 MeV, 6 MeV and 10 MeV was placed in the center of the beam hole. The were generated 504 input files for the simulation. The running on the cluster ARGOS of all these files generated 504 output files for all combinations of radii and energies.

In order to analyze the output files from MCNPX simulations it was developed a new fortran code which read the basic information from the output files. The aim of this code was to calculate the neutron detection efficiency for all of the geometries simulated in order to find the optimal geometry which has a compromise with the flattest and highest neutron detection efficiency for the neutron energy range shown above. The example of some neutron detection efficiency curves simulated can be observed on Figure 3.13 and Figure 3.14. These figures present neutron detection efficiency curves for some combinations of inner and outer ring radii. As can be seen in Figure 3.13 an increase of the inner ring radius reduces the efficiency for energies less than 1 MeV. For neutron energies greater than 1 MeV, the value of the inner ring radius has low influence to the neutron detection efficiency. That means if we want to

increase the neutron detection efficiency at low neutron energies the inner ring should be set as close as possible to the beam hole. On the other hand, as can be seen in Figure 3.14, the neutron detection efficiency has a maximum for a neutron energy depending on the radius of the outer ring. The neutron energy where maximum is seen, increases according to the outer ring radius increment, but the neutron detection detection efficiency reduces. This result means that to flatten the neutron detection efficiency we have to combine the radii of both rings.

Analyzing all the combinations of both ring radii, the optimal configuration is inner ring radius equal to 11 cm because this radius gives high and flat neutron detection efficiency for the low energy range (See Figure 3.13). To define the optimal outer ring radius has been used the efficiency factor (F) defined above. According to the cases of Figure 3.16 the efficiency factors (See equation 3.3) were calculated for two neutron energy ranges. One range (reduced range) is from 0.01 MeV to 1 Mev and the other (full range) is from 0.01 MeV to 6 MeV. The values of the efficiency factors can be observed on table 3.7 and table 3.8 respectively. In case of full energy range the smallest value of the efficiency factor is $F = 1.61$ which corresponds to 20 cm of outer ring radii. In case of reduced energy range the smallest value of efficiency factor corresponds to $R = 18$ cm. It was difficult to drill the polyethylene matrix with a radius of 18 cm because the distance between the proportional counters will be very small which implies two problems. The first one is polyethylene damage and the second one is an uncomfortable manage of the counters and its connectors. In order to avoid these problems the final decision was to set the outer ring radius at $R = 20$ cm. This radius was chosen as optimal for the detector construction. According to the Figure 3.17 the value of Efficiency factor (F) is $F = 1.22$ which is the minimum value obtained for energy range from 0.01 MeV to 1 MeV.

In Figure 3.15 is shown the total neutron detection efficiency from 0.01 MeV to 6 MeV neutron energies together with neutron detection efficiency related with both rings individually.

Outer ring radii (cm)	Efficiency Factor
22 cm	1.7
21 cm	1.64
20 cm	1.61
19 cm	1.68
18 cm	1.65
17 cm	1.78
16 cm	1.87
15 cm	1.98

Table 3.7: Efficiency factor for all energy range at inner ring radius r=11 cm

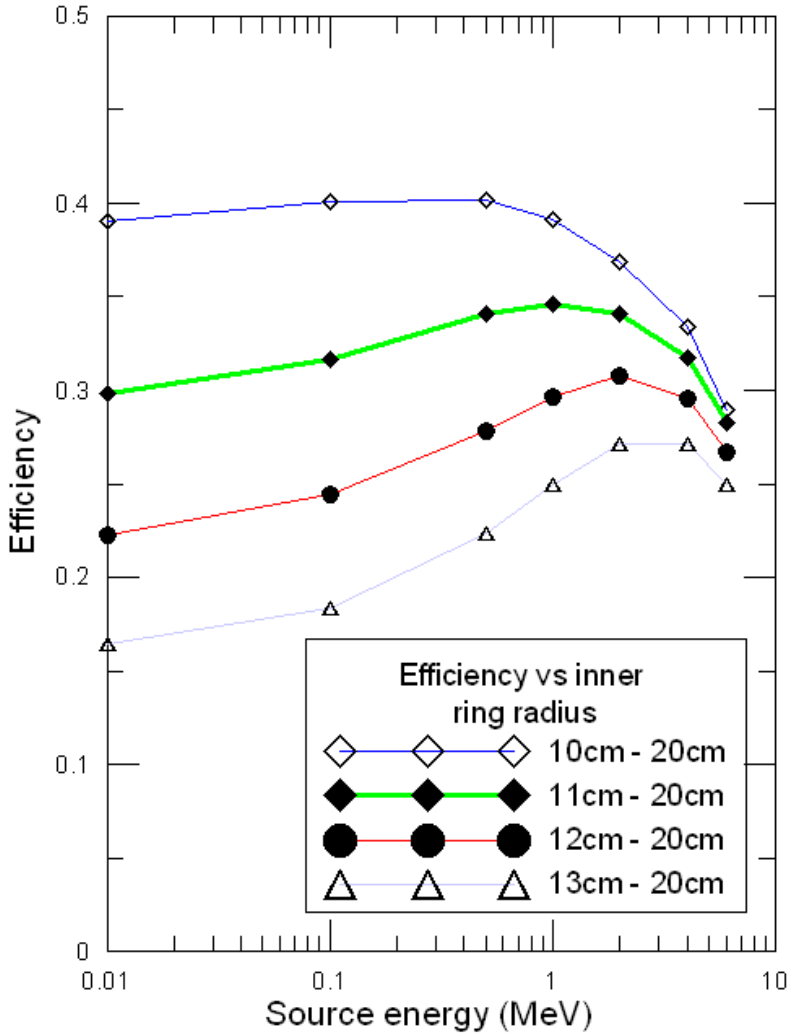

Figure 3.13: Simulated inner ring neutron detection efficiency for different inner ring radii at a fixed outer ring radius of 20 cm

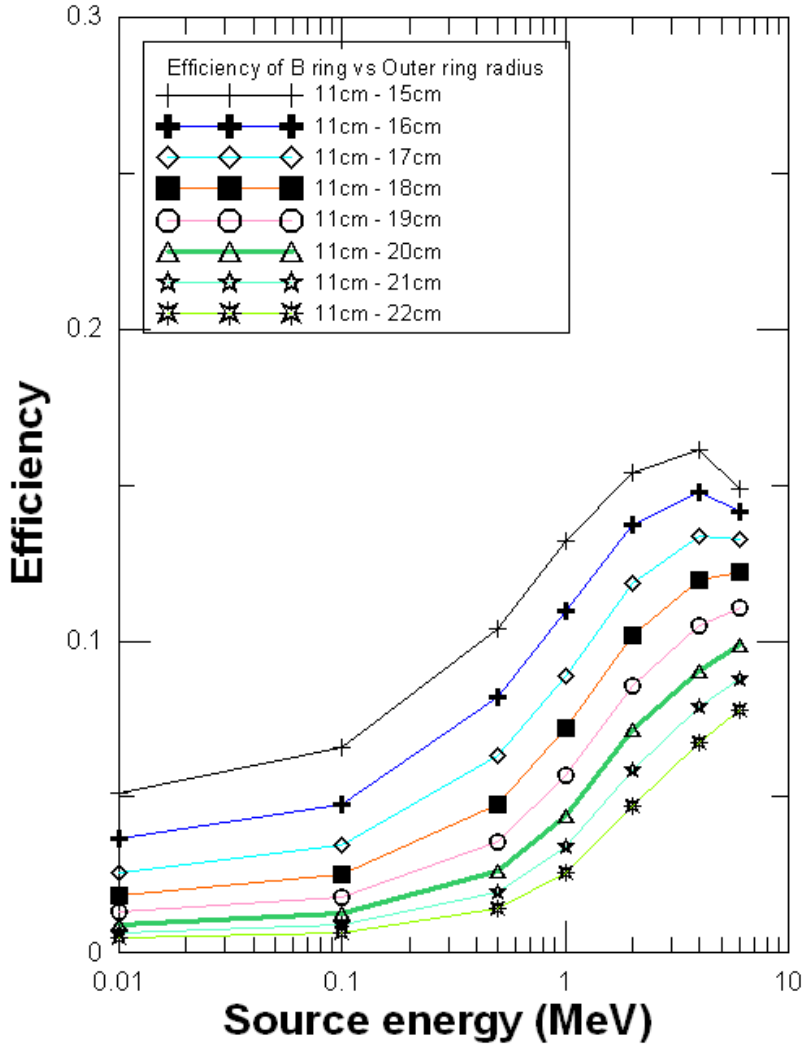

Figure 3.14: Simulated outer ring neutron detection efficiency for different outer ring radii at a fixed inner ring radius of 11 cm

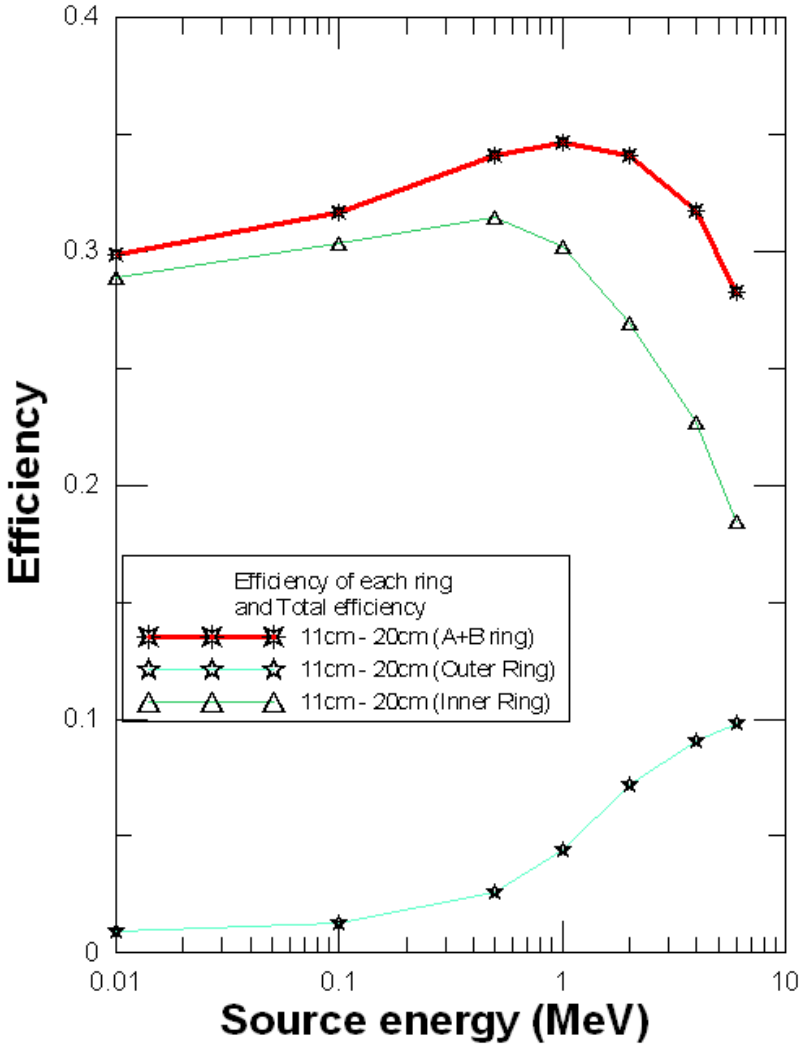

Figure 3.15: Simulated inner ring, outer ring and total neutron detection efficiency for inner ring radius equal to 11 cm and outer ring radius of 20 cm

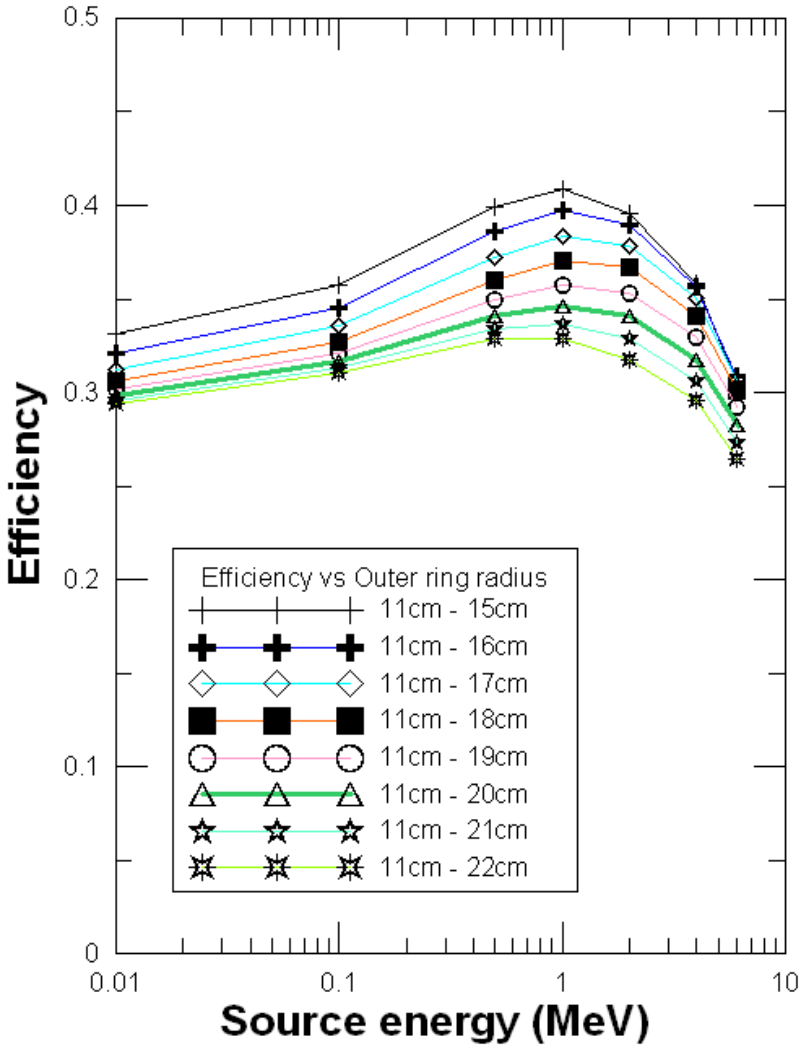

Figure 3.16: Example of efficiency curves from the simulation for different outer ring radii, for inner radius set to 11 cm

Outer ring radii (cm)	Efficiency Factor
22 cm	1.3
21 cm	1.27
20 cm	1.22
19 cm	1.19
18 cm	1.15
17 cm	1.17
16 cm	1.78
15 cm	1.24

Table 3.8: Efficiency factor for energy range from 0.1 Mev to 1 Mev and inner ring radius r=11 cm.

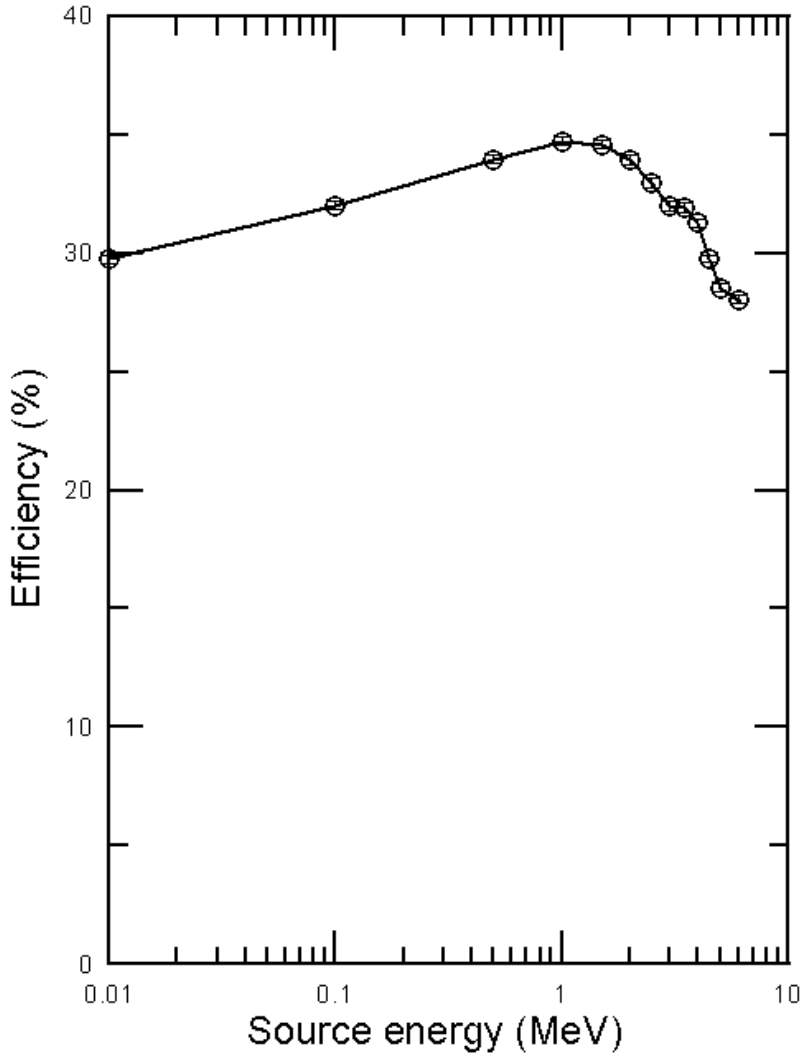

Figure 3.17: Logarithmic plot of efficiency as a function of neutron source energy for final design of the detector. R_H=5 cm, R_A=11 cm, R_B=20 cm

3.8.2 Background and shielding

In order to evaluate the effect of the neutron background and design the neutron shielding, the next mcnpx simulation were done. The simulated optimal geometry was surrounded by a sphere. This sphere simulated background neutron source. It is important to find optimal protection from the background. Background on the experiment can be of two origins. The first one is a cosmic background and the second one is background from the experimental facility such as accelerator. A fraction of cosmic background is attenuated by building structures because walls and roof are thick and made of concrete. The background contribution from the accelerator is not well known including neutron flux and neutron energy spectrum. As the real flux and energies of the background neutrons are unknown, we suppose that it is the same like flux from the radioactive nuclide to be studied.
In order to make background protection the detector was covered with polyethylene shielding on four sides. In this simulation the neutron source was a sphere located outside surrounding the detector. The neutrons of energies 0.01 MeV, 0.1 MeV, 0.5 MeV, 1 MeV, 2 MeV and 5 MeV were emitted inside the sphere (See Figure 3.18). The neutron propagation time for

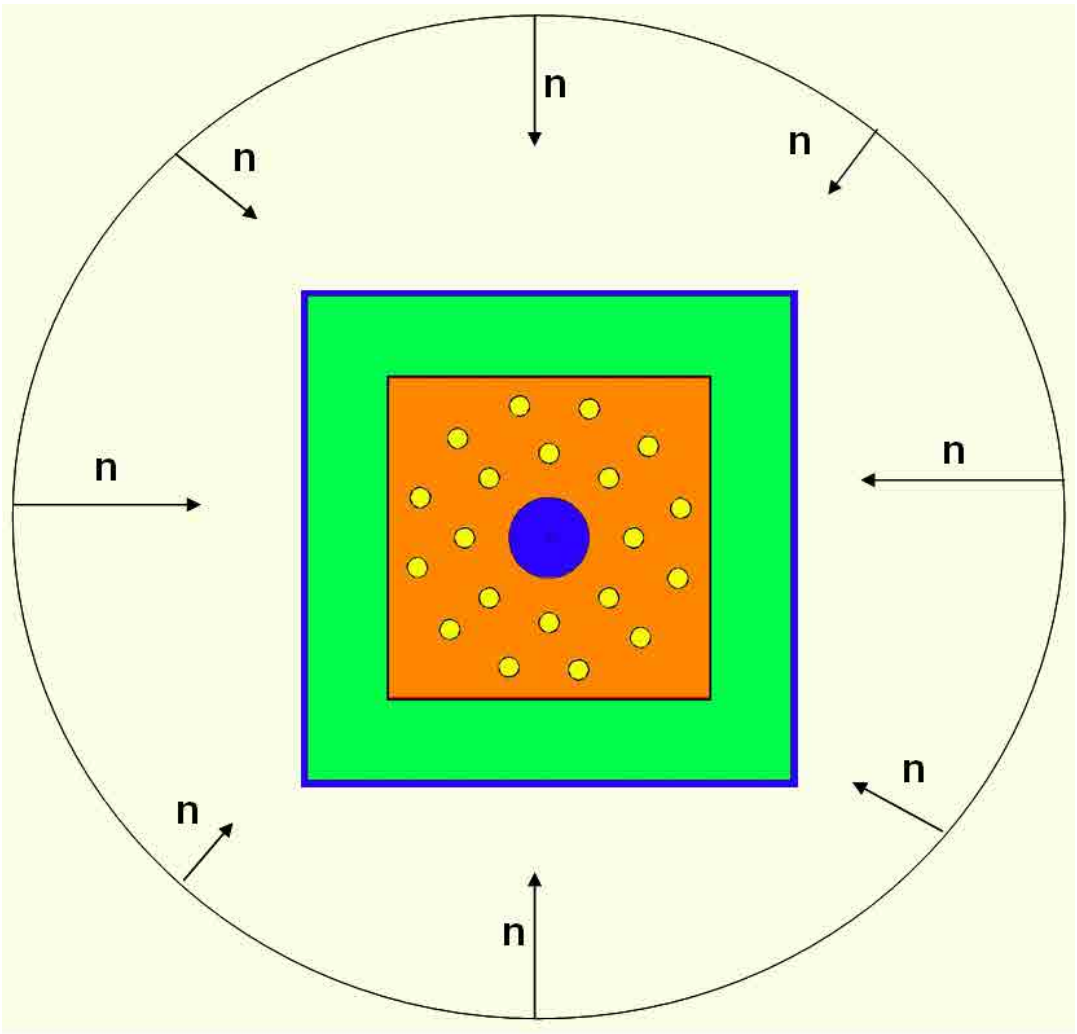

Figure 3.18: Study of background shielding. Sphere is a neutron source for background study.

this simulation was set to infinite. The aim of this simulation was to choose the shielding dimensions and to determine the possibility to use a cadmium layer between matrix of the detector and shielding. Cadmium is usually employed to capture thermal neutrons. In this setup the background shielding will moderate the background neutrons and the cadmium layer will capture them. The neutron can be also captured in the polyethylene. In this case cadmium layer will not make a large contribution in the shielding.
This simulation was made for shielding of 5 cm, 10 cm, 15 cm, 20 cm and repeated for the same shielding, but 0.5 mm of Cd between the shielding and matrix of the detector. The results of the simulation can be observed on Figure 3.19. The background detection efficiency without shielding ranges from 4.5% to 17% depending of the background neutron initial energy. This phenomena make a large uncertainty for neutron detection. But with the polyethylene shielding this "efficiency" is lower. For example, the shielding of polyethylene without Cd-layer decrease the background neutron detection from 0.5% to 5% depending of initial background neutron energy. Adding a layer of cadmium the detection of neutrons from background decreases from 5% to 4% for neutron energy of 5 MeV. So the contribution of this layer is not significant. And as the adding the cadmium will increase the price of the detector this layer will not be added.

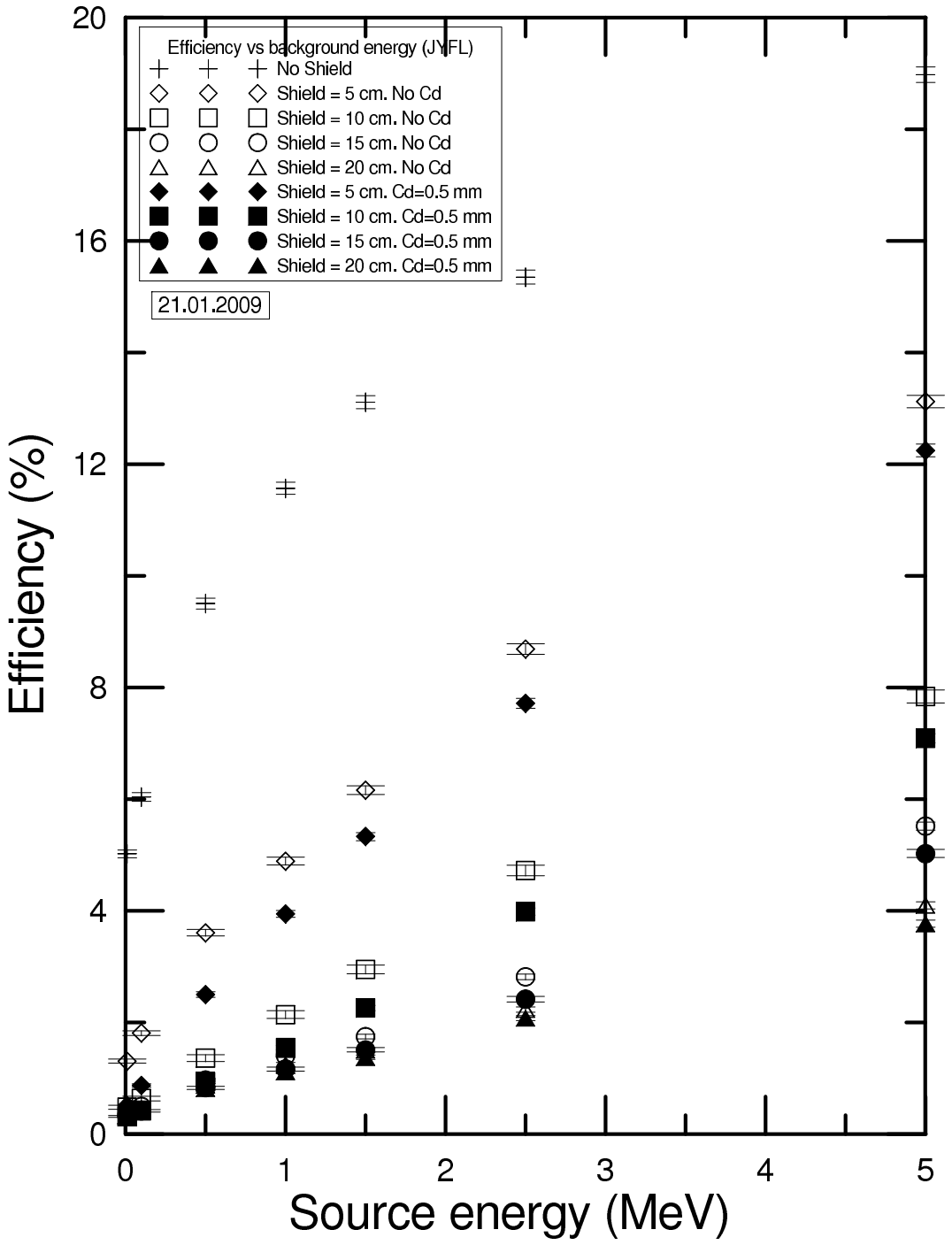

Figure 3.19: Neutron background detection

3.8.3 Neutron propagation time in the detector

It is important to know the neutron propagation time in order to have an idea about the trigger window of the experiment. One of possible setup of the experiment will be the neutron

detector with β-detector inside the beam hole. After the β decay of the radioactive nuclide the β-detector will detect this particle and mark the start time stamp for detecting the neutrons. The experiment will not use the trigger and the data will be captured continuously in order to record as much data as possible.
With the optimal configuration the next simulation was done. For neutron point source of 1 MeV the efficiency of the detection was simulated versus neutron propagation time. For the time range from 0 μs to 250 μs the time bin was set to 10 μs. The results can be observed on Figure 3.20.

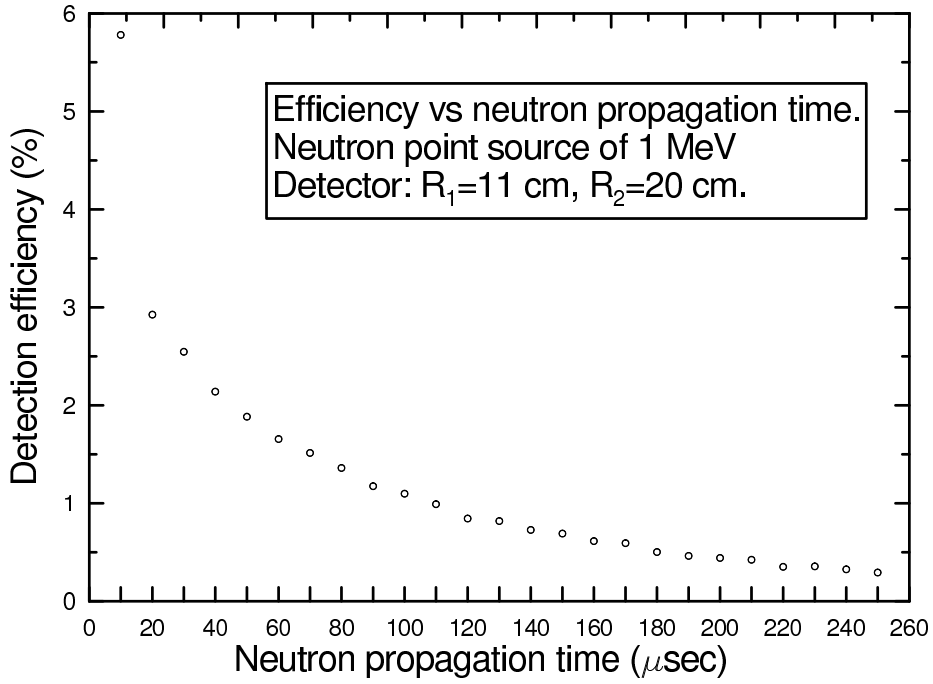

Figure 3.20: Propagation time contribution for detection efficiency. Differential efficiency

According to the simulation the propagation time larger than 200 μs does not contribute much into the efficiency, but it can contaminate the output signals from detector with neutrons from the background. It is important to find a compromise between the efficiency and trigger time. The simulation of efficiency for the optimal configuration of the neutron detector was repeated for neutron propagation time 200 μs and infinite time. The result of this simulation can be observed on Figure 3.21

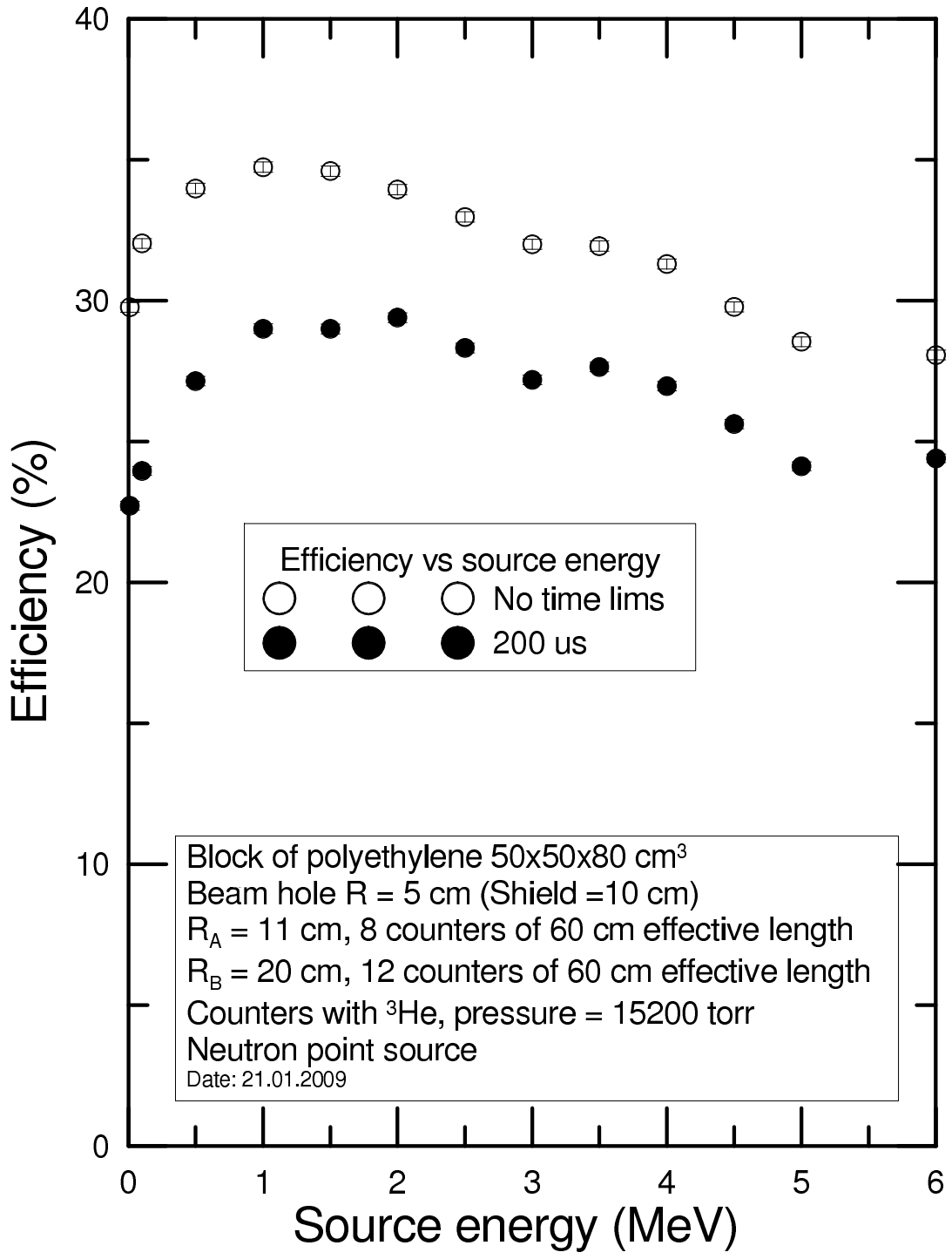

Figure 3.21: Simulated efficiency of final setup as a function of neutron source energy for different neutron propagation time

3.9 Detector construction

3.9.1 Main characteristics and materials

According to the simulation and electronic tests the detector should consists on a of matrix of polyethylene 50x50x80 cm^3 with 20 ^{3}He proportional counters inside. This matrix of polyethylene will be made of some polyethylene layers with 10 cm thin. The length of proportional counters should be 60 cm. In order to cover this length seven or eight layers of polyethylene should be used. In order to fix this layers together four additional holes will be made. It is necessary make a beam hole in the center of the matrix in order to deliver radioactive nuclei inside the detector. It is necessary to include a shielding around the detector. This shielding is 20 cm thin and covers the detector on 4 sides. The schematic view of the detector is presented on Figure 3.22 The weight of all this device is about 700 kg. This value can be confirmed multiplying the volume of the polyethylene by its density which is about 0.97 g/cm^3.

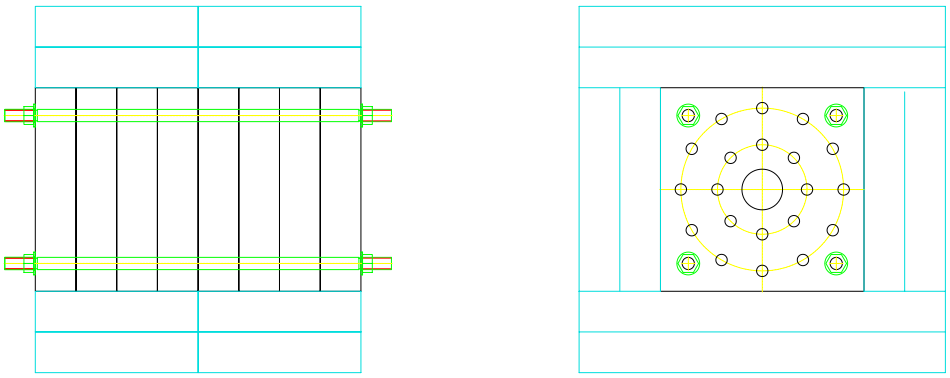

Figure 3.22: View of polyethylene matrix with 20 holes for the proportional counters and 4 additional holes to fix the polyethylene layers

3.9.2 Platform for the detector

As the weight of the neutron detector will be about 700 kg special platform have to be done. This platform should provide easy adjustment in order to fix the detector‘s position so as beam pipe or tape system would be in the center of the beam hole. The platform should have wheels in order to move the detector in the experimental area. It is also important to have a possibility to fix its position. The scheme of the platform is presented on Figure 3.23. There are wheels in order to move the table with the detector in the experimental area. There are special pads near the wheels. This pads let to fix the table position in order not to move it. These pads also give an opportunity to correct the inclination of the floor in order to have the detector‘s position aligned. There is a special tray on the table. This tray let by special wheel to move the detector in the beam axis. This mechanism lets the target to enter inside the polyethylene matrix.

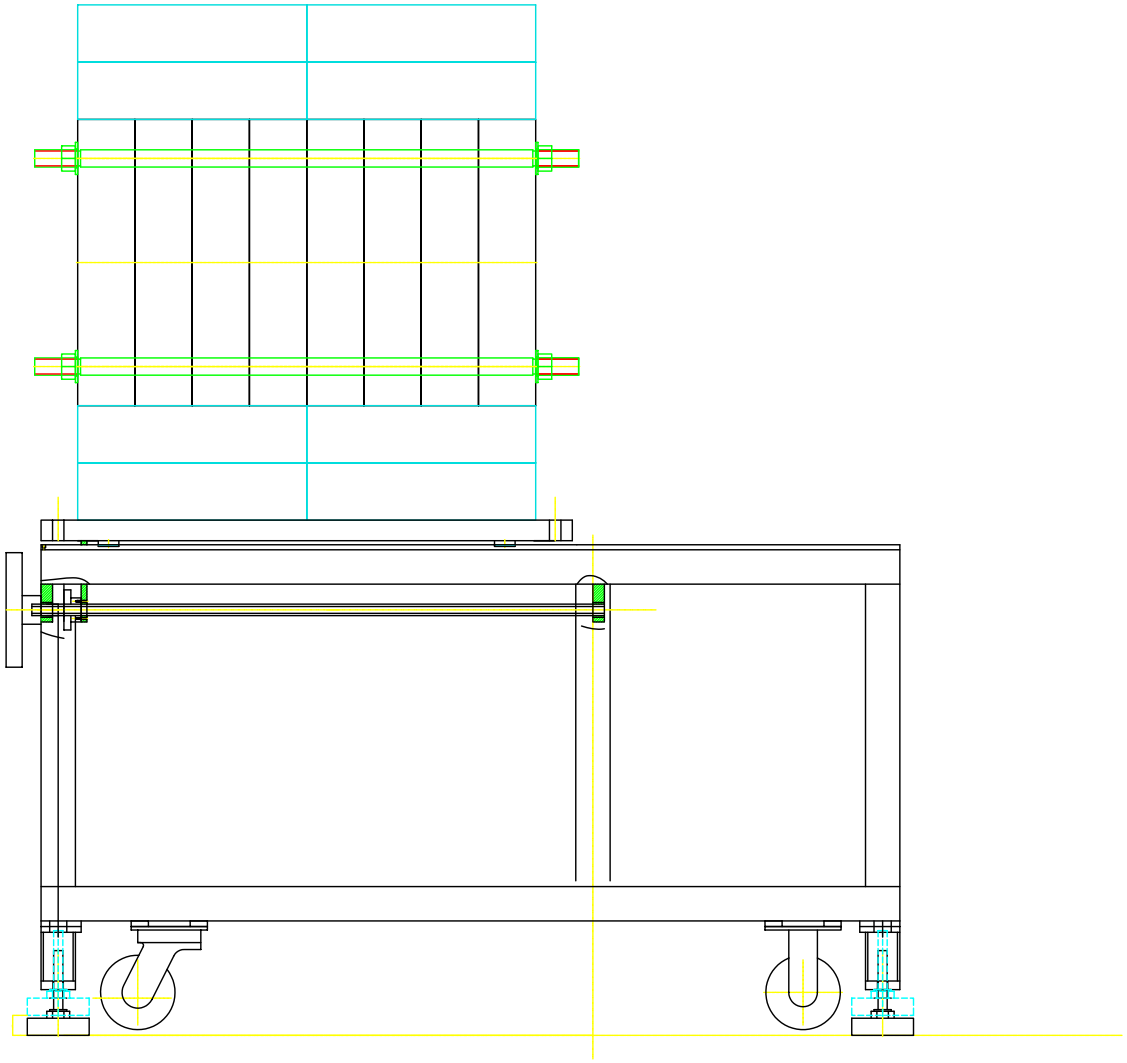

Figure 3.23: View of table support for the neutron detector

3.9.3 Simulation conclusions

This section describes the conclusions based on simulations done in previous sections. The main characteristics obtained with the simulation are shown on table 3.9.

These data was obtained taking in account physics, economics and engineering problems. The main physics objective is a flat and high efficiency for wide energy range in order to obtain correct data. The flat efficiency helps to decrease uncertainty on β - delayed neutron emission calculation. The background protection is also important task for the neutron detector in order to decrease the background contamination. It was described in previous section the origins of background source
The economy objective was to make this detector not very expensive. In order to reduce the costs of the detector the optimal material and optimal number of ^{3}He counters were chosen. The engineering problem is related with the dimensions of the detector, and its weight. These

Total dimensions of the detector	90x90x80 cm^3
Material of the detector	Polyethylene
Dimensions of matrix	50x50x80 cm^3
Shielding	20 cm
Cd layer	No
Beam hole radius	5 cm
Total number of counters	20
Number of rings	2
1st ring radius	11 cm
Number of counters in the 1st ring (inner ring)	8
2nd ring radius	20 cm
Number of counters in the 2nd ring (outer ring)	12
Matrix weght	630 kg
Mean efficiency for 0.01 MeV to 1 MeV	(26.74 +/- 3.25)%
Mean efficiency for 0.01 MeV to 6 MeV	(27.69 +/- 3.00)%
Efficiency factor (F) for 0.01 MeV to 1 MeV	1.22
Efficiency factor (F) for 0.01 MeV to 6 MeV	1.61

Table 3.9: Main characteristics of the neutron detector

characteristics are important for the detector movement and its installation in experimental are. Other important things are polyethylene matrix mechanizing, platform design for this matrix. This platform had to be able to provide fine adjustment on the beam in the experimental area. As the detector will be used in assembly with other equipment it was designed for it.
According to the simulation the data described above are optimal for these conditions.

Chapter 4

Electronics and Validation of the Simulations

4.1 Introduction

A test of ^{3}He and BF_3 counters and electronics has been performed in order to validate MCNPX as a simulation tool, check the electronics and the proportional counters for the design of the 4π neutron detector for JYFL laboratory.
In order to validate our simulation, two preliminary tests and simulations were done. These tests were performed in CIEMAT (Madrid) and in UPC-SEN laboratory (Barcelona). These simple tests were reproduced with MCNPX in order to compare them.

4.2 The first preliminary test

This test was done to validate the neutron detection efficiency of different proportional counters to choose the optimal counters to be used in our neutron detector.

4.2.1 Experimental setup

The first preliminary test was done in CIEMAT laboratory. Three different types of counters have been used during the experiment. They are a position sensitive proportional counter and standard one filled with BF_3 and a position sensitive proportional counter with ^{3}He as detecting gas. The picture and scheme of the setup used for the experiment can be observed on Figure 4.1 and Figure 4.2 . The counters were held by two bars at a distance of 60 cm from the table to reduce its influence on neutron moderation and prevent scattering. The neutron source (Figure 4.3 and Figure 4.4) was placed inside a polyethylene matrix (Figure 4.5) that was attached to the center of counter. This geometry has been used to simplify the simulation on MCNPX

Figure 4.1: Experimental setup. Counter is held by bars. The neutron source is placed inside the polyethylene matrix which is attached to the center of the counter.

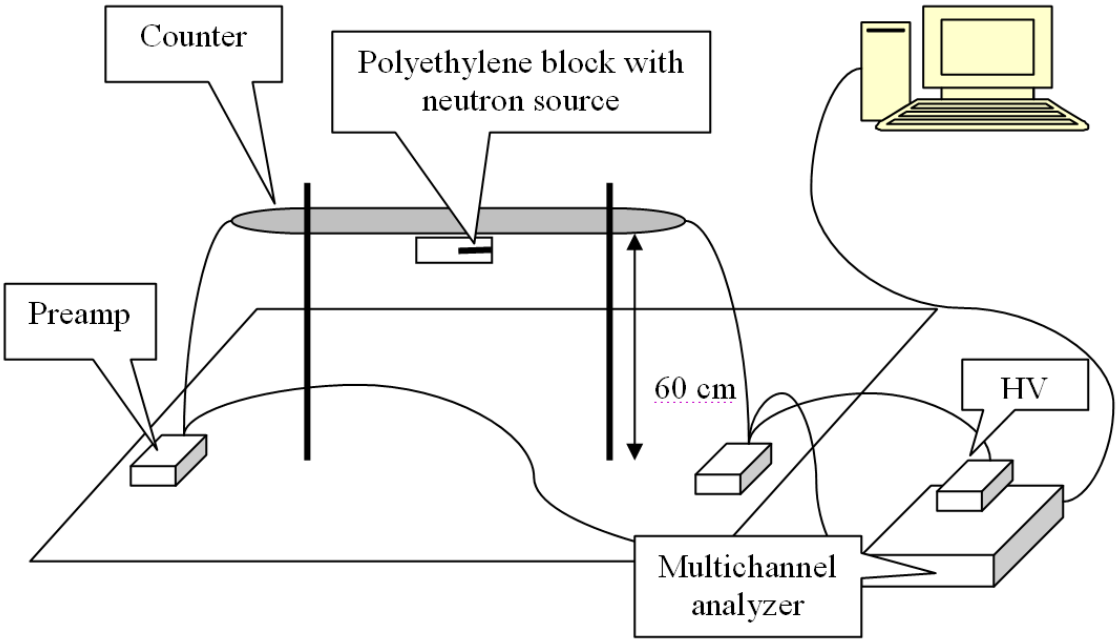

Figure 4.2: Scheme of experimental setup.

The neutron source used during the experiment was a vial with a 5 ml solution of ^{252}Cf, The source activity is 10 kBq with 3% spontaneous fission and 3.75 neutrons per fission, which gives about 1100 neutrons per second. The average neutron energy will be considered to be 2.2 MeV for the simulations.

Figure 4.3: Neutron source used in CIEMAT laboratory.

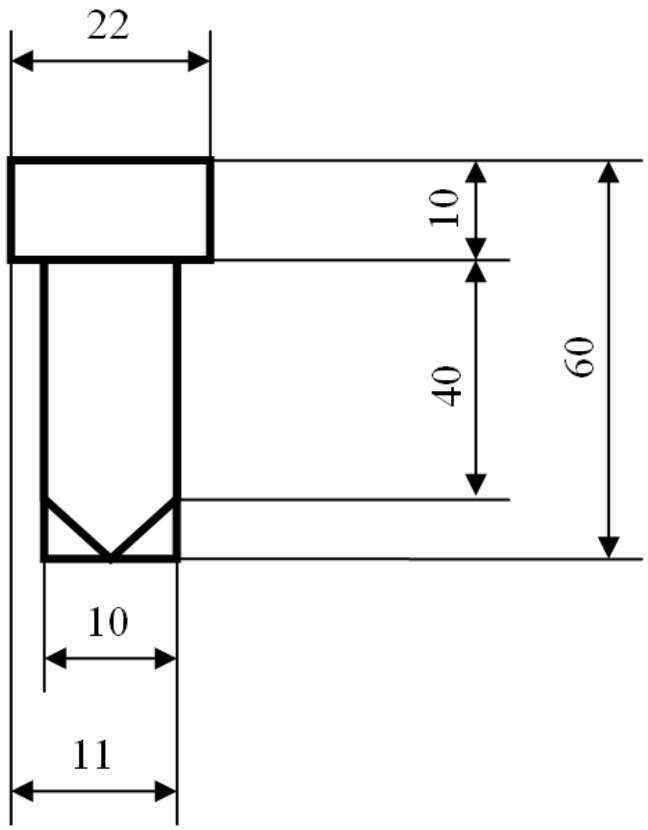

Figure 4.4: Neutron source scheme (units in mm).

Detector Characteristics

Three different types of detectors have been used. They have been manufactured by LND inc. and their characteristics are presented in Table 4.1. The anode of the 3 detectors had SHV connectors.

Electronics

Standard electronics have been used during the test. The preamplifiers ORTEC 142PC have been coupled directly to the ends of the counter tubes (Figure 4.2 and Figure 4.6). These preamplifiers provide the interface between the counter tube and the amplifier or the acquisition system and they also provide the high voltage through one end of the counter. In standard detectors the signal is collected through one end. In position sensitive detectors the signal is collected through both ends. The difference in the amount of charge collected from both ends provides the information on the position of the neutron.

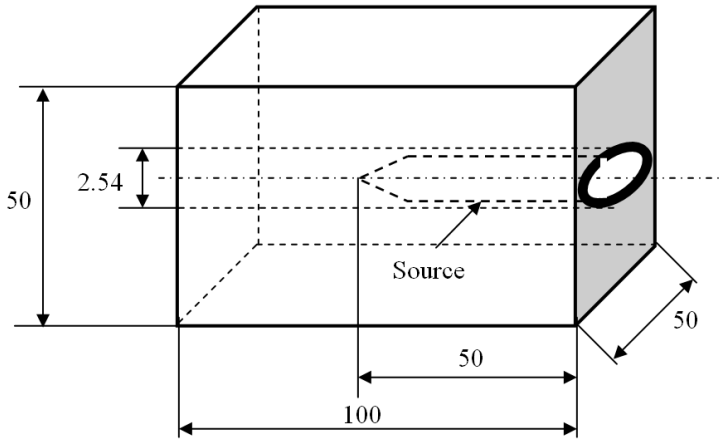

Figure 4.5: Block of polyethylene with neutron source inside (units in mm).

Model	Gas	Length x diam (cm)	Pressure Partial/ Total (torr)	Volume (cm^3)	Wall thickness (mm)	Anode diameter (μm)	Cathode	Voltage (Volts)	Features
20358	BF_3 (96% ^{10}B)	37.5x5.08	550	760.06	0.508	50	Stainless steel	1800	Standard
202105	BF_3 (96% ^{10}B)	48.8x2.54	700	247.3	0.508	11	Stainless steel	1400	Position sensitive
252231	^3He+Ar	50.0x2.54	3800/ 7600	253.35	0.508	11	Aluminium	1200	Position sensitive

Table 4.1: Summary of the main characteristics of the three proportional counters used

Data Acquisition System

The signals from the three detectors were recorded in commercial data acquisition systems DSA-2000 manufactured by Canberra. The signal from the amplifier is digitized after some pre-conditioning and amplification, and then it is sent to the PC for data acquisition and visualization. For the position sensitive detectors, the position sensitive feature was not exploited since the signals from the two ends were merged into one and sent to the acquisition system.

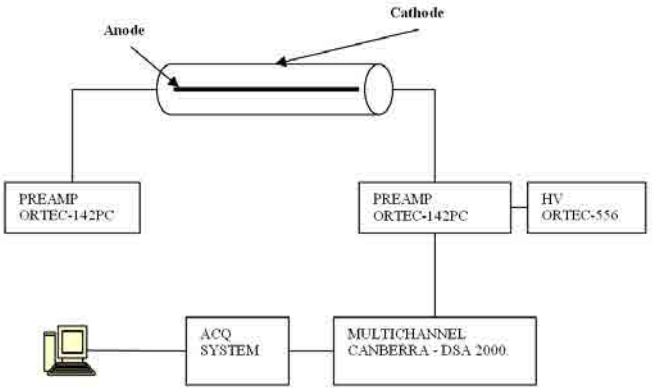

Figure 4.6: Electronic scheme used at CIEMAT laboratory.

Measurements

Each counter was connected as shown on Figure 4.6 and measurements were taken during 40000 seconds. The obtained data was compared with a simulation in MCNPX.

Response Function

A voltage of 1400 Volts was applied to one end of the position sensitive ^{3}He proportional counter. The signal from the preamplifier was recorded with the DSA-2000 Canberra module using as a filter parameters for rise time 2.0 μs and for the flat top 0.8 μs. The gain value of the internal amplifier was set to 15x1.2. The response obtained is shown on Figure 4.7.

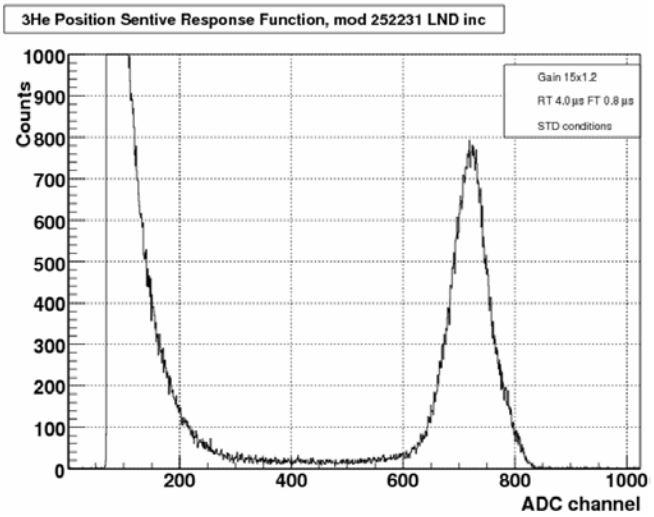

Figure 4.7: Response function for ^{3}He position sensitive detector model 252231.

Two different BF_3 proportional counters have been tested, a position sensitive proportional counter and a standard one. The detectors were placed in the same conditions as the ^3He proportional counter. The neutron source was placed in the polyethylene matrix. The voltage was set to 1200 Volts for the position sensitive detector and to 1800 Volts for the standard one. The signals from the preamplifiers were recorded with the DSA-2000 Canberra module using as a filter parameters for rise time 2.0 μs and 0.8 μs for flat top. The gain value of the internal amplifier was set to 15x1.2. The response obtained is shown on Figure 4.8 for the position sensitive counter and on Figure 4.9 for the standard one.

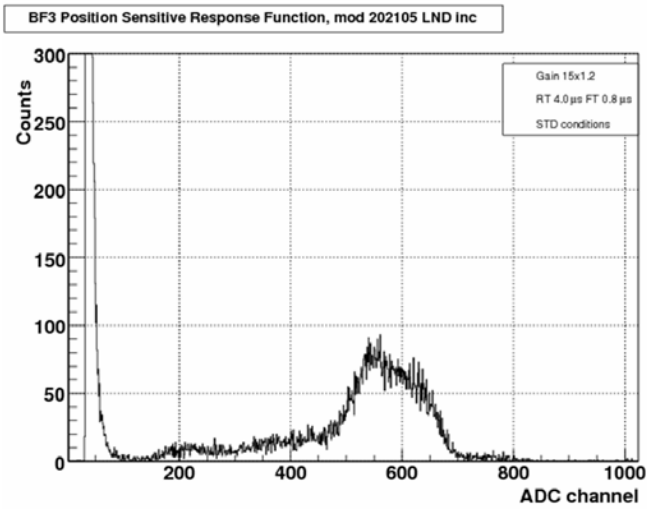

Figure 4.8: Response function for BF_3 position sensitive detector model 202105.

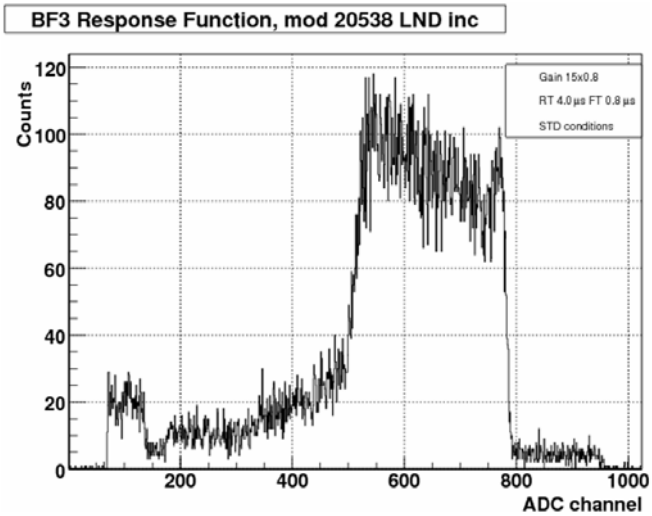

Figure 4.9: Response function for BF_3 position sensitive detector model 20538.

Background Measurements

In order to study the influence of background the same measurement as before was made for the three counters but without the neutron source. The detectors have been placed in the same conditions as in the previous experiment with the neutron source (see Figure 4.6). The measurements were taken during 216000 seconds. The responses obtained during the background measurements are shown on Figure 4.10 for ^{3}He counter. The response function for BF_3 is shown on Figure 4.11 for position sensitive counter and on Figure 4.12 for the standard one.

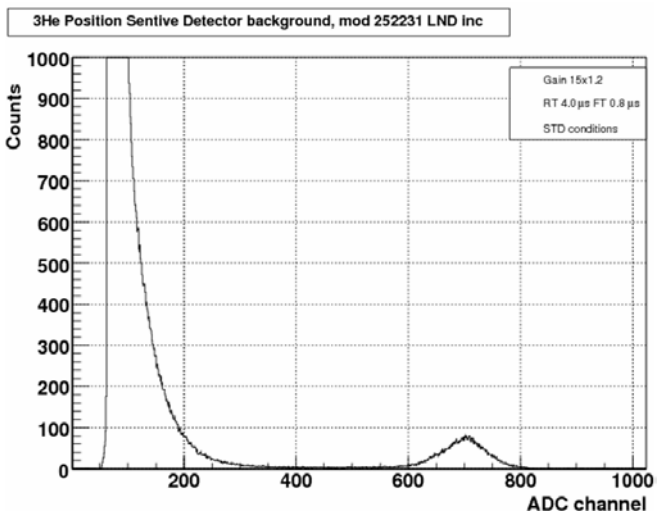

Figure 4.10: Response function for background measurement with ^{3}He counter model 252231.

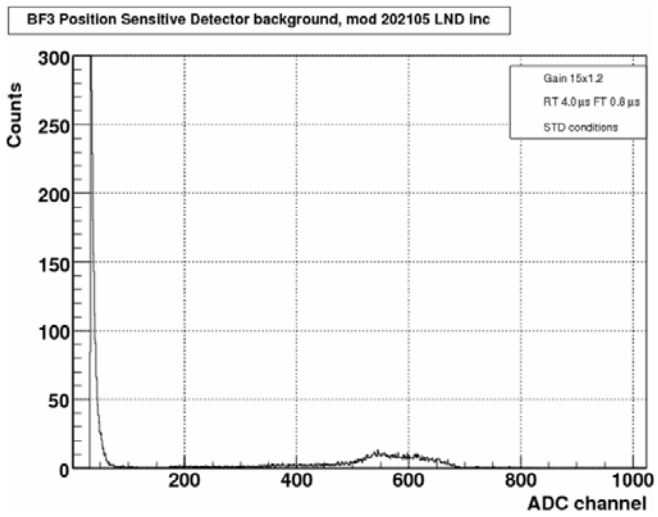

Figure 4.11: Response function for background measurements with BF_3 position sensitive counter model 202105.

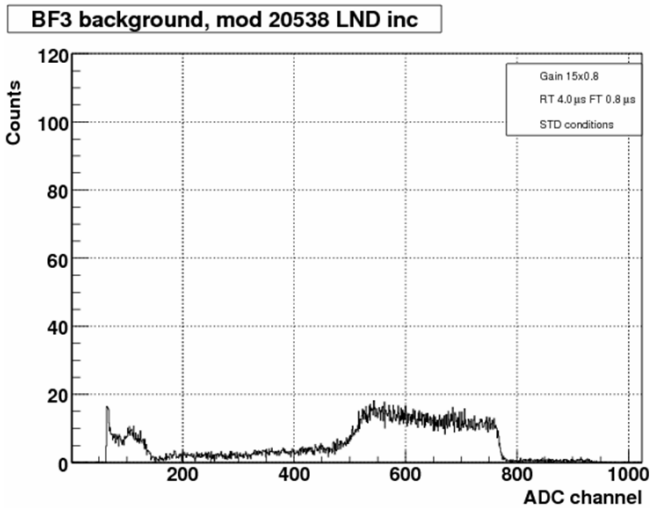

Figure 4.12: Response function for background measurements with BF_3 standard counter model 20538.

DATA analysis

In order to analyze the data the next things were done. The number of neutrons detected from background (N_b) were measured during a time of t_b=216000 seconds. The neutron rate of background is $\dot{N}_b = \frac{N_b}{t_b}$ with uncertainties $\sigma_{\dot{N}_b} = \sqrt{\frac{\dot{N}_b}{t_b}}$ The measurements with neutron source were performed during t_m=40000 seconds. The neutron rate was $\dot{N}_m = \frac{N_m}{t_m}$ with uncertainties $\sigma_{\dot{N}_m} = \sqrt{\frac{\dot{N}_m}{t_m}}$.

The efficiency of the detection (η) was calculated according to the equation 4.1, where $\dot{N}_s$ is the number of neutrons emitted from the ^{252}Cf source per second. In this case it corresponds to $\dot{N}_s = 1100n/s \pm 15\%$

$$\eta = \frac{(\dot{N}_m - \dot{N}_b)}{\dot{N}_s} * 100\% \tag{4.1}$$

The uncertainty of the efficiency corresponds to equation 4.2

$$\sigma_\eta = \sqrt{(\frac{\partial \eta}{\partial \dot{N}_m}\sigma_{\dot{N}_m})^2 + (\frac{\partial \eta}{\partial \dot{N}_b}\sigma_{\dot{N}_b})^2 + (\frac{\partial \eta}{\partial \dot{N}_s}\sigma_{\dot{N}_s})^2} \tag{4.2}$$

The measured efficiency is presented in table 4.2

MCNPX Simulation

These experimental conditions were simulated in MCNPX. The block of polyethylene with dimensions of 100x50x50 mm and with a hole inside with diameter of 25.4 mm to put the neutron source. In order to simplify the influence of the room's walls around the experimental setup a concrete sphere around the detector was simulated. As MCNPX does not reproduce the spectra from the reaction in the gas, it only provides us with the efficiency of the detector from the ratio of neutrons detected and emitted.
The simulation results together with experimental values are presented in Table 4.2 and there is good agreement between simulations and experimental data for ^{3}He counter and larger error between simulation and experimental data for the BF_3 counters. After different checks no errors have been found in the MCNPX simulations that could explain the difference of results in the case of the BF_3 gas. One of possible thing which affected to the measurements was mechanical and electrical noise. During the measurements in one laboratory there was noise from the vacuum pump and in other laboratory there was noise from the central heating and air conditioning. This noise could not be rested absolutely because of irregularity of these equipment working. The counter with ^{3}He was not such sensible to this influence.

Data	BF_3 Model 20358	BF_3 Model 202105	^{3}He Model 252231
Experimental	(0.06 ± 0.01)%	(0.028 ± 0.004)%	(0.16 ± 0.02)%
MCNPX data	(0.046 ± 0.003)%	(0.020 ± 0.001)%	(0.15 ± 0.02)%
(Exp-MCNPX)/(Exp) (%)	28%	28%	5%

Table 4.2: Detection efficiency of counters.

Conclusions and Future Measurements

One of the difficulties during the measurements was the presence of electronic noise in the experimental room. Two different experimental rooms were used in CIEMAT in order to

improve the conditions for the measurement. The first room had a vacuum pump which produced a very high level of electronic noise therefore the experiment was moved to a second room. However in this room there was noise from the ventilation system during the morning so the measurements were only possible during the afternoon and night

Some other measurements was carried out at the UPC after the setup of laboratory.

4.2.2 The second preliminary test

According to the previous simulation 20 proportional counters with ^{3}He detecting gas, with 2.5 cm in diameter and 60 cm of effective length will be used for the detector construction. In order to be able to construct the detector 22 proportional counters were bought. This counters were manufactured by LND Inc. and their characteristics can be observed on table 4.3 The design of this experiment was made in order to analyze next data:

- To check the functionality of the counters
- Length of signal cable between the counter and pre-amplifier
- To check the influence of the electronics warming
- Spectrum of the neutron detection in these counters

After performing this test the results will be useful to make correct scheme of the experiment.

Experimental setup

During the test 22 proportional counters were tested in SEN-UPC laboratory. They are filled with ^{3}He as detecting gas. All the ^{3}He counters have been manufactured by LND Inc. and their characteristics are presented in Table 4.3. The anode of the counters has SHV connectors. The second preliminary experimental setup is presented on Figure 4.13. The

Counter	Gas	Maximum length (mm)	Effective length (mm)	Maximum diameter (mm)	Effective diameter (mm)	Gas pressure (torr)	Cathode material
2527 LND Inc	^{3}He	686.84	604.8	25.4	24.38	15200	Stainless Steel

Table 4.3: Summary of the main characteristics of the proportional counters used at the tests and for the neutron detector construction

counters one by one were put inside of polyethylene block with dimensions 20x20x20 cm^3. There are 4 holes in the polyethylene block. These holes have distance among each other 10 cm. The neutron source was placed in the bottom left hole and the counters were placed in the top left hole. So the distance between the counter and neutron source was 10 cm. This geometry was reproduced in MCNPX simulation.

There were two different electronic schemes during the test because new equipment was ordered, but some measurements were made before this new equipment was delivered. The electronic schemes of the setup used for the experiment can be observed on Figure 4.14 (1st scheme) and Figure 4.15 (2nd scheme).

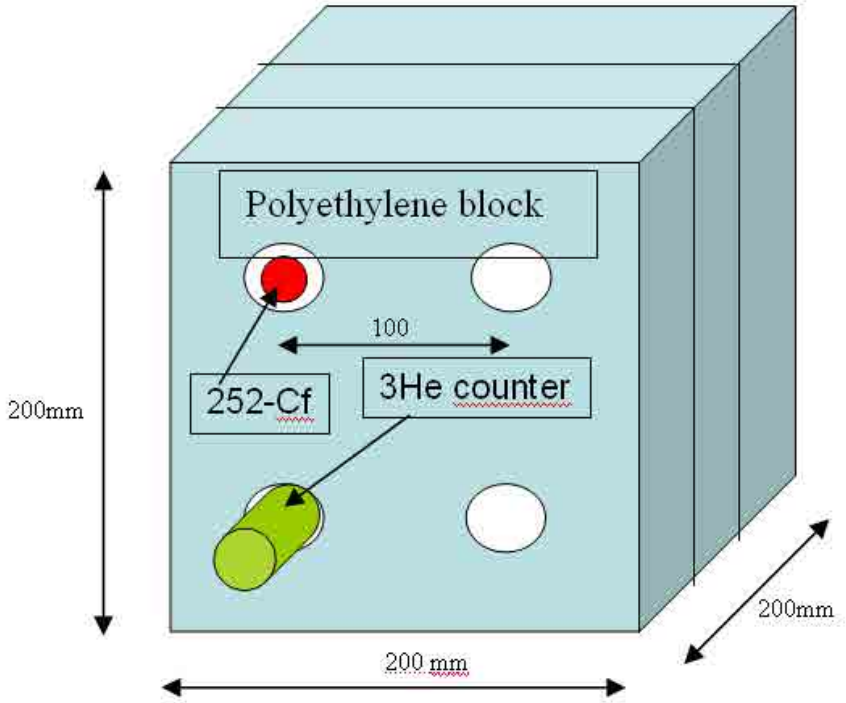

Figure 4.13: Experimental setup for simple test

Here is a list of components used in scheme from Figure 4.14:

- Pre-amplifier Mesytec MPR-16 for 16 channels
- Amplifier Mesytec STM-16+ for 16 channels
- Multiport II by ORTEC is channel analyzer for one channel
- PC with Windows XP operation system and Genie-2000 software
- Power supply by ISEG. Model NHQ2003M for two channels

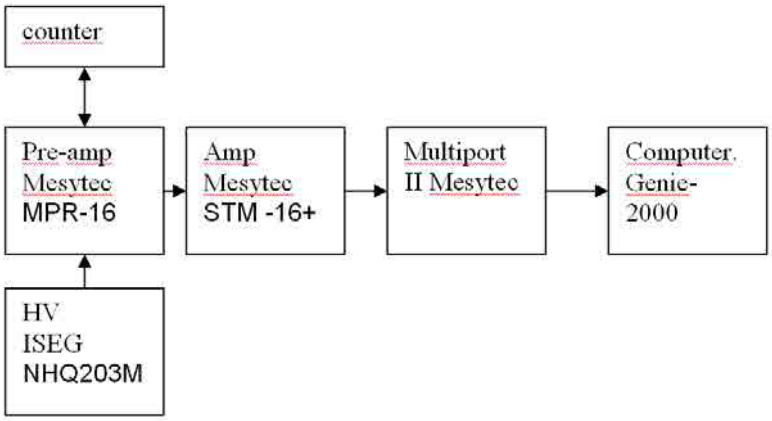

Figure 4.14: Electronic scheme 1

Here is a list of components used in scheme from Figure 4.15:

- Pre-amplifier Mesytec MPR-16 for 16 channels
- Amplifier Mesytec STM-16+ for 16 channels
- ADC Canberra for one channel
- AIM Canberra for 16 channels. Model 556A
- PC with Windows XP operation sistem and Genie-2000 software
- Power supply by ISEG. Model NHQ2003M for two channels

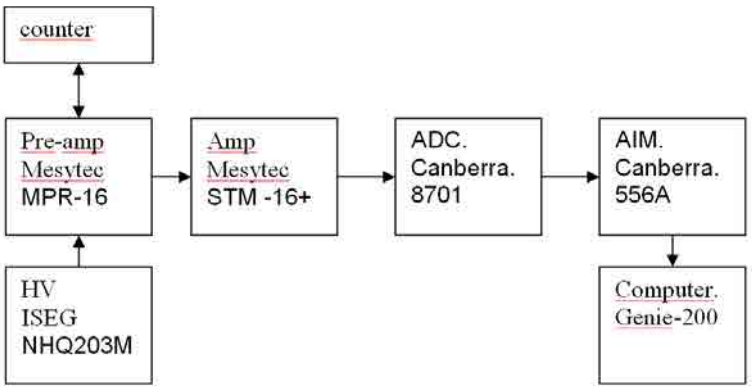

Figure 4.15: Electronic scheme 2

The neutron source used during the experiment was a vial with a 1 ml solution of ^{252}Cf, The initial source activity (at December 2007) was 9.9 kBq with 3% spontaneous fission and 3.5 neutrons per fission.

Electronics and data acquisition

During the test ISEG NHQ203M module was used to supply the High Voltage (See Figure 4.16. This module has two output channels and provides tension up to till 3 kV per channel. It has low ripple (<0.05 V) which is important for this test since the noise of electronics produces more false counts in low channels. In order to make the test clear the noise must be as low as possible. The preamplifiers MESYTEC MPR-16 were connected to channel

Figure 4.16: ISEG HV power supply

14th directly to the ends of the counter tubes. This preamplifier has 16 channels. As this preamplifier provides the high voltage through one end of the counter, the HV module was also connected to this preamplifier (see Figure 4.14 and Figure 4.15). This preamplifier was connected to the amplifier MESYTEC STM-16+ which is manufactured by Mesytec and has 16 channels. Since different electronic components were available during the test two different electronic schemes were used. First the electronic scheme from the Figure 4.14 was used and then other equipment was bought for new laboratory and this equipment was used for the second electronic scheme (see Figure 4.15) for the measurements.
Two types of data acquisition systems were used during the measurements. In the first one the output from the amplifier were connected to Canberra module Multiport II and it sent the signal to the PC with Genie-2000 software. After buying the new equipment in the second electronic scheme the signal from the amplifier were digitized in module ADC 8701 manufactured by Canberra and then it was sent to the Canberra AIM 556A module which sent the data to PC for data acquisition and visualization. The commercial software Genie-2000 was used for data recording in the PC.

Measurements

The aim of the measurements was to check the response of all the counters and electronics. The counters one by one were connected to the channel number 14 of the pre-amplifier. The measurements were taken during 2000 seconds. In order to make this measurement different steps were performed.

- The first measurement was to check the electronics with "hot" and "cold" start. "Cold start" means beginning the data taking after switching on the electronics without waiting any time. "Hot start" in this work means beginning data taking after warming up the electronics for 5 hours after switching it on. This measurement was taken during 1000 seconds.
- The influence of cable length between the counter and pre-amplifier was checked. The cable lengths 5 cm, 50 cm, 75 cm and 100 cm were checked.
- Other measurement was done in order to check the response from each channel of pre-amplifier and amplifier. For these measurements only one counter was connected to the all channels one by one. For all these channels the energy spectra were obtained. The measurements were taken during 4000 seconds.

Response plots

In order to check the influence of warming up the electronics the next tests were done. Firstly the energy spectrum was obtained after switching on the equipment. This measurement is called "cold" start. The data taking after warming up the equipment for 5 hours is called "hot start" in this work. A voltage of about 2202 $\pm$ 2 V was applied to end of the ^{3}He proportional counters. The electronic scheme was the same as on Figure 4.14. The signals from them were recorded with Genie-2000 software. The cable length between preamplifier and amplifier was 5 cm. The measurements were taking during 1000 seconds.

Channel	1-25	26-80	81-150
Cold	1479	3372	12420
Hot	1560	3261	12290
Cold-Hot/hot%	-5.2%	1.5%	1%

Table 4.4: Cold and hot start table

The response function for "cold" and "hot" start is presented on Figure 4.17. In this figure can be observed the electronic noise in channels from 0 to 20. The next peak in channel 25 corresponds on first wall effect and the second wall effect could be observed in channels near 80, but it is overlapped with the main peak of energy deposition. The main peak corresponds to the energy 765 keV and it is around channel 98. The wall effect arises because the proton and triton daughter products of the reaction have discrete energies (573 keV and 191 keV respectively) and their ranges in the detector are usually larger than the dimensions of the detector. When one of the daughter products collides with the wall of the detector, its energy

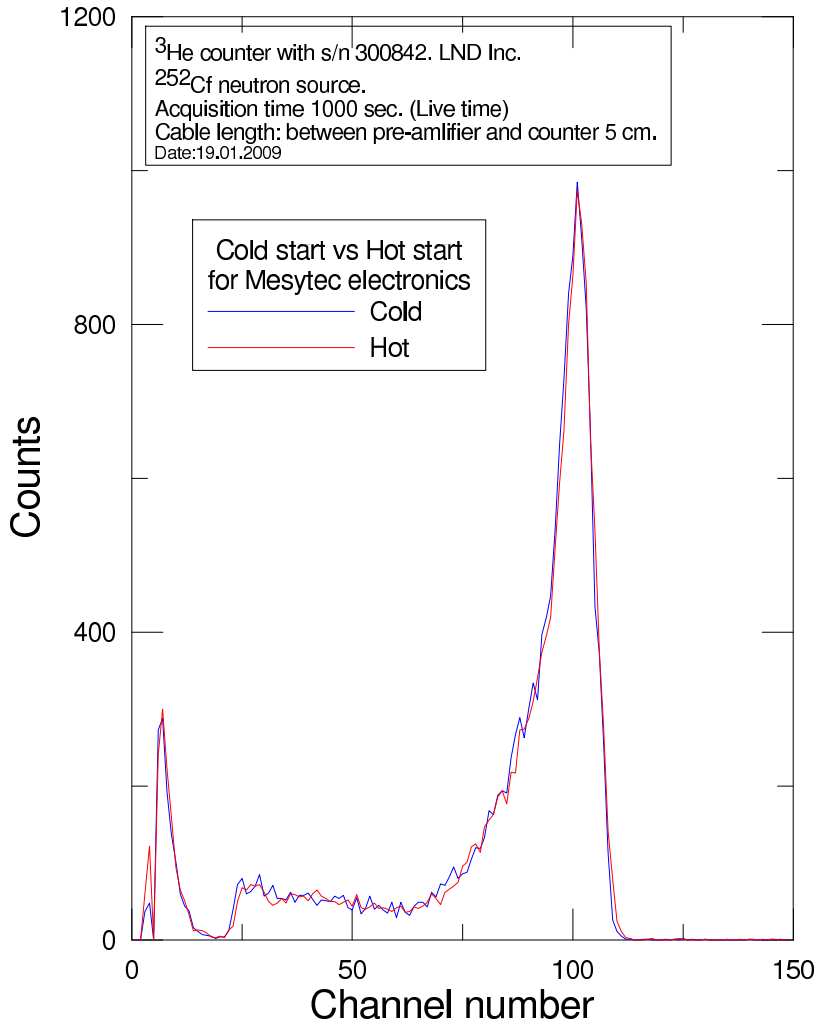

Figure 4.17: Response function for "hot" and "cold" start

is dissipated and does not contribute to the full energy peak, thus creating the discrete steps in the spectrum. The total number of counts for channels from 0 to 150 for "hot" start corresponds to 17211 and for "cold" start 17111 which has a relative difference of 0.58% According to Figure 4.17 there is no significant difference between the "hot" and "cold" start. The table 4.4 shows three parts of the spectrum. The first one is from channels from 1 to 20 which corresponds to noise. Their difference is about 5%. The next region corresponds to two wall effects. Their difference is about 1.5% and the last region corresponds to main peak. The difference between hot and cold start is about 1%. So, as the difference gives about 1% of uncertainty to make the measurement quicker it is possible to take data after connecting the electronics and it is not necessary to wait for the warming up of the electronics after each connection.

Counters spectra

Following measurements were made according the same electronic scheme on Figure 4.14. These measurements were made during 20000 seconds for each counter. The cable length between the counter and preamplifier was 5 cm. The counters were connected one by one to channel 14 of the preamplifier. For the neutron source used was a ^{252}Cf. The typical response function is present on Figure 4.18.

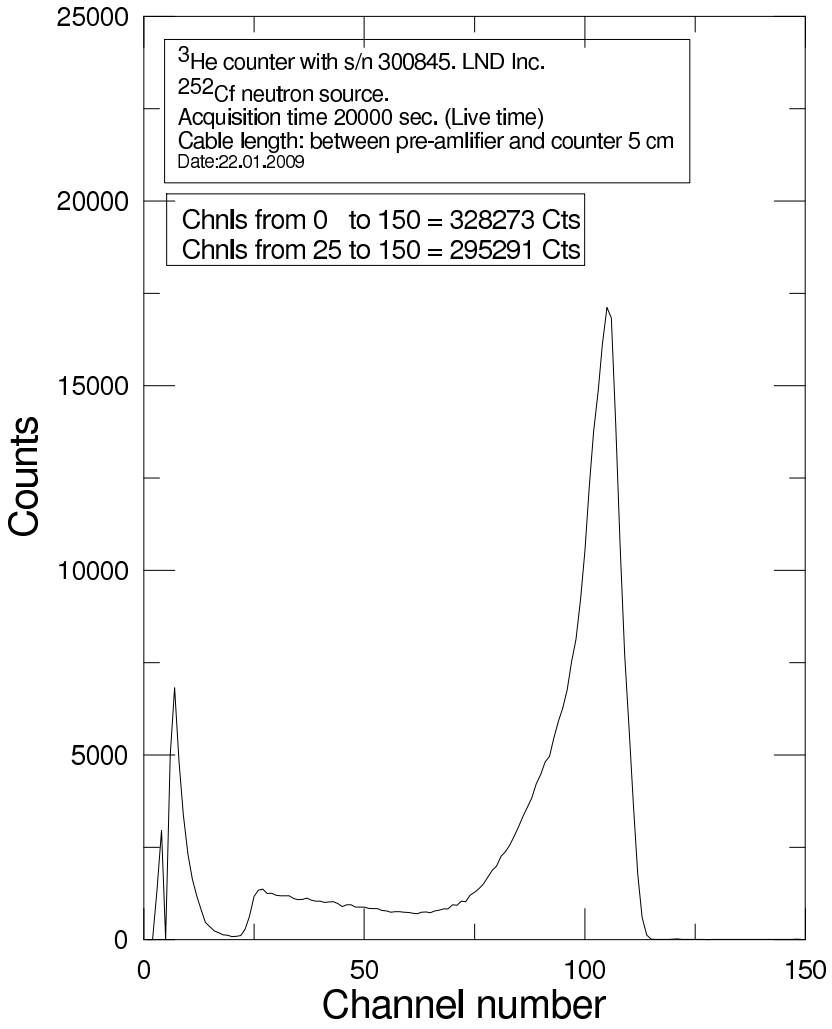

Figure 4.18: Response function for counter with s/n 300845. Electronic scheme from Figure 4.14 was used.

After some series of measurements new equipment was bought and delivered and the laboratory and electronic scheme was changed. The new electronic scheme was changed according to the Figure 4.15. Cable length between preamplifier and amplifier was 5 cm. A high voltage of 2202 $\pm$ 2 V was applied. In order to make validation of these different schemes the measurement with the counter with s/n 300845 were made for two different electronic schemes. The response function can be observed on Figure 4.19.

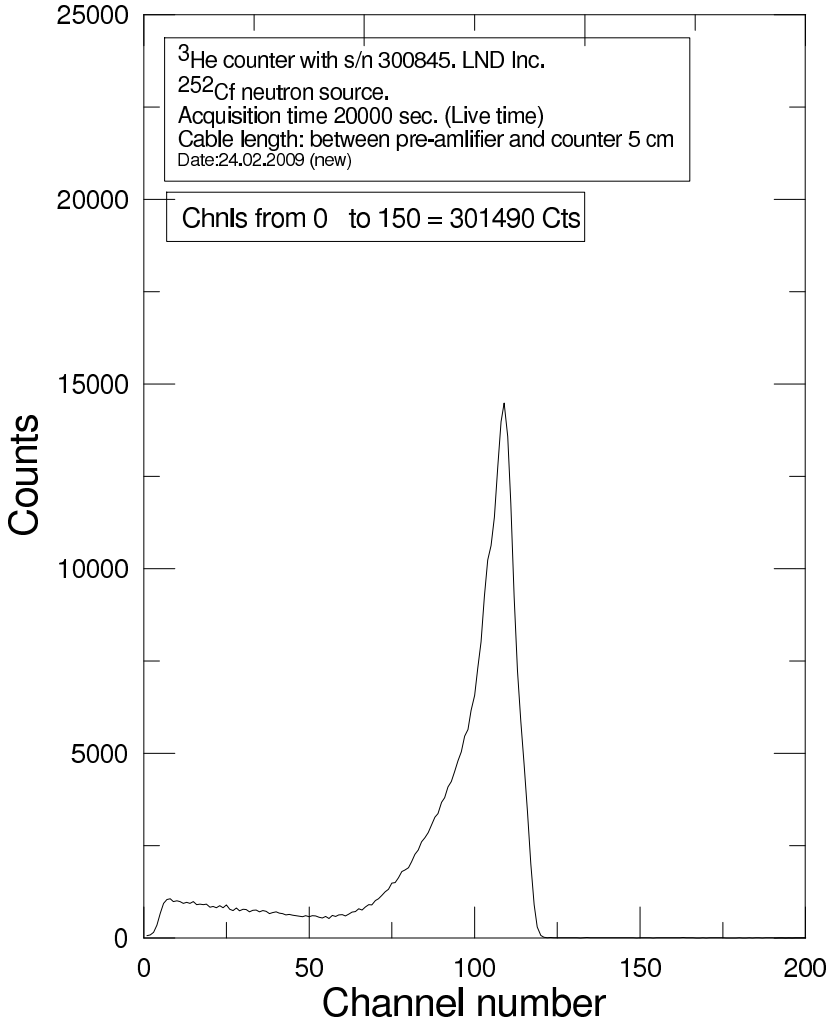

Figure 4.19: Response function for counter with s/n 300845. Electronic scheme from Figure 4.15 was used.

The total number of counts in the new scheme is 301490 counts and in old one is 328273 counts or 295291 counts if the first 25 channels are discriminated. This was done because using the 1st electronic scheme there is noise in the low energy channels. This noise produces false counts and influes on the total number of counts. So the difference between these two schemes is 2%. For this calculation the noise in low channels was excluded

The next measurements were made with electronic scheme from the Figure 4.15. The cable length and HV were the same as in the 1st scheme. The cable length between preamplifier and amplifier was 5 cm. The measurements were taking during 20000 seconds. A high voltage of 2202 $\pm$ 2 V was applied.

As it can be observed on Figure 4.20 the counter with s/n 301259 has noise in the low channels. In order to check if there was any error in the measurement the data taking was repeated twice with measurement time 10000 seconds. The results can be observed on Figure 4.21.

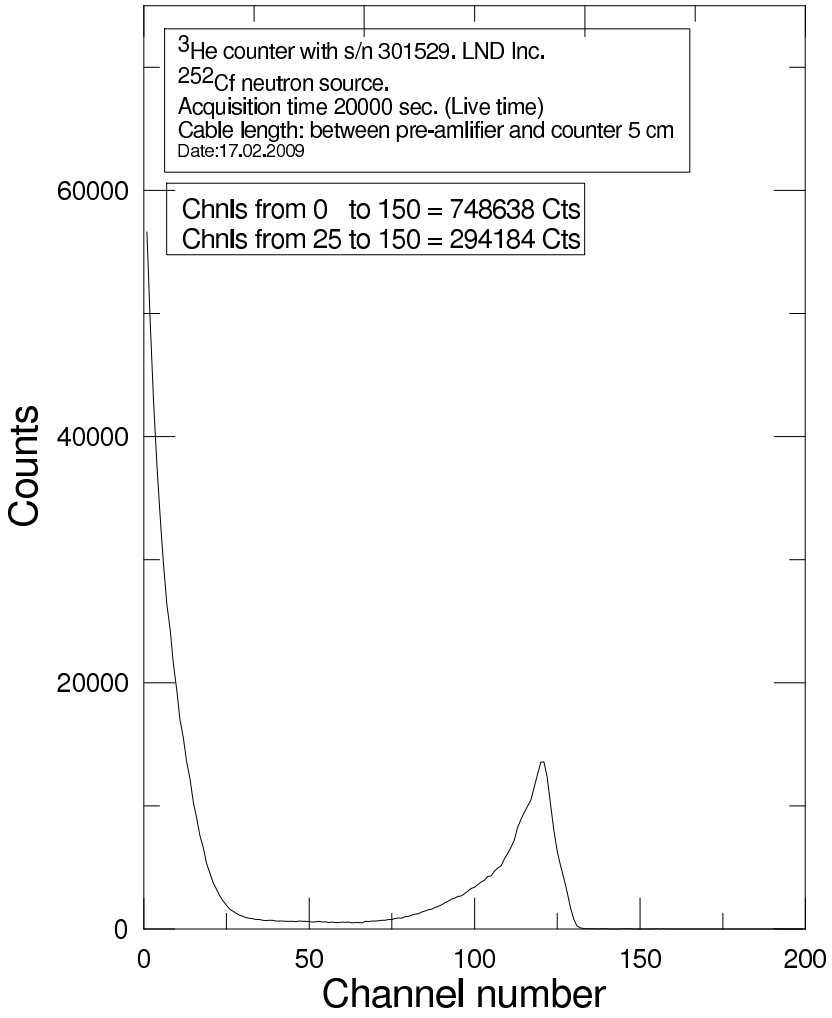

Figure 4.20: Response function for counter with s/n 301529. Electronic scheme from Figure 4.15 was used.

This counter showed noise in the second set of data in the low channels. It was sent to LND Inc. in order to be repaired. The number of counts in each counter is presented in Table 4.5. For the counters which were connected using scheme from Figure 4.14 the sum of counts from channel 25 to 150 were taken in order to remove noise and for the counters which were connected using scheme from Figure 4.15 the sum from channel 0 to 150 was taken.

s/n	Number of counts	Efficiency (%)	Type of scheme
300840	296047	2.20	1
300841	304812	2.27	1
300842	316339	2.35	1
300843	308455	2.30	2
300844	292259	2.17	1
300845	295291	2.20	1
300845	301490	2.20	2
300846	294110	2.19	1
300847	305727	2.27	1
300848	297503	2.21	1
300849	308542	2.30	2
300850	305711	2.27	2
300851	306832	2.28	2
301523	305443	2.27	2
301524	302657	2.25	2
301525	302423	2.25	2
301526	305173	2.27	2
301527	302216	2.25	2
301528	303631	2.26	2
301529	748638	5.57	2
301530	301752	2.25	2
301531	304807	2.27	2
301532	301894	2.25	2

Table 4.5: Number of counts in each counter.

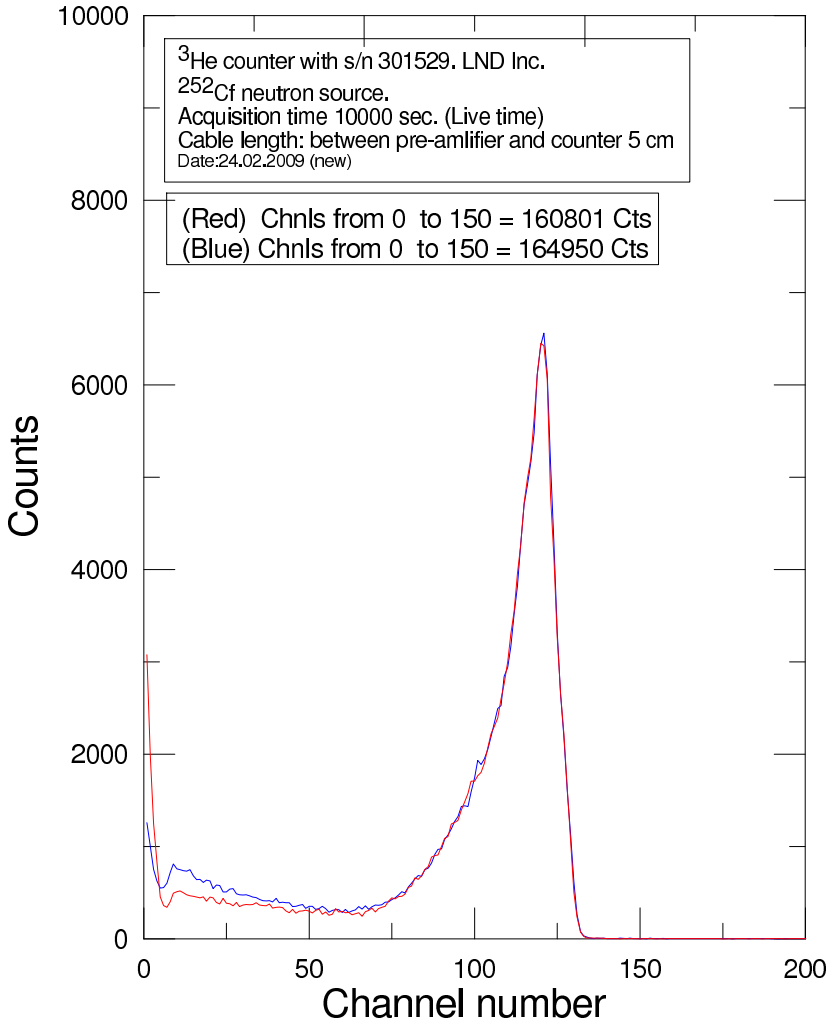

Figure 4.21: Response function for counter with s/n 301529. Electronic scheme from Figure 4.15 was used.

Test of influence of cable length

During the following measurements the influence of cable length between the counter and pre-amplifier was checked. The cable lengths tested were 5 cm, 50 cm, 75 cm and 100 cm. The number of counts for these lengths can be seen in Table 4.6. This test was made with counter with s/n 300851. The response function can be seen on Figure 4.22. The amplitude of the spectrum decreases from channel 111 to 105 for the cable lengths 5 cm and 100 cm. The number of counts decreases as the cable length increases because of signal loss due to the impedance and capacity of the cable and as the cable length increases the number of counts the length of the cable chosen was 75 cm. It is also enough to connect the tubes with pre-amplifiers and the noise which produces in the cable is less than noise in the cable of 100 cm. Since the cable length that will be used in the neutron detector in JYFL will be 75 cm the next measurements were made with this cable length.

Cable length	Counts	Difference number of counts relative to cable of 5 cm (%)	Peak channel	Peak channel difference relative to cable of 5 cm (%)
5 cm	306832	0	111	0
50 cm	300216	-2.16	110	-0.9
75 cm	308945	0.69	108	-2.70
100 cm	324455	5.74	105	-5.47

Table 4.6: Number of counts for different cable length.

Tests of channels of pre-amplifier and amplifier

These measurements were made in order to check all the channels of the preamplifier and amplifier. The counter with s/n 300851 was chosen for the measurements and the time of measurements was set to 4000 seconds. The typical response function can be observed on figure Figure 4.23. The summary of number of counts in each electronic channel is presented in Table 4.7.

The mean value of the counts is 61084 with variance 1508 which corresponds to 2.46% of error. All the channels give similar results inside the error range 2.5%. It seems the electronics works well.

MCNPX Simulation

The obtained experimental data was compared with results of simulation in MCNPX. The geometry of the test (see Figure 4.13) was reproduced in the simulation code. The only simplification was with neutron energy spectrum. The neutron energy was set to 2.2 MeV.

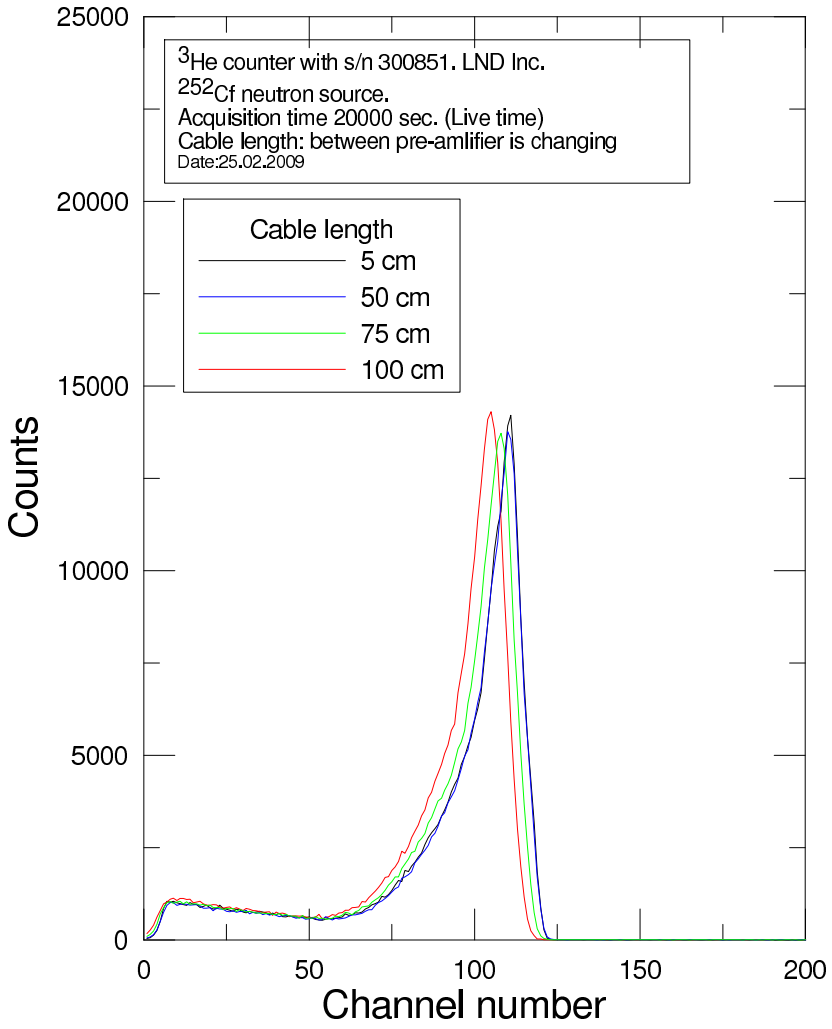

Figure 4.22: Response function for counter with s/n 300851. Electronic scheme from Figure 4.15 was used. The cable length between the preamplifier and the counter was 5 cm, 50 cm. 75 cm and 100 cm.

The aim of the simulation was to obtain the efficiency of the setup and compare this data with experimental ones.

The simulation results are presented in Table 4.8 and there is good agreement between simulations and experimental data for ^{3}He counters. The mean value of experimental efficiency of the counters is presented in Table 4.8. Data from counter with s/n 301529 was excluded from the calculation of mean value of experimental efficiency as it had high noise.

Conclusions after test at SEN laboratory

After this test at SEN laboratory the following conclusions have been drawn:

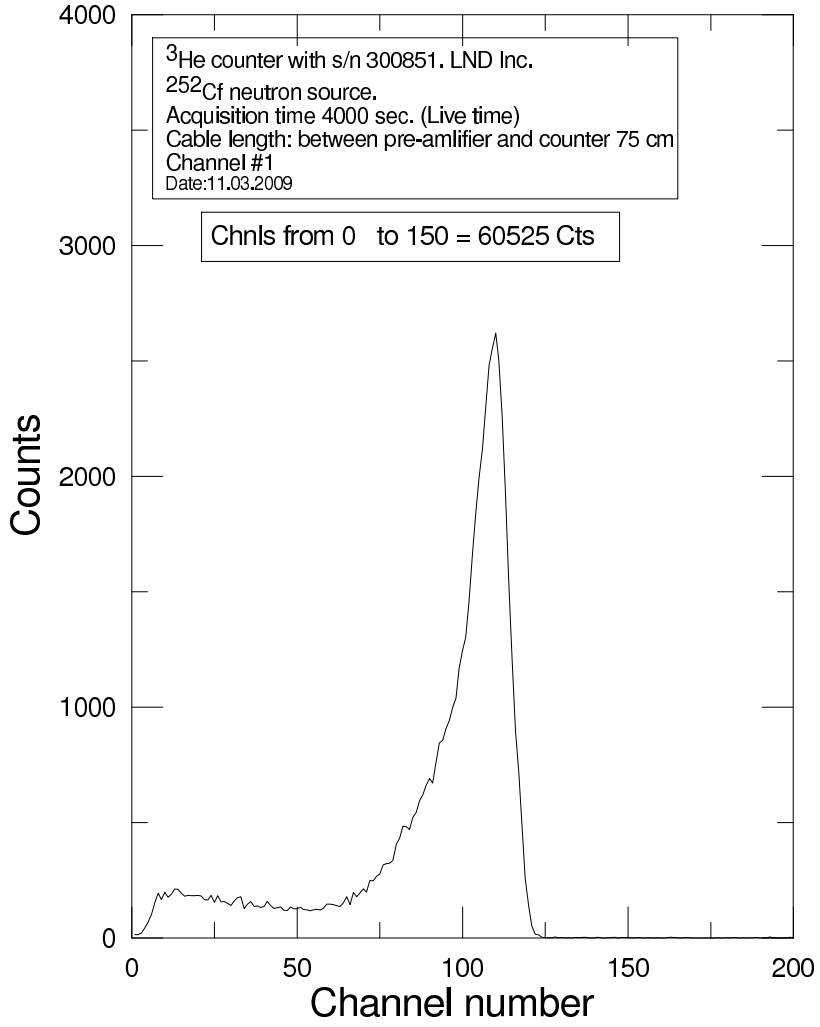

Figure 4.23: Response function for channel 1 and counter with s/n 300851. Electronic scheme from Figure 4.15 was used. The cable length between the preamplifier and the counter was 75 cm.

- Most of the counters are accepted to be used at the future experiment. One counter needs to be changed.
- All the channels of the electronics work well.
- There is no influence of "hot" or "cold" start for the electronics equipment.
- The cable length between the preamplifier and amplifier will be 75 cm.
- The experimental and simulation results are in good agreement.
- The electronic modules MESYTEC STM-16+ and MPR-16 will be used for the neutron detector.
- The High Voltage module NHQ203M will be also used for the detector.

Channel #	Number of counts. Chnnls from 0 to 150
1	60525
2	62593
3	61785
4	60130
5	59817
6	60266
7	60428
8	60016
9	60638
10	59909
11	60156
12	60074
13	59788
14	59576
15	59832
16	59985

Table 4.7: Number of counts in each channel.

Data type	Efficiency (%)
Experimental data	2.26 ± 0.09
MCNPX data	2.41 ± 0.07

Table 4.8: Experimental and simulated (MCNPX) detection efficiency of the counters.

Two additional modules of preamplifiers and amplifiers MESYTEC have been bought. The test of the channels of the equipment was repeated with the second equipment MESYTEC. The test was made according to the scheme from Figure 4.15

Chapter 5

Experimental test of the detector

5.1 Full detector test at UPC

This chapter is about test of the neutron detector in UPC laboratory (Barcelona) and JYFL laboratory (Finland). The test of the detector is a result of all previous works which were done to design this detector. The main objective of this chapter is to explain that the neutron detector works according to the main requirements.

5.1.1 Efficiency test

In order to validate the simulation data and check the electronics to be used in Finland (JYFL) full test should be done. This test was performed at UPC laboratory in July 2009. The test was made with our ^{252}Cf neutron source (See chapter 3).
During the test the efficiency of the detector was checked and a neutron moderation time was measured. This test was performed with collaboration of IFIC(Valencia) and CIEMAT (Madrid). The IFIC participation involved providing a DAQ system for the test. CIEMAT provided NaI(Tl) detector to detect γ from the ^{252}Cf fission. The test was performed during 3 days. The were performed the measurements of neutron detection from the source and background measurements. Other important thing were done is a measure of neutron moderation time. The neutron detector can be observed on figure 5.2. The detector was mounted, but the polyethylene shielding was not placed around the detector due it's large weight and because of the limitation on floor resistance of the building. The acquisition system, which can be observed on figure 5.3, was provided by colleagues from IFIC (Valencia). The main module was Struck SIS 3006 and the software of the acquisition system was developed by the IFIC (Valencia). The SIS3306 board is used for the readout of high resolution detectors, accelerator controls and other applications.

The neutron source was inserted in a special frame in order to be fixed and have exact position to repeat the experiment at the same conditions. See figure 5.4

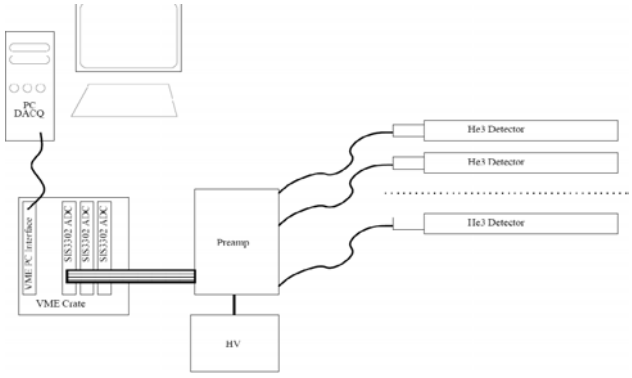

Figure 5.1: DAQ for neutron detector

The experiment was done with 20 proportional counters. These proportional counters were assembled inside the polyethylene matrix with dimensions 50x50x80cm^3 in two rings. The first ring contained 8 counters and second ring contained 12 counters. This polyethylene

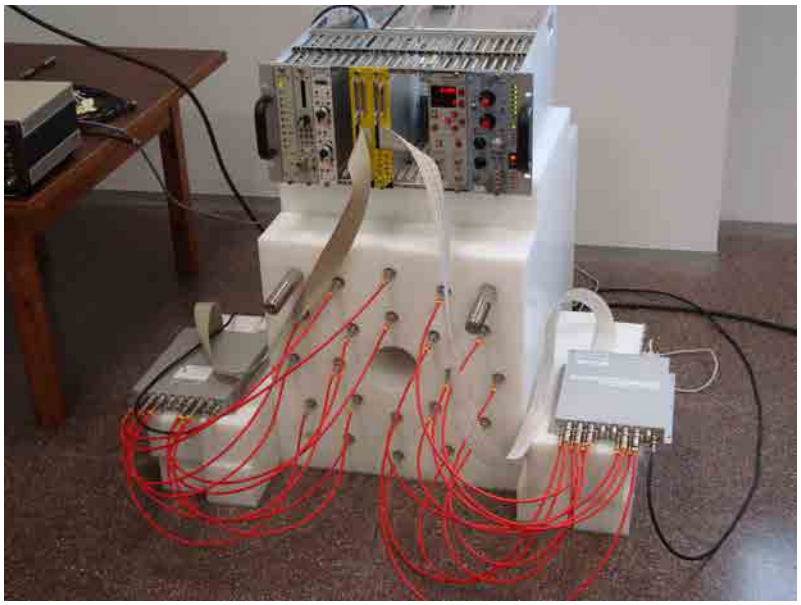

Figure 5.2: Neutron detector at the test in SEN

Figure 5.3: DAQ system for the test at SEN

matrix has a central hole in order to set the neutron source. This structure was chosen according to the previous MCNPX simulation in order to have the efficiency curve as flat as possible for wide range of initial neutron energy. The NaI(Tl) detector was inserted inside the central hole as close as possible to the neutron source in order to detect the γ from the fission. This detector will be used to obtain the neutron moderation time inside the polyethylene. The typical neutron energy spectrum can be observed on figure 5.5. There is the first wall effect which corresponds to the energy 191 keV and the second wall effect which

Figure 5.4: Neutron source for test at SEN

corresponds to 574 keV. The second wall effect is closed by the spectrum curve. The main peak corresponds to full energy deposition and it is 765 keV.

The efficiency (η_d) of the neutron detector obtained by MC simulations (See Chapter 3) can be observed on figure 5.6 for neutron energies up to 6 MeV. The efficiency measured in this experiment have a value of (29±4)% which is in accordance with MC simulation. This value is represented as a red spot in figure 5.6. The efficiency and its uncertainty were calculated according to the equations 5.1 and 5.2.

$$\eta_d = \frac{\sum N_i}{N_{source}} * 100\% \tag{5.1}$$

$$\sigma^2_{\eta_d} = \sum (\frac{\partial \eta_d}{\partial N_i})^2 * \sigma^2_{Ni} + (\frac{\partial \eta_d}{\partial A})^2 * \sigma^2_A \tag{5.2}$$

Where η_d is the efficiency, N_i is the number of counts in each counter and N_{source} is the number of emitted neutrons from ^{252}Cf source.

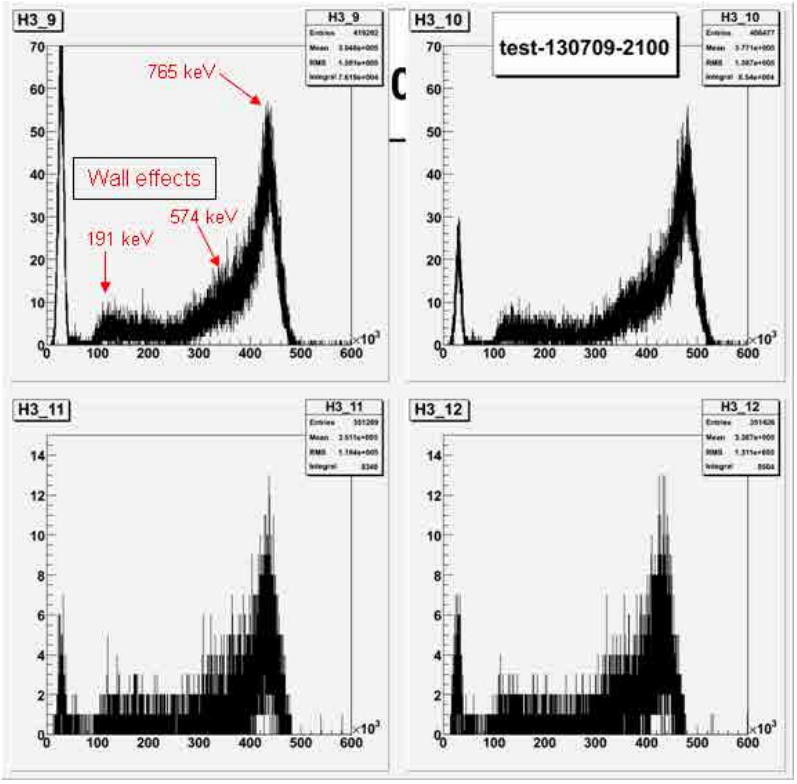

Figure 5.5: Neutron energy spectrum

$$\eta_d = \frac{\sum(\dot{N}_g) - \sum(\dot{N}_b)}{\dot{N}_{source}} \tag{5.3}$$

$$N_{N_i} = N_{g_i} - N_{b_i} \tag{5.4}$$

$$\sigma_{N_i} = \sqrt{N_{g_i}} \tag{5.5}$$

$$\sigma_{N_{b_i}} = \sqrt{N_{b_i}} \tag{5.6}$$

$$\sigma_{N_i} = \sqrt{\sigma^2_{N_{g_i}} + \sigma^2_{N_{b_i}}} \tag{5.7}$$

Where N_{b_i} is a background counts in one counter, N_{g_i} is a gross counts in one counter and N_{N_i} is a net counts in one counter.

This efficiency was calculated by analyzing the spectrum files from the experiment. The number of detected neutrons was calculated by including all events from the spectrum, but cutting the noise from the fist $80\text{x}10^3$ channels of the spectrum (see figure 5.5). The data obtained at the experiment are presented on table 5.1

Counter number	Counts	Pulser
1	15299	691341
2	15545	691346
3	16046	691370
4	15270	691414
5	16909	691401
6	15284	691319
7	122222	691542
8	125439	691455
9	124480	691558
10	122429	691528
11	15729	691311
12	15177	691321
13	15030	691315
14	15179	691442
15	15272	691334
16	15450	691315
17	124341	691478
18	121313	691465
19	121367	691492
20	123274	692067

Table 5.1: Experimental data obtained during July experiment at UPC

The pulser was set to 10 MHz, where N_i is the number of neutrons detected in each counter and N_{source} is a number of neutrons emitted from the Cf source. The uncertainty of the efficiency in this case is very large. The contribution to the uncertainty comes from the count rate and from the uncertainty of the activity of the ^{252}Cf source. In order to decrease the uncertainty of the efficiency we need increase the measure time and decrease the uncertainty of the neutron source. But it is impossible to decrease the uncertainty of the neutron source in this laboratory. It corresponds to 15 % and it comes from the manufacturer. The efficiency of the measurement and simulation efficiency can be observed on figure 5.6. Next measurements with this detector will be made in JYFL (Finland). The neutron source will have less uncertainty and the efficiency can be checked with better resolution.

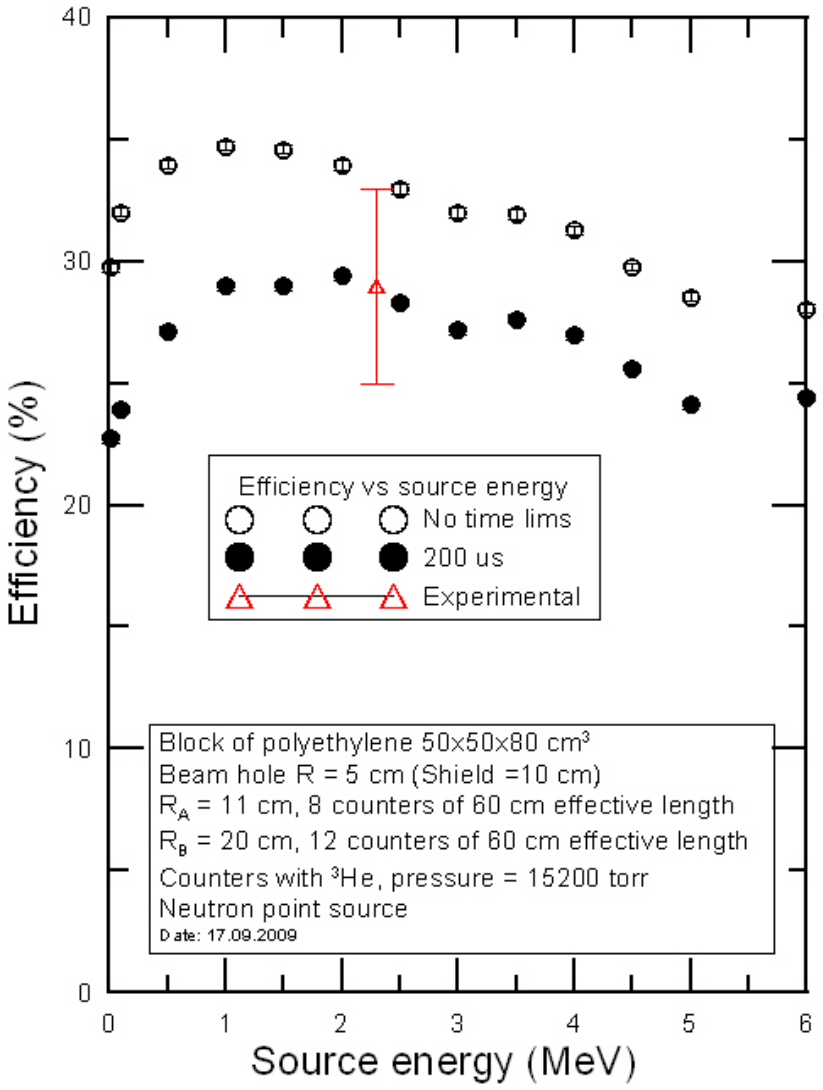

Figure 5.6: Efficiency of the neutron detector vs simulation

5.1.2 Measurement of neutron moderation time

One of the important task consists in distinguish the β-delayed neutrons from background neutrons in order to measure neutrons only from β-decay and not contaminate the detector with false signals from the background.
The main idea for this measurements is γ detection from ^{252}Cf decay. In order to make this measurements a NaI(Tl) detector was used. This detector was put in the center of the neutron detector close to ^{252}Cf source and detected γ from the decay of ^{252}Cf. The scheme of β - delay neutron emission and gamma emission can be observed on figure 5.7. The detector NaI(Tl) detected γ from the emitter after spontaneous fission of ^{252}Cf and the proportional counters detected neutron from the emitter. The time between the γ detection and neutron detection is called a moderation time. In order to evaluate the optimal moderation time a simulation was done where the efficiency of the detector was a function of moderation time. This function is presented on figure 5.8 and it shows the optimal time should be about 200 μs because after this time the efficiency does not change so much.
In order to validate simulation data the measurements with NaI(Tl) detector were performed with a ^{252}Cf source which decays via either alpha emission (96.9%) or spontaneous fission (3.1%). An average of 3.7 neutrons are emitted in each spontaneous fission. The neutron emission is accompanied with γ emission. The measurements were performed by finding the time between the detection a γ and neutron detection. The NaI(Tl) detector was installed inside the neutron detector near the Cf-source in order to detect the γ. The neutrons were detected by proportional counters. The time difference between two signals from NaI(Tl) detector and proportional counters is the neutron moderation time. The experimental

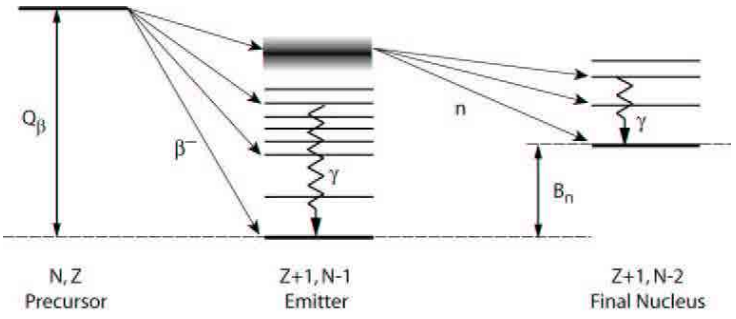

Figure 5.7: Scheme of β delay neutron emission

results of this measurement can be observed on figure 5.9. During the first 10 μs there are about 950 counts in all the proportional counters. Next 10 μs gives about 530 counts. It is easy to observe that during this time the number of counts decreases about 50 %. If experimental and simulation results are compared there is a coincidence (Figure 5.9 Figure 5.8 respectively). During the first 10 μs and the next 10 μs the decreasing is the same for the simulation and experiment. According to the simulation the neutrons measured during first

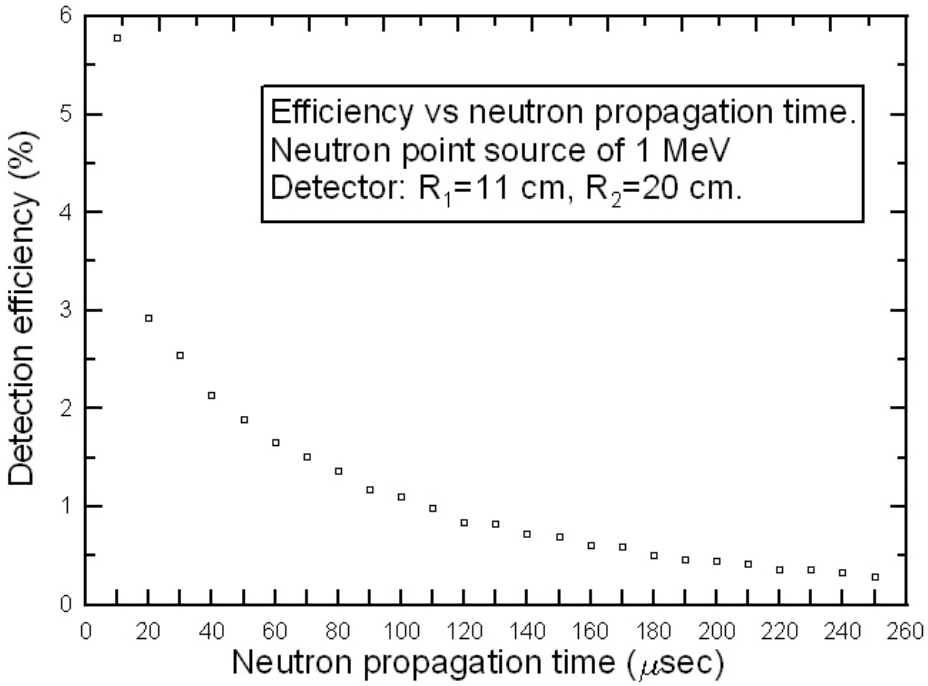

Figure 5.8: Neutron detection vs propagation time. Simulation results

10 μs is twice then the number of neutrons detected after next 10 μs as it can be seen in the experimental results (Figure 5.9).

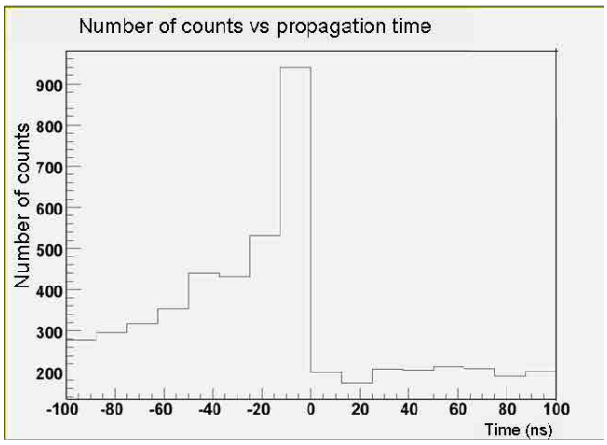

Figure 5.9: Neutron detection vs propagation time. Experimental results

5.2 Experiment at JYFL

The test of the detector was performed at University of Jyväskylä (JYFL). The aim of this test was to validate the characteristics of the neutron detector such as efficiency and moderation time. In order to do it we need to measure the β delayed neutron emission from well-known nuclei to validate the values measured, comparing with referenced data. The nuclei measured [6] at JYFL were ^{94}Rb, ^{95}Rb, ^{88}Br, ^{138}I, ^{138}Te. This detector is a prototype of large detector at DESPEC (GSI) experiment. After the experiment at JYFL we should answer to the next questions:

- Does the experimental efficiency of the detector corresponds to simulation efficiency?
- Does the obtained data with well-known nuclei correspond to the table values?
- Is this detector adequate prototype for the neutron detector for DESPEC experiment?

5.2.1 Facility at JYFL

The measurements were performed the at Ion Guide Isotope Separator On-Line (IGISOL) facility (See figure 5.10). It based on the ion guide technique which is stopping the primary ions from nuclear reactions in noble gas, typically in helium. Because of the high ionization potential of helium, the stopped species are preserved as ions long enough to be evacuated from the stopping volume still as ions. Another option is to use voltages inside the ion guide to drift the ions through the gas. At the IGISOL, ions are extracted from helium using a diKerential pumping system and mass separated using a dipole magnet with a mass resolving power (MRP) of about 500. This is adequate to select an isobar - species with the same mass number A - to be sent to subsequent spectroscopy, or to double Penning trap system for more refined purification. The purification with trap system is sufficient to separate the diKerent species within the isobar, resulting in truly monoisotopic beams of the studied species. The MRP of this separation can easily exceed 105. Beta, gamma, and beta delayed neutron decay studies significantly benefit from such sources and a vivid research program is established around the decay studies of the purified sources. The tape system (JYFLTRAP) is an intrinsic part of the IGISOL facility. In addition to beam purification, it can be used as an instrument to determine very precisely atomic masses. Atomic masses of over 200 neutron-rich nuclei have been measured with JYFLTRAP with an accuracy of a few keV. At the IGISOL facility the particle induced fission of natural uranium and thorium targets used to produce neutron rich species for nuclear spectroscopy studies. The chemical insensitivity of the ion guide technique makes it also an attractive approach to study the fission yield distributions. Due to the ion production mechanism of IGISOL only directly produced ions are detected and hence independent fission product yields are measured.

At IGISOL the beam hits a thin target and products high charged ions. After acceleration to about 40 kV the beam is separated by a dipole magnet. A good features of this technique are the fast (sub-millisecond) release, and chemical non-selectivity making it possible to produce even the most refractory of elements. In relation with nuclear fission, the IGISOL method has led to the production of neutron-rich nuclei with beam intensities approximately 10^5 ions/s. The typical transverse emittance of an extracted ion beam is about 1.2π mm mrad and the

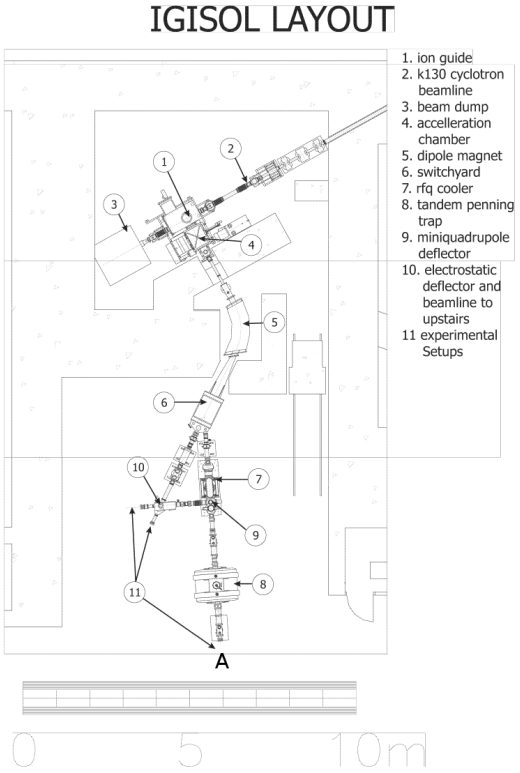

Figure 5.10: IGISOL layout

energy spread is relatively large, up to 50 eV. In order to reduce these physical parameters an additional cooling is required. On the figure 5.10 look for point number 8. After each measurement, a moving tape extracts daughter nuclei from the center of the neutron detector, in order to eliminate the background from these nuclei. The neutron detector was placed on the point "A" of this scheme.

5.2.2 Detector configuration in the experimental area

The experiment setup is based on three detection systems. The first one consists on 20 ^{3}He proportional counters to detect the neutrons, the second one is a HPGe-detector to measure gamas emitted by nuclei decay and the last one is a Si-detector to measure β particles from

the decay. The configuration can be seen on Figure 5.11.

The main idea of this detectors assembly is a detection of all particles involved in beta-decay. The nuclei from the beam was implanted to the center of the neutron detector. After some time the nuclei were moved away by tape system (see Figure 5.14 and Figure 5.15) which was used to eliminate the contamination by daughter nuclei. The frequency at which the nuclei are moved away from the center of the detector (by means of the tape system) depends on each nuclide and the period is equal to seven times of the half-lifes of each nuclide.

Following a β decay the nuclide emits a γ particle which can be used as a starting time stamp in the DAQ system. These particles are measured with HPGe-detector that is located at the center of the polyethylene matrix, close to the Si detector and the tape where nuclei have been implanted. The Si detector was used to detect β-particles. After detecting these two particles the delayed neutron was detected by ^{3}He counters. The main configuration of the experiment setup is shown in Figure 5.11

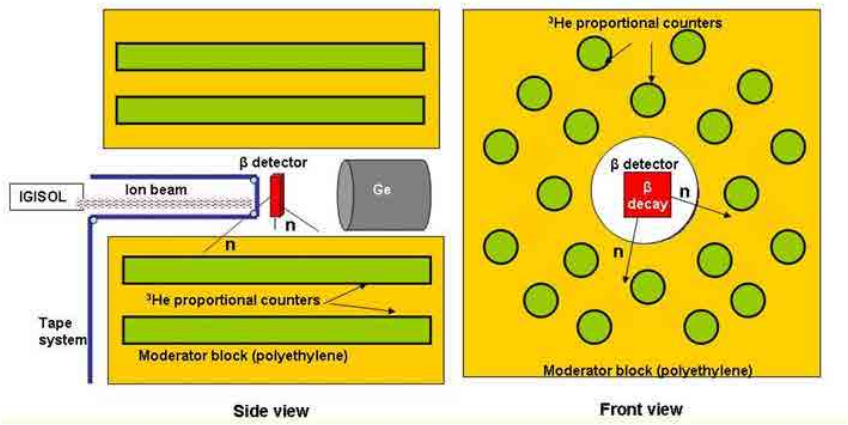

Figure 5.11: The detectors assembly at the experiment

In Figure 5.12 is shown a picture of the neutron detector with HPGe-detector. The detector was placed in the experimental area and the beam pipe (Figure 5.13) was placed inside the beam hole of the detector. The position of the polyethylene matrix was adjusted (by means of a table designed for this experiment) to set the end of the beam pipe at the center of the beam hole and the center of the polyethylene matrix in order to maintain the symmetry and the 4π geometry.
The analysis of data measured with the HPGe and Si-detector will help to find the neutron moderation time after β-decay.
As this experiment is triggerless we can not use START and STOP triggering signals, in this case we use labels "start time stamp" and "stop time stamp" for data analysis. In order to determine the neutron moderation time we need to know the start time stamp. This time stamp is provided by the γ detected by HPGe-detector. The stop time stamp is provided the signal by the neutron proportional counters. The neutron moderation time is the time difference between start and stop time stamps. Si-detector worked also as additional detector for start time stamp in order to substitute the HPGe-detector in same cases. And it is also a confirmation of β decay event.

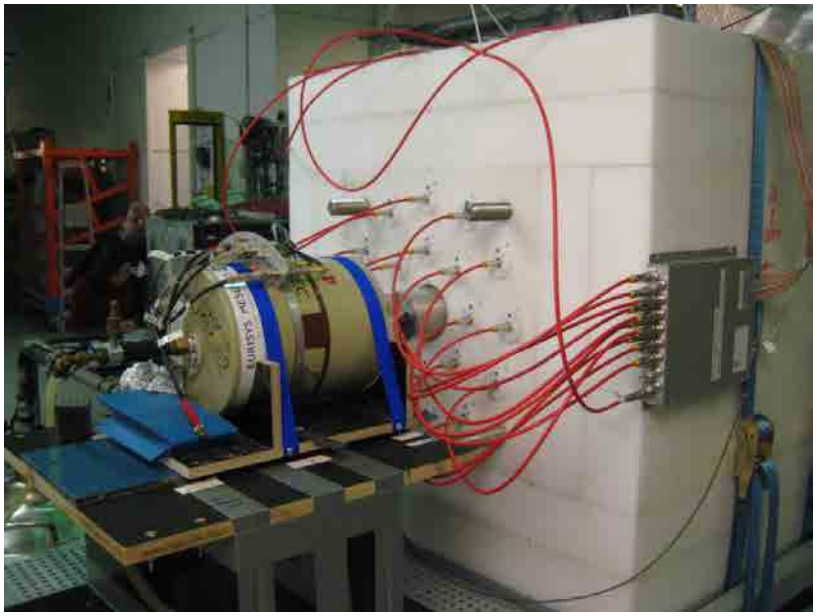

Figure 5.12: Neutron detector on the beam and HPGe-detector

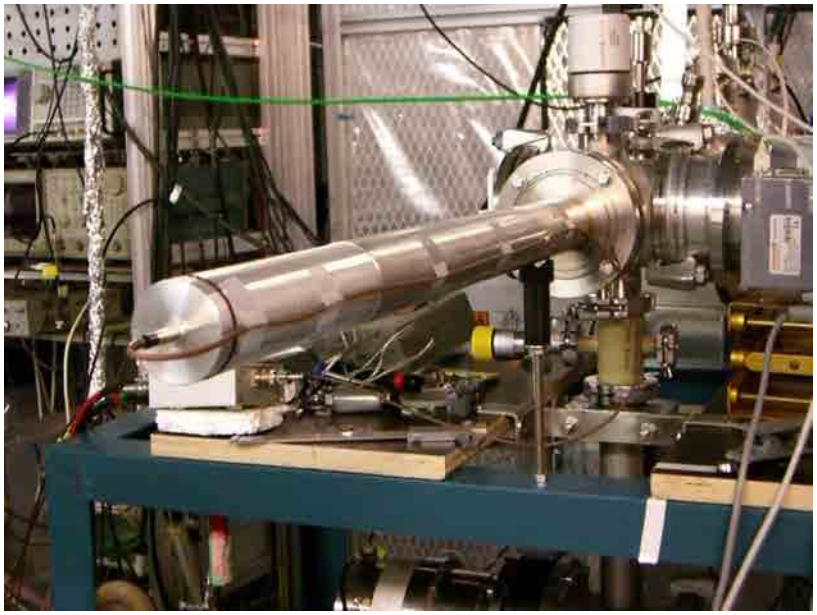

Figure 5.13: Beam tube with Si-detector inside

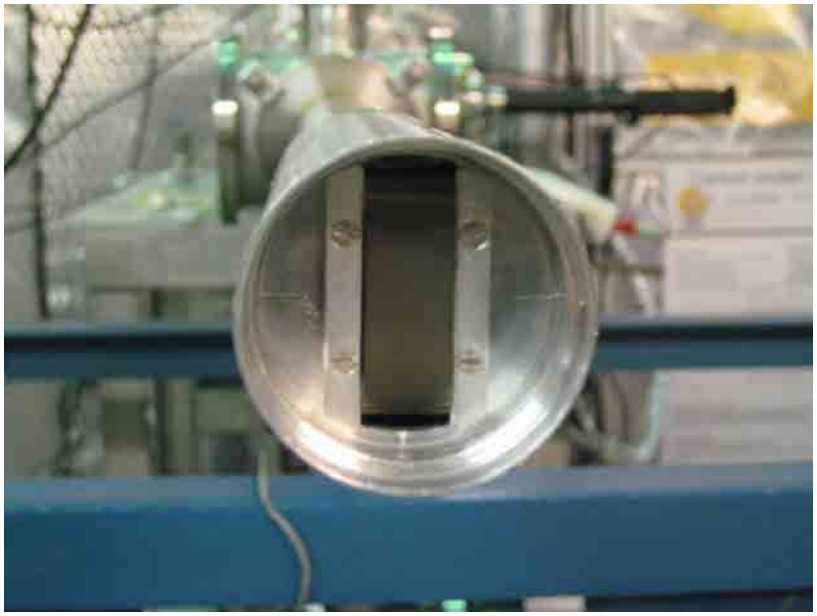

Figure 5.14: Beam tube with tape integrated inside

Figure 5.15: The tape system on the experiment

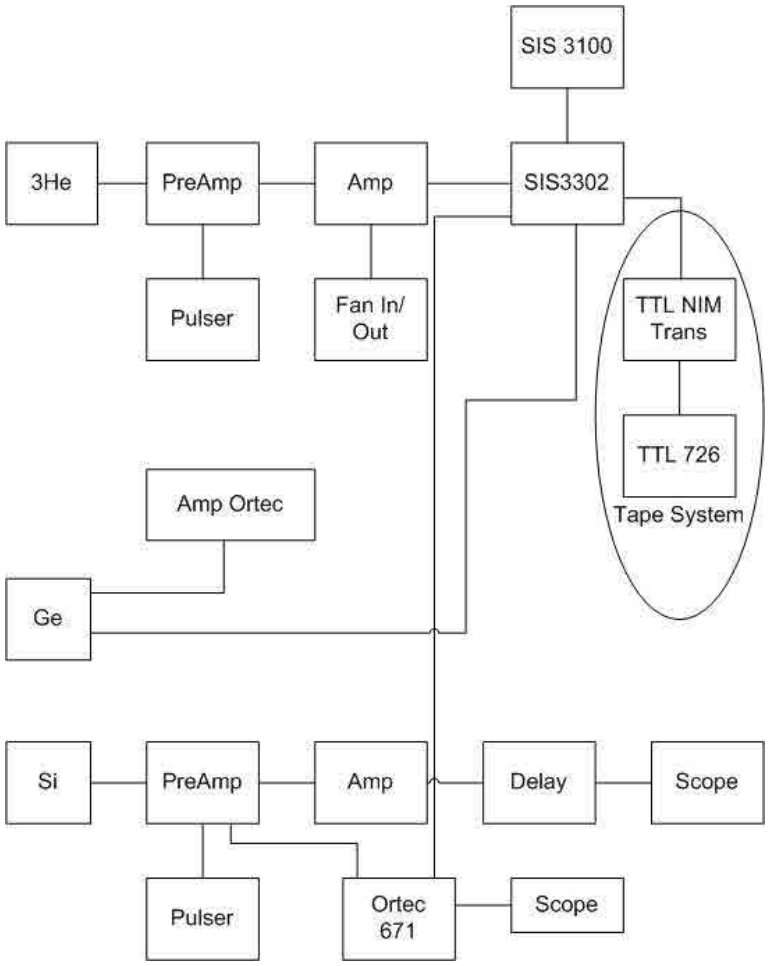

Figure 5.16: Electronics scheme at JYFL experiment

5.2.3 Electronics at experiment

The scheme of the experiment is presented on Figure 5.16. There are three schemes which show the connection of three main detectors.

The first detector is the ^{3}He neutron detector for detection the neutrons from the beta decay. Gammas are detected by HPGe-detector and β-particles are detected by Si-detector. Data from these three detectors will be analyzed in order to find the efficiency of the detector, neutron moderation time and β delay emission probability. The analysis process scheme is presented on Figure 5.17. There are four main time lines for each detector and pulser. The gama detection gives a start time stamp. The β delay neutron emission is confirmed by the detection in coincidence of a neutron and a β particle. The pulser gives the time reference during all the experiment time. As the frequency of pulser is well-known and controlled by us, the time elapsed between each event can by calculated easily. A neutron detection generates a signal for stop time stamp. The moderation time is a time difference between gamma and neutron detection.

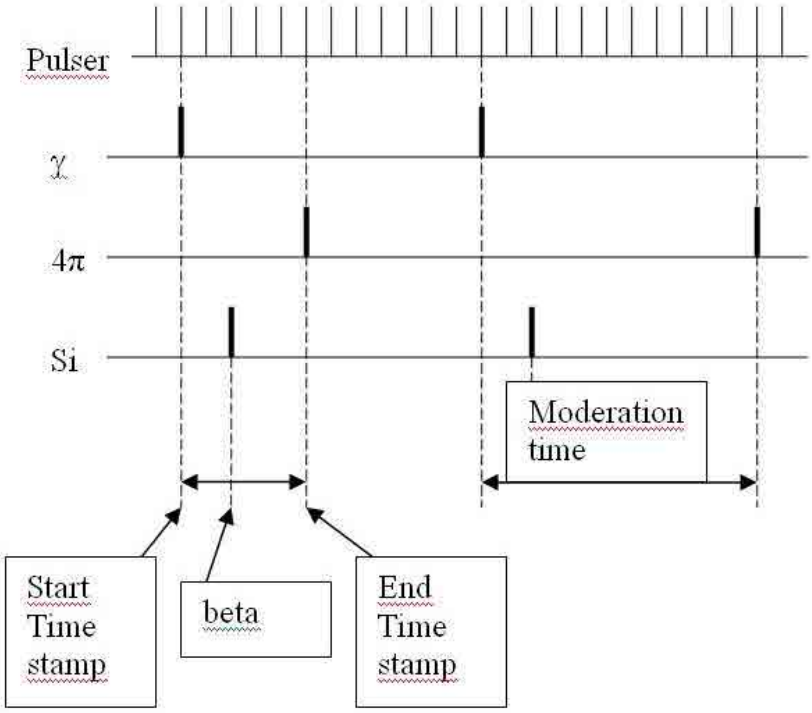

Figure 5.17: Analyzing scheme at JYFL experiment. Valid event

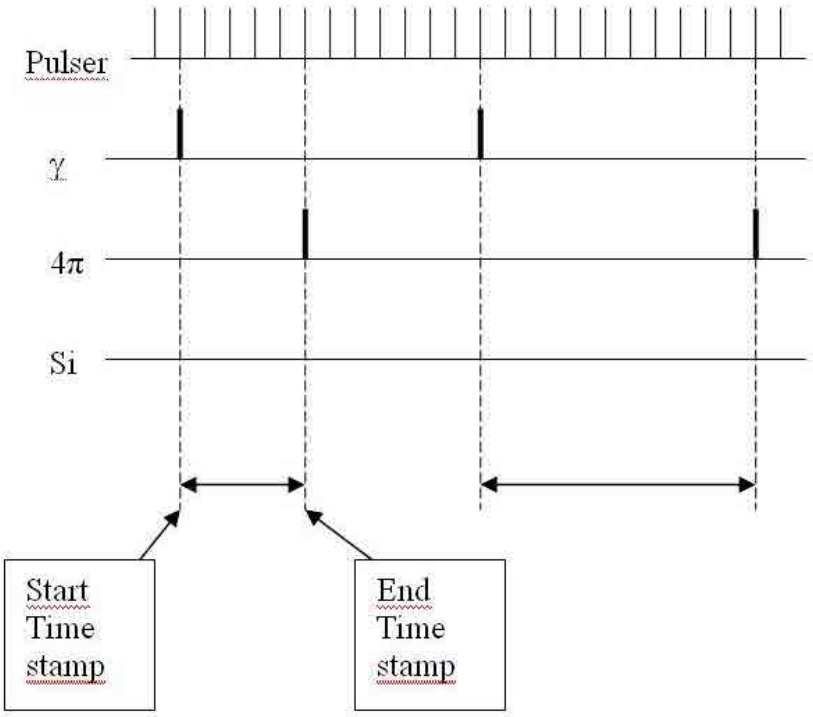

Figure 5.18: Analyzing scheme at JYFL experiment. Not valid event

The event can not be taken in account if information is lost. For example on the Figure 5.18 There is no information from the Si-detector about β - detection. It can not be sure in N_β event so this event will not be taken in account for analyzing.

The main electronics components involved in the scheme are:

- High Voltage. The bias voltage of proportional counters was set to 1800V. There were two HV with 16 channels each in order to power all the counters. The HV module manufacturer is ISEG.
- Pre-amplifier. Two pre-amplifiers by Mesytec with 16 channels each one. Twenty channels were used for proportional counters. One channel was used for Si detector and one channel for HPGe detector. Other ten channels were not used at the experiment
- Amplifier. The same manufacturer as pre-amplifiers and also with 16 channels each one.
- Pulser. Is used as a time reference. This component sends the signal with fixed frequency.
- Sis 3302 is 100 MHz 16-bit VME Digitizer by Struck manufacturer is used to collect all the data from the all components of the scheme.
- Sis 3100 is PCI/cPCI to VME interface card combination was used to send the data from VME module to PC. And afterwards analyzer the data to meet the requirements of demanding VME data acquisition systems

The signals from proportional counters of the neutron detector were sent to the preamplifier. The signals from the pulser was connected to the same preamplifier. The pulser was used to have a time reference during for the data analyzing. The signal from the amplifier was synchronized with the movement of the tape. The transformed signal was sent to the Struck SIS3302 ADC module. Si-detector sent the signals to the preamplifier and pulser was also connected to the preamplifier. These two different pulsers were used for independent time reference peaks. Analyzing the number of counts in the peak from the pulser the measurement time can be received. HPGe-detector sent the signal directly to the Struck SIS3302 ADC module. The three signals from three detectors was digitaged in the SIS3302. This board was chosen because the board is used for the readout of high resolution detectors, accelerator controls and other applications. After the digitalization the signals were sent to Struck SIS3100 module. It is a PCI/cPCI to VME interface card. It is optimized for low latency high speed readout.

5.2.4 Measurements and data analysis

During the measurements the following nuclei were tested: ^{94}Rb, ^{95}Rb, ^{88}Br, ^{137}I, ^{138}Te. These nuclei are well known and we use them as a reference in order to check the detector's properties at the experiment. The data of these nuclei are presented on Table 5.2

Isotope	$T1/2$	Decay Modes
^{94}Rb	2.702 s	β^-: 100.00% ;β^-n: 10.50%
^{95}Rb	377.7 ms	β^-: 100.00%;β^-n: 8.70%
^{88}Br	16.29 s	β^-: 100.00%;β^-n: 6.58%
^{137}I	24.5 s	β^-: 100.00%;β^-n: 7.14%
^{138}Te	1.4 s	β^-: 100.00%;β^-n: 6.3%

Table 5.2: Characteristics of Isotopes at the experiment at JYFL

These nuclei were implanted on the tape and this tape extracted the daughter nuclei from the center of neutron detector. The movement of the tape was synchronized with the time of the decay of each nucleo in order to have the decay in the center and not contaminate the detector with daughter nuclei.

The implantation time of each nuclide is equal three half-lives of the nuclide implanted and remains in that position during seven half-lives. After this time period the tape is moved and removes daughter nuclei from that position. In order to obtain the neutron ratio per a decay the next calculation should be done. Firstly the beta spectrum in the silicon detector was obtained. This spectrum can be observed on Figure 5.19. This figure shows the number of electrons for each channel where channels represent deposited energy.

There was a neutron spectrum obtained from the neutron detector. This spectrum can be observed on Figure 5.20. This figure shows the number of neutrons for each channel where channels represent deposited energy.

The Figure 5.21 and Figure 5.22 represents a number of events during the time. They were fitted by Bateman equations The First part of each figure is a time of grow the number of events. In this case it was a time of implantation and the decay part shows the decay during

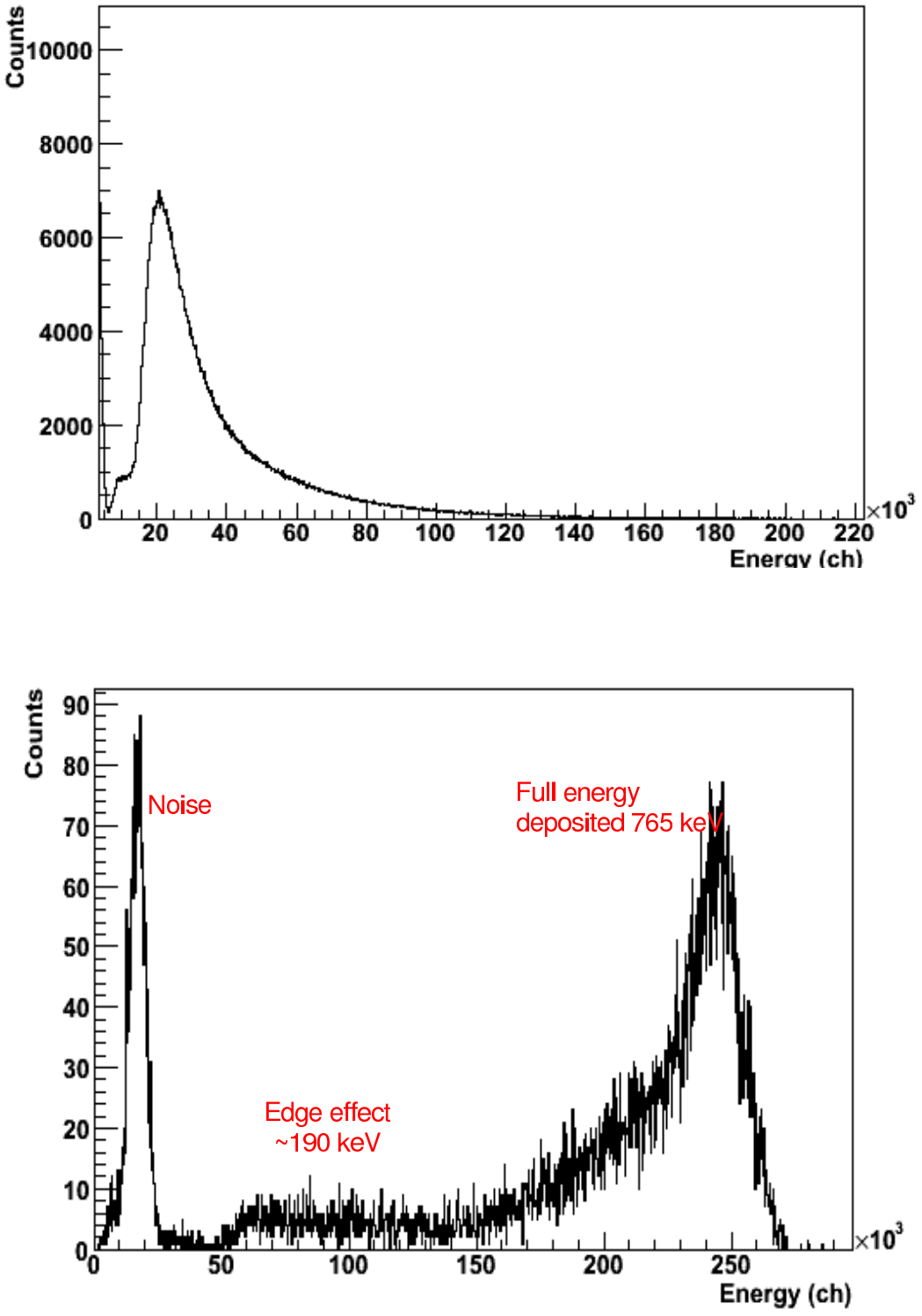

Figure 5.20: Neutron detector neutron spectra

the 7 half-life time. The next plot (Figure 5.23) was constructed by coincidence of neutrons in neutron detector and beta decay in Si-detector with opened time window for 1 ms.

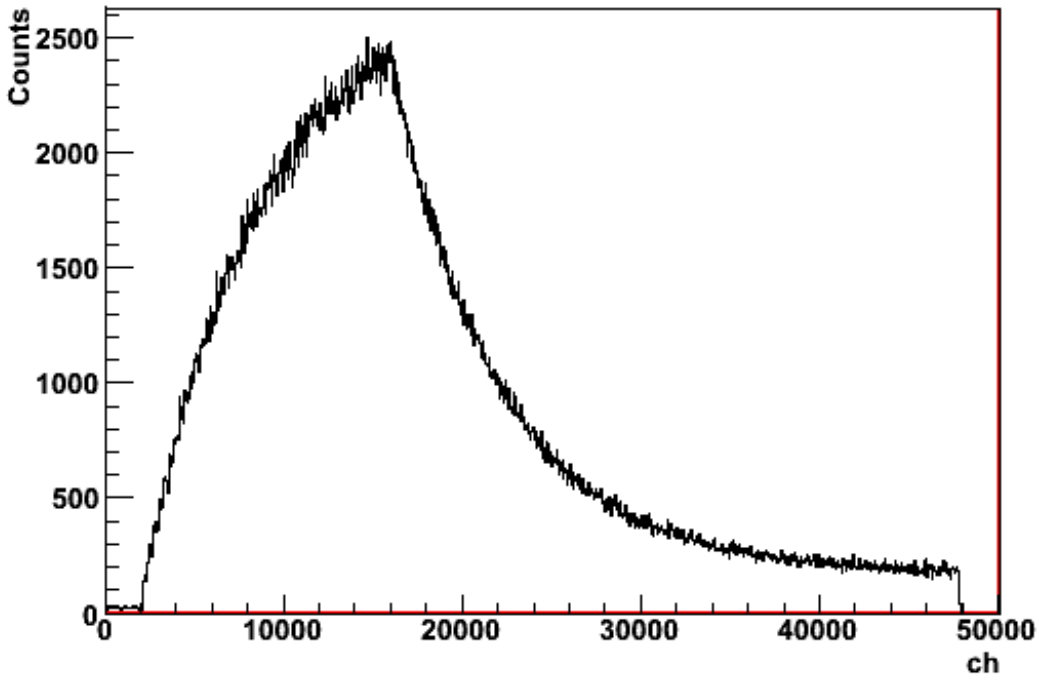

Figure 5.21: Time silicon detector

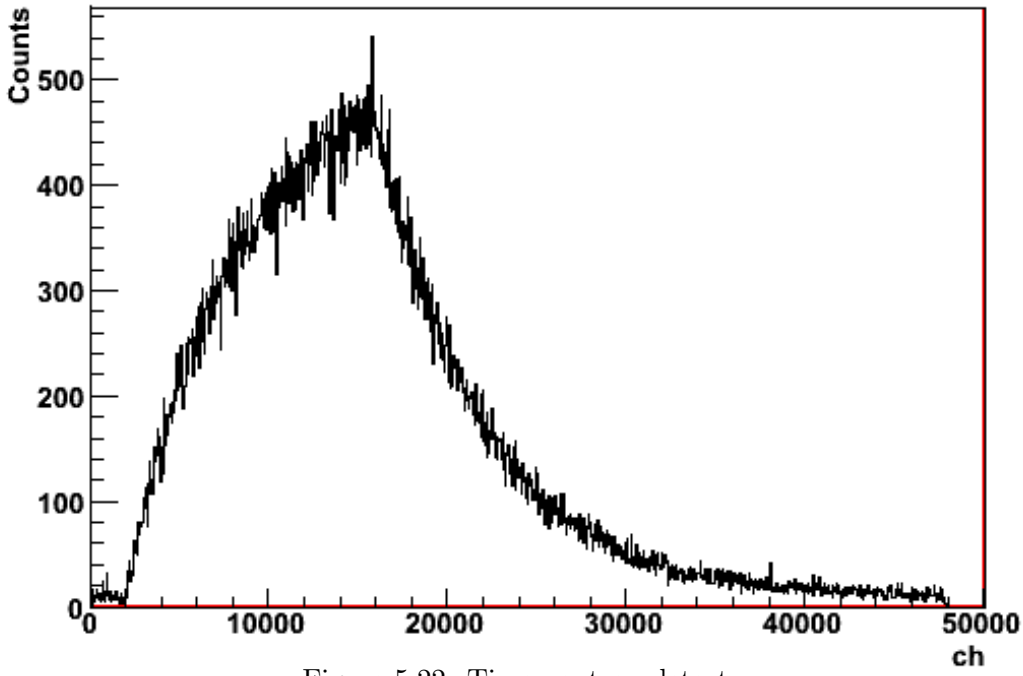

Figure 5.22: Time neutron detector

The neutron emission probability was calculated by equation 5.8

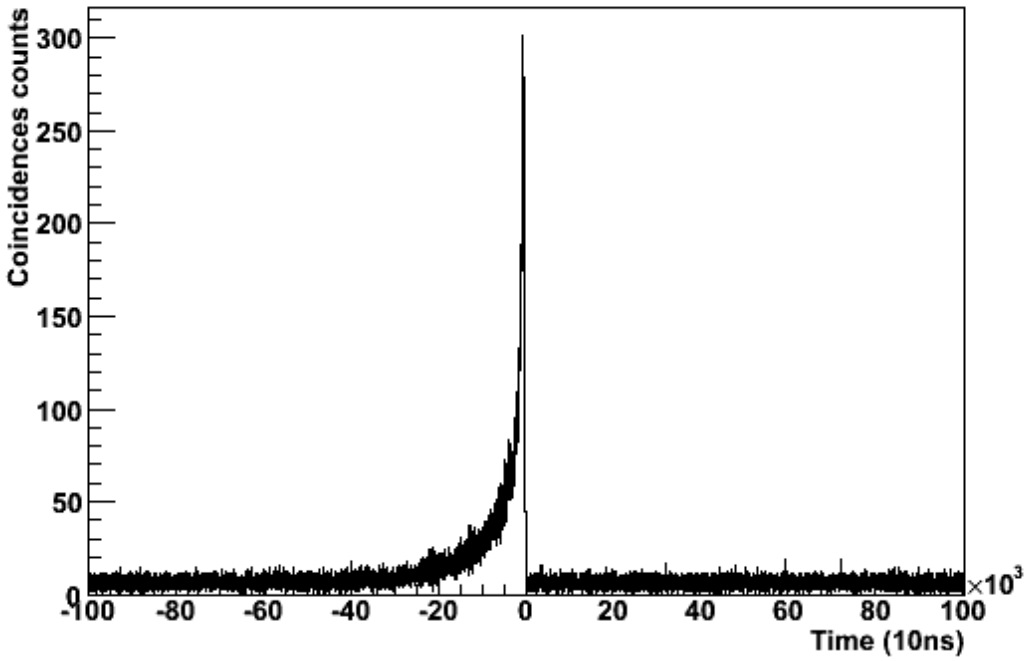

Figure 5.23: Moderation time

$$P_N = \frac{1}{\varepsilon_N} \frac{N_{N\beta}}{N_\beta} \tag{5.8}$$

Where $N_{N\beta}$ is a number of $N\beta$ registered events. N_β is a number of β registered events and ε_N is neutron detector efficiency. These values can be obtained analyzing the experimental data.

5.2.5 Results

The main objective of this work was to test the neutron detector at the experiment and to verify it working with described electronics. The electronics on the experiment worked according to its requirements. It gave an opportunity to obtain the neutron spectra after the decay. It was important to test the measurements with other detector such as Si-detector and HPGe-detector. During the work at JYFL it was done. This measurement lets to obtain neutron moderation time in the polyethylene matrix.
Coincidence of all these measurements helps to obtain neutron ratio per a decay for each nucleo measured.

This detector is based on ^{3}He as a detection gas. This choice was done because ^{3}He has higher cross-section for the reaction with neutron. This property increases the probability of neutron detection and increases the efficiency of the detector. There were some tests with BF_3 detector done. This tests were described in previous chapter.

In order to calculate the experimental efficiency of the detector, The P_n values of ^{88}Br and ^{95}Rb were used as references. From these two values the average detection efficiency for the neutron detector is (27.1 +/- 0.8)/(see Table 5.3). This neutron detector has very small uncertainty. The error of the ratio is less than 4% This results are better than other experiments provide. The NERO experiment has uncertainties about 9%

Isotope	P_n(%)	N_β	$N_{\beta\ n}$(%)	Efficiency (%)
^{88}Br	6.58 +/- 0.18	867701	14350	27.6 +/- 0.7
^{95}Rb	8.73 +/- 0.20	588116	13301	26.6 +/- 0.8

Table 5.3: Detection efficiency obtained using ^{88}Br and ^{95}Rb as calibration

According to the experimental results [14] for ^{94}Rb and ^{138}I can be observed on table 5.4. The comparation of the values of P_n for the JYFL experiment and other one gives a good agreement. It means that the neutron detector designed in this thesis gives the aim described in the introduction of this

Isotope	N_β	$N_{\beta\ n}$	P_n(%)	Works
^{94}Rb	3.005	83.768	10.28 +/- 0.31	This detector
^{94}Rb	-	-	10.01 +/- 0.31	Rudstam [15]
^{94}Rb	-	-	9.1 +/- 0.1	Pfeiffer [16]
^{138}I	343,890	4,955	5.32 +/- 0.2	This detector
^{138}I	-	-	5.46 +/- 0.18	Rudstam [15]
^{138}I	-	-	5.17+/-0.36	Pfeiffer [16]

Table 5.4: Nuclei at JYFL experiment compared to other authors

Chapter 6

Conclusions

6.1 Conclusions

The detector designed in this work was developed as a prototype for DESPEC experiment (future FAIR facility at GSI) and tested at JYFL facility in University of Jyväskylä (Finland) in order to find delayed neutron emission rate per β-decay. In order to design it, firstly was studied the 4 π neutron detectors state of the art. As the base to design the neutron detector, the NERO detector experiment was taken in account. The NERO detector is formed by three rings of proportional counters of different types. The aim of this work is to find the optimal configuration of a prototype for the detector to be used in the DESPEC experiment where the neutron detection efficiency should be as flat as possible for a wide neutron energy range. In this case the energy range is from thermal neutrons to 6 MeV.
The design was performed by means of Monte Carlo simulations using the MCNPX code. The design and optimization implies the following parameters: the proportional counters detection gas (BF_3 or ^3He), the length of the proportional counters, the number of the counters and its distribution inside the moderator. Also MCNPX code let us to choose the moderator and shielding materials and dimensions in order to protect the detector from the background neutrons. In the table 6.1 there is a description of the main properties of the final configuration of the detector designed in this work.

Total dimensions of the detector	90x90x80 cm^3
Material of the detector	Polyethylene
Dimensions of matrix	50x50x80 cm^3
Shielding	20 cm
Cd layer	No
Beam hole radius	5 cm
Detection gas	^3He
Gas pressure	15200 torr (20 bar)
Total number of counters	20
Number of rings	2
1st ring radius	11 cm
Number of counters in the 1st ring (inner ring)	8
2nd ring radius	20 cm
Number of counters in the 2nd ring (outer ring)	12
Matrix weght	630 kg
Mean efficiency for 0.01 MeV to 1 MeV	(26.74 +/- 3.25)%
Mean efficiency for 0.01 MeV to 6 MeV	(27.69 +/- 3.00)%
Efficiency factor (F) for 0.01 MeV to 1 MeV	1.22
Efficiency factor (F) for 0.01 MeV to 6 MeV	1.61

Table 6.1: Main properties of the neutron designed detector

In order to choose electronics for data acquisition system (DAQ) for the detector, some preliminary tests were done at CIEMAT and UPC laboratories. These tests were done to find electronics components and the best HV wiring types and lengths for the detector. The efficiencies obtained by the tests were validated by MCNPX simulations in order to design the main detector
After choosing the type of proportional counters, moderator, electronics and shielding the

complete test at UPC laboratory was done. This test was done in collaboration of IFIC and CIEMAT. The aim of this test was to validate the electronics for the future experiment at JYFL.
The definitive validation, done in this work, was a test at JYFL facility in Finland in order to measure the β delayed neutron emission rates of known nuclei as ^{94}Rb, ^{95}Rb, ^{88}Br, ^{138}I, ^{138}Te and compare the rates obtained at JYFL with those published by other groups (See table 6.2).

Isotope	N_β	$N_{\beta\ n}$	$P_n(\%)$	Works
^{94}Rb	3.005	83.768	10.28 +/- 0.31	This detector
^{94}Rb	-	-	10.01 +/- 0.31	Rudstam [15]
^{94}Rb	-	-	9.1 +/- 0.1	Pfeiffer [16]
^{138}I	343,890	4,955	5.32 +/- 0.2	This detector
^{138}I	-	-	5.46 +/- 0.18	Rudstam [15]
^{138}I	-	-	5.17+/-0.36	Pfeiffer [16]

Table 6.2: Nuclei at JYFL experiment compared to other authors

The conclusion of the experiment is that the data obtained are in concordance with other published data, which validates the design of the neutron detector performed in this work.

Future activity to be done is the neutron detector design for DESPEC experiment, based on this prototype and results obtained in this work. This implies the change of the dimensions of the beam hole (to allocate the implantation equipment inside the detector), increase the number of counters and number of rings in order to increase the detection efficiency and make it flatter for wider neutron energy range (up to 10 MeV). Also is needed a calibration of the neutron detector, in a reference laboratory, in order to validate the results.

Bibliography

[1] U. Bosch-Wicke R. Biittger H. Klein J. Daughtry V. Kunze, W.D. Schmidt-Ott. A modular 4π counter for beta-delayed neutrons. *Nuclear insauments and Methods in Physics Research A*, 361:263–269, 1995.

[2] W. K. Kellogg P. R. Wrean, R. W. Kavanagh. Total cross sections and reaction rates for ^{19}f(α,n) ^{22}na, ^{22}ne(p,n) ^{22}na, and their inverses. *PHYSICAL REVIEW C*, 62, October 2000.

[3] B. Pelowitz. *MCNPX USER MANUAL*. University of California at Los Alamos National Laboratory, 2.5.0 edition, April 2005.

[4] P.T. Hosmer. Beta-decay studies ^{78}ni and other neutron-rich nuclei in the astrophysical r-process. phd thesis of p.t. hosmer. michigan state university 2005.

[5] A. Denker H. W. Drotleff J. W. Hammer H. Knee R. Kunz, S. Barth and A. Mayer. Determination of the ^{9}be(α,n)^{12}c reaction rate. *PHYSICAL REVIEW C*, 53(5):193–194, 1996.

[6] F. Calviño G. Cortes C. Pretel A. Poch UPC-Barcelona Spain M.B. Gómez Hornillos, V. Gorlychev. Proposal for the jyfl accelerator laboratory.

[7] P. Enflo. Advanced implantation detector array (aida): Technical specification.

[8] C. J. Read. Technical proposal for the design, construction, commissioning and operation of the hispec/despec experiment at the low-energy branch of the super-frs facility.

[9] T.W. Crane and M.P. Baker. *Neutron detectors*.

[10] Geant4 Collaboration. *Introduction to Geant4*. CERN.

[11] Alberto Fass'o Johannes Ranft Alfredo Ferrari, Paola R. Sala. *Fluka: a multi-particle transport code*. CERN-INFN.

[12] Josep Sempau Francesc Salvat, José M. Fernández-Varea. Penelope-2008: A code system for monte carlo simulation of electron and photon transport.

[13] Josep Pujal Curià. *Argos cluster welcome document*. UPC-SEN.

[14] V. Gorlychev et al. Beta-delayed neutron emission studies. *Hyperfine interact.*

[15] Rudstam et al. Delayed neutron branching ratios of precursors in the fission product region. atom. data nucl. data tab. 53, 1 (1993).

[16] Pfeiffer et al. Status of delayed neutron precursor data: half lives and neutron emission probabilities. prog. nucl. energy 41, 39 (2002).

[17] Charles Louis Xavier Joseph de la Vallée Poussin. A strong form of the prime number theorem, 19th century.